THE ROLE OF CROSSTALK BETWEEN THE ARYL HYDROCARBON RECEPTOR AND TRANSLOCATOR PROTEIN IN MODULATION OF GENE EXPRESSION AND CELLULAR HOMEOSTASIS

By

Michelle Megan Steidemann

A DISSERTATION

Submitted to
Michigan State University
in partial fulfillment of the requirements
for the degree of

Pharmacology & Toxicology-Environmental Toxicology-Doctor of Philosophy

2023

ABSTRACT

The complexity of biological cells requires the use of multiple proteins and pathways to maintain a level of homeostasis in changing environments. The aryl hydrocarbon receptor (AHR) is a ligand-activated transcription factor that binds to numerous aromatic environmental pollutants, including 2,3,7,8-tetrachlorodibenzo-ρ-dioxin (TCDD). The AHR regulates the expression of a battery of genes, most notably drug metabolizing enzymes. While environmental sensing has long been the most studied activity of AHR, there has always been the assumption that AHR could have another function mediated by an endogenous ligand(s). Proposed endogenous ligands of the AHR include cholesterol-related, heme-related, and tryptophan-related molecules. Growing evidence for AHR to be partially localized to mitochondria leads to the hypothesis that AHR could have an impact on this organelle's activity. Interestingly, another mitochondrial protein, translocator protein (TSPO) is associated with many of the putative AHR endogenous ligands. Due to the shared mitochondrial localization and ligands, the goal of this research was to determine if AHR and TSPO exhibited signaling crosstalk. Transmission electron microscopy was employed to visualize mito-AHR at a high magnification to confirm the suborganellar location. CRISPR technology was used to knock out AHR and TSPO individually in mouse cell lines; BV-2 (microglia), Hepa1c1c7 (liver), and MLE-12 (lung). The influence of AHR and TSPO was studied by treating MLE-12 cells with an AHR ligand (TCDD), TSPO ligand (PK 11195), or both and then collecting the RNA for comparison. RNA-sequencing demonstrated that loss of either AHR or TSPO altered the expression of nuclear-encoded mitochondrial genes including *Micu2,* which is a component of mitochondrial calcium transport. AHR and TSPO both also influenced the expression of mitochondrial-encoded genes for the electron transport system.

TSPO knockouts were found to have significantly decreased expression of LRRK2, a protein linked to the development of Parkinson's disease. AHR loss also appeared to have some effect on LRRK2. The LRRK2 protein is associated with the exterior of mitochondria and has been associated with mitochondrial dynamics. This dissertation provides evidence that AHR and TSPO are involved in maintaining mitochondrial homeostasis. Many diseases including Parkinson's can be linked to mitochondrial dysfunction and environmental pollutants. It will be crucial to understand the relationship between endogenous functions of AHR and TSPO and how that could be used to prevent loss of mitochondrial homeostasis due to environmental exposures.

ACKNOWLEDGMENTS

To have reached this point is amazing to me and I am so grateful for everyone along the way who has helped me. I would like to first thank Dr. John LaPres who, from the moment he gave me a spot in his lab, was always there to support me. I appreciated that he gives all of his students freedom in research and encourages us to "not let a thing like fear stop you." He is a great example of a director, professor, and mentor.

I would like to thank all of my graduate mentors, Dr. Teri Lansdell, Phillip Lamoureux, Dr. Ronghui Pan, and Dr. Hye Jin Hwang for each giving me a unique bit of knowledge during my first year at MSU. Thank you to Hye for passing on the mito-AHR project and so many new lab techniques to me. Thank you to Dr. Peter Dornbos for teaching me qRTPCR and other lab protocols. I wish I could have learned more about statistics from him. I would like to thank Dr. Amanda Jurgelewicz for being a great lab partner during my later years. She would always be so willing to help and have such well organized, easy to follow instructions. Thank you to all of the many undergraduate, summer, or rotational students over the years. I would like to thank Ayman Taher for being my first mentee and for being so excited for the research. I would like to apologize to Zach D'Haem who had to learn how to perform Western blotting from me. He was such a receptive and truly kind lab member. He has all the skills to be a great doctor. I would like to thank Kalin Bayes and Lizbeth Castro for helping create the CRISPR knockout cell lines that were used in this dissertation.

Dr. Shelagh Ferguson-Miller deserves so many thanks for this dissertation. She was the one who first noticed the overlap of ligands between AHR and TSPO. She was always so invested in helping me to succeed in research. I would like to acknowledge Dr. Jian Liu for all of his work with TSPO including the kynurenine binding assay described in this dissertation and

corresponding paper. I so appreciate all the help Dr. Alicia Withrow gave me with the TEM.

I would like to thank all of my committee members, Dr. Norbert Kaminski, Dr. Robert Roth, Dr. Jamie Bernard, and Dr. Keith Lookingland. Many thanks to them for all of their questions and suggestions for my research. I appreciated that they would always make the time for me even when I gave them late notice.

I would like to thank all of the Pharm/Tox department including all of the professors who instructed me in my first two years to professors who were willing to just talk with me about experiment issues. I would like to thank Dr. Anne Dorrance and Dr. Karen Liby for being such helpful graduate advisors. Thank you to Jake Wier and Meagan Kroll for helping me with all the degree requirements and organization. On the EITS side, thank you to Kasey Baldwin and Amy Swagart for helping me stay informed and involved in the toxicology. Thank you to the Pharm/Tox, EITS, and graduate school for the funding that allowed me the time to continue with my research. Thank you to the Biochemistry department for adopting me into the building along with Ron Norris and Nichole Daly for always being there when a machine would go down.

I would like to thank my brother Mike, who was always the example I wanted to be. He was the reason I wanted to go to Michigan State, and he always looked out for his little sister. Thank you to my parents for being there from every soccer game, to late night school report, to high school musical. I would like to thank my Dad who amazed me with science when he extracted iron from Wheaties. I would like to thank my best friend and person who is every part of my life, my Mom. She has always done everything for me, and I could never actually thank her enough.

"Break a beaker" all future graduate students.

TABLE OF CONTENTS

LIST OF ABBREVIATIONS

ABCA1	ATP binding cassette subfamily A member 1
ABCA3	ATP binding cassette subfamily a member 3
ACTB	Beta-actin
AHR	Aryl hydrocarbon receptor
AHRR	Aryl hydrocarbon receptor repressor
AIP	Ah receptor-interacting protein
ANT	Adenine nucleotide translocase
ARNT	Aryl hydrocarbon receptor nuclear translocator
ATP	Adenosine triphosphate
Cas9	CRISPR-associated protein 9
cDNA	Complementary DNA
CRAC	Cholesterol recognition amino acid consensus
CTSC	Cathepsin C
CTSH	Cathepsin H
CRISPR	Clustered regularly interspaced short palindromic repeats
CYP1A1	Cytochrome P450 Family 1 Subfamily A Member 1
CYP1A2	Cytochrome P450 Family 1 Subfamily A Member 2
CYP1B1	Cytochrome P450 Family 1 Subfamily B Member 1
DEG	Differentially expressed gene
DRE	Dioxin response element
DTT	Dithiothreitol
EDTA	Ethylenediaminetetraacetic acid

EGTA	Ethylene glycol-bis(2-aminoethylether)-*N, N,N',N'*-tetraacetic acid
EHBP1L1	EH domain-binding protein 1-like 1
EPA	Environmental Protection Agency
FPKM	Fragments per kilobase per million mapped reads
GPR39	G-Protein Coupled Receptor 39
GSTK1	Glutathione S-transferase kappa 1
HAH	Halogenated aromatic hydrocarbon.
HPRT	Hypoxanthine phosphoribosyltransferase 1
HSP90	Heat shock protein 90
IARC	International Agency for Research on Cancer
IMM	Inner mitochondrial membrane
IMS	Intermembrane space
IP_3R	Inositol 1,4,5-trisphosphate receptor
LAMP1	Lysosomal associated membrane protein 1
LPS	Lipopolysaccharide
LRRK2	Leucine-rich repeat kinase 2
MAM	Mitochondrial-associated membrane
MCU	Mitochondrial calcium uniporter
MICU2	Mitochondrial calcium uptake 2
MitoDNA	Mitochondrial DNA
Mito-AHR	Mitochondrial AHR
MLE-12	Mouse lung epithelial 12
MPP^+	1-methyl-4-phenylpyridinium

MPTP	1- methyl-4-phenyl-1,2,5,6-tetrahydropyridine
MT1	Metallothionein 1
MtCK	Mitochondrial creatine kinase
MTT	Thiazolyl blue tetrazolium bromide
NAD	Nicotinamide adenine dinucleotide
NFATC2	Nuclear Factor of Activated T Cells 2
NQO1	NAD(P)H: quinone oxidoreductase 1
OMM	Outer mitochondrial membrane
PAH	Polycyclic aromatic hydrocarbon
PAS	Per-Arnt-Sim
PBR	Peripheral-type benzodiazepine receptor
PD	Parkinson's disease
PET	Positron emission tomography
PK	PK 11195
PTPC	Permeability transition pore complex
P38 MAPK	p38 Mitogen Activated Protein Kinase
QRTPCR	Quantitative Real-Time Polymerase Chain Reaction
RAB10	Ras-Related GTP-Binding Protein 10
RIPA	Radio-immunoprecipitation assay
SDS-PAGE	Sodium dodecyl sulfate–polyacrylamide gel electrophoresis
SMDT1	Single-pass membrane protein with aspartate rich tail 1
SFTPB	Surfactant associated protein B
SFTPC	Surfactant associated protein C

TCDD	2,3,7,8-tetrachlorodibenzo-*p*-dioxin
TEM	Transmission electron microscopy
TSPO	Translocator protein
TspO	Tryptophan-rich sensory protein
VDAC	Voltage-dependent anion channel
WT	Wild type
2,4-D	2,4 dichlorophenol
2,4,5-T	2,4,5-trichlorophenol
3-MC	3-methylcholanthrene
18s	18S Ribosomal

CHAPTER 1: INTRODUCTION

Times Beach, MO chemical disaster

It was going to be a resort town. Times Beach, Missouri, was a small town just southwest of St. Louis founded in 1925. The hardships of the Depression and World War II, however, would prevent the city from becoming that planned getaway for the wealthy and instead developed into an area of mostly low-middle class houses. Dirt roads remained into the 1970s and created a lot of dust in the town. To remedy this situation, Russell Bliss was hired to spray waste oil on the roads to prevent dust production. The problem was that Bliss had combined the oil with waste he had been hired to remove from a Northeastern Pharmaceutical & Chemical Company facility which was contaminated with 2,3,7,8-tetrachlorodibenzo-*p*-dioxin (TCDD) (Hites, 2011). Bliss additionally had used the oil on horse tracks throughout Missouri and horses at these stables started to die along with birds, dogs, and cats (Carter et al., 1975). The U.S. Center for Disease Control started to investigate the cause of the illnesses in 1971 but it was not until 1982 that the Environmental Protection Agency (EPA) even announced a plan to test the soil in Times Beach. It would take the surrounding Meramec River flooding in December of 1982 to force the evacuation of the Times Beach inhabitants and for the town to finally be abandoned. In 1983, the EPA reported that some soil samples from around the roads contained up to 100 ppb TCDD (Environmental Protection Agency, n.d.). The EPA bought out the town using Superfund money and undertook a massive incineration of all TCDD-contaminated soil. The remains of the disaster were covered by a massive mound of dirt. The town has never been inhabited again, but by 1999 the region was ready to be used again for recreational activity and the Route 66 State Park was opened. Times Beach is a cautionary tale about how quickly the environment can become hazardous due to human activity or accidents but also how it can be

remedied if action is taken.

The aryl hydrocarbon receptor (AHR)

The aryl hydrocarbon receptor (AHR) was discovered because it acts as a transcription factor receptor for a variety of environmental pollutants including TCDD. Bleiberg et al. (1964) examined cases of factory workers involved in the production of 2,4 dichlorophenol (2,4-D) and 2,4,5-trichlorophenol (2,4,5-T), chemicals used for herbicides. Several workers presented with chloracne and porphyria, which would come to be known as classic symptoms of TCDD exposure. In a desire to learn how TCDD could be elucidating toxic effects, Poland & Glover (1976) analyzed cytosolic fractions from responsive and nonresponsive mice to identify what was causing the induction of aryl hydrocarbon hydroxylase activity. They discovered that the response was caused by one protein that they termed the induction receptor. The Ah receptor was subsequently isolated from mouse liver by Bradfield, Glover, and Poland (1991) and the cDNA was characterized by Burbach, Poland, and Bradfield (1992). There have subsequently been AHR-related proteins found in *C. elegans* (Powell-Coffman et al., 1998), fruit flies (Duncan et al., 1998), and zebrafish (Tanguay et al., 1999) indicating that the receptor might have a conserved function. Currently no homologs of AHR are known to exist outside of the animal kingdom.

AHR has been grouped into the Per-Arnt-Sim (PAS) domain family of proteins due to shared structure in base domains. The other proteins in this family help to regulate circadian rhythms (period, Per)(Reddy et al., 1986) and multicellular development (single-minded, Sim)(Nambu et al., 1991). There are PAS proteins in bacteria; including one in *Sinorhizobium meliloti* that senses oxygen (FixL), and in fungi, including Wc-1 which coordinates the circadian blue-light responses of *Neurospora crassa* (Taylor & Zhulin, 1999). The complexity of cells

requires proteins that have the ability to sense the environment and then be able to regulate genes in order to produce a targeted response.

When unbound, the mammalian AHR is predicted to be located primarily in the cytosol bound to the Ah receptor-interacting protein (AIP, also known as ARA9 and XAP2) (Carver et al., 1998; Ma & Whitlock, 1997; Meyer et al., 1998; Meyer & Perdew, 1999) and a heat shock protein 90 (HSP90) dimer (Perdew, 1988) (Fig. 1.1). The HSP90 proteins are responsible for the stabilization of the AHR-AIP complex through a c-terminus that binds to AIP and a middle domain that binds AHR (Bell & Poland, 2000). Lipophilic ligands for the AHR like TCDD can pass through plasma membranes. Once a ligand binds to AHR, the HSP90 proteins dissociate, and their absence uncovers the nuclear localization signal (Ikuta et al., 1998). It is still unclear if the AIP molecule accompanies AHR into the nucleus, and it could be that the constituents of the nuclear complex might even vary among species. Once AHR is inside of the nucleus, it forms a heterodimer with the aryl hydrocarbon receptor nuclear translocator (ARNT) (Probst et al., 1993). When bound, the AHR-ARNT heterodimer can act as a transcription factor and bind to regions of DNA that contain the sequence 5'-GCGTG-3', termed dioxin response elements (DREs or XREs) (Denison et al., 1988). There are DREs present throughout the genome, and many influence the expression of genes encoding drug metabolizing enzymes that act to modify chemicals for increased excretion from the body. The classic battery of genes induced by AHR activation includes *cytochrome P450 family 1 subfamily a member 1 (Cyp1a1), cytochrome P450 family 1 subfamily a member 2 (Cyp1a2)* (Nukaya & Bradfield, 2009), *Cytochrome P450 Family 1 Subfamily B Member 1 (CYP1B1)* (Sutter et al., 1994), and *NAD(P)H: quinone oxidoreductase 1* (*Nqo1*) (Prochaska & Talalay, 1988). AHR also acts as a transcription factor for the expression of the *aryl hydrocarbon receptor repressor* (*Ahrr*) providing negative feedback for its own

activity (Mimura et al., 1999). Adaptive immunity B cells are proposed to have around seventy-eight genes that are direct AHR target genes (De Abrew et al., 2010). Interactions of the AHR with other receptors and signaling pathways could influence many more genes indirectly (Köhle & Bock, 2007).

Possible portion of AHR localizes to mitochondria

While the established path of AHR is from cytosol to nucleus, there is a possibility that unbound AHR could also be present within mitochondria. It is not a novel idea for a ligand-activated transcription factor to be in mitochondria. For example, the estrogen (Cammarata et al., 2004; S.-H. Yang et al., 2004), glucocorticoid (Psarra et al., 2005; Scheller et al., 2000), and thyroid hormone receptors (Hashizume & Ichikawa, 1982; Morrish et al., 2006) have all been found there.

The LaPres lab began to actively pursue the idea of AHR in mitochondria after it was found by tandem affinity purification that AHR interacts physically with ATP5α1, a component of ATP synthase that is located in the matrix, in a ligand-dependent manner (Tappenden et al., 2011). Cellular fractionation of mouse primary liver and cell cultures showed that AHR is present in mitochondrial fractions (Hwang et al., 2016; Tappenden et al., 2011). By progressively solubilizing the membranes of isolated mitochondria and exposing to a protease, Hwang et al. (2016) determined that the mitochondrial-AHR (mito-AHR) pool was located within the intermembrane space of the organelle. Through the use of mitochondrial targeting signal (MTS) prediction programs MitoProtII and MitoFates, it was determined that there is a predicted MTS in AHR, but this has not been decisively proven (Hwang, 2015). Currently, the role AHR could be playing in mitochondria is not known. If AHR does have a function in mitochondria it might be through the binding of an endogenous ligand, that environmental toxicants disrupt.

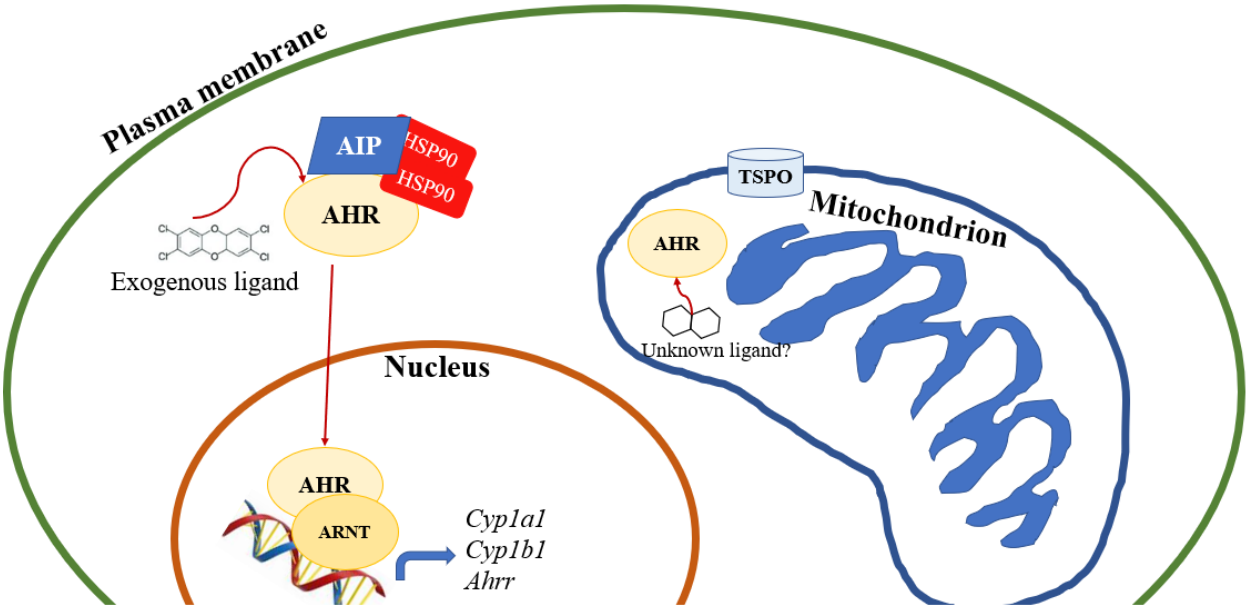

Figure 1.1 Canonical cytosol-to-nucleus AHR pathway and proposed mitochondrial localization. Traditional pathway describes ligands binding to the aryl hydrocarbon receptor (AHR), Ah receptor-interacting protein (AIP), and heat shock protein 90 (HSP90) dimer complex in the cytosol. Ligand binding causes the disassociation of the HSP90 dimer, the uncovering of the AHR nuclear translocation signal, and movement of AHR into the nucleus. AHR forms a heterodimer with the aryl hydrocarbon nuclear translocator (ARNT) and acts as a transcription factor at dioxin response elements (DREs). AHR-ARNT regulates the expression of a battery of genes including *Cyp1a1*, *Cyp1b1*, and *Ahrr*. Proposed mito-AHR shown in the intermembrane space of the mitochondrion with translocator protein (TSPO) in outer mitochondrial membrane.

Mitochondria

Mitochondria are highly dynamic organelles involved in cellular energy production, calcium homeostasis, and apoptotic signaling. They contain both an outer mitochondrial membrane (OMM) and inner mitochondrial membrane (IMM) (Sjostrand, 1953). The region between the two membranes is called the intermembrane space (IMS) and the region within the IMM is the matrix. The IMM is made up of many folded regions called cristae (Palade, 1952). While mitochondria cannot replicate autonomously, they can undergo fission and fusion processes to exchange molecules, meet regional needs of the cell, and maintain the health of mitochondria (Detmer & Chan, 2007). Mitochondria also contain their own circular genome

(Anderson et al., 1981; Nass & Nass, 1963), RNA polymerase (Ringel et al., 2011), and ribosomes (Sharma et al., 2003). Both human and mouse genomes contain thirteen protein encoding genes (Anderson et al., 1981; Bibb et al., 1981). These genes provide the sequences for proteins that make up complexes in the IMM called electron transport complexes. The other components of the complexes are encoded by nuclear genes. It is through the coordination of these complexes that mitochondria produce energy in the form of adenosine triphosphate (ATP). It is thought that the folded structure of the IMM allows for more surface area for the electron transport complexes. NADH dehydrogenase is designated as complex I. It oxidizes NADH, then passes electrons to reduce ubiquinone, and as a result pumps protons into the IMS from the matrix (Hatefi et al., 1962; Ohnishi et al., 2018). Complex II is called succinate dehydrogenase and it is unique in that it is also part of the citric acid cycle. It functions to oxidize succinate to fumarate and pass electrons to oxidized ubiquinone (Singer & Kearney, 1954; Yu & Yu, 1981). Complex II does not pump protons into the IMS. Complex III is known by numerous names including ubiquinol: cytochrome c oxidoreductase and cytochrome bc_1. It oxidizes ubiquinone, passes electrons to oxidized cytochrome c, which allows for the movement of protons into the IMS (Hatefi et al., 1962; Xia et al., 2013). The name of complex IV is cytochrome c oxidase and it removes electrons from a reduced cytochrome c to reduce O_2 and pump electrons into the IMS (Ferguson-Miller & Babcock, 1996; Yoshikawa et al., 1998). The result of pumping the protons into the IMS is an electrochemical gradient across the IMM. ATP synthase (complex V) is the protein complex that couples the movement of protons down the gradient from the IMS into the matrix to ATP production (Racker, 1964). Mitochondria use about 72% of cellular oxygen for the direct production of ATP (Rolfe & Brown, 1997) and this provides the majority of energy for the cell.

TCDD effect on mitochondrial efficiency

It is crucial that the mitochondrial membrane potential is maintained in order to continue to produce enough ATP. The LaPres lab has collected evidence that TCDD has the ability to alter the charge gradient within mitochondria. Using flow cytometry, it was demonstrated that TCDD exposure for 6 hours causes the hyperpolarization of the mitochondrial membrane potential in AHR+/+ mouse B cell line (CH12.LX) (Tappenden et al., 2011). This hyperpolarization occurs even with cotreatment of mitomycin c, which is a global transcription inhibitor, indicating that this effect is not mediated through AHR acting as a transcription factor (Tappenden et al., 2011). To determine if AHR was required for this change in membrane potential, an AHR-/- B cell line (BCL1) was treated with TCDD but there was no change in membrane potential from control (Tappenden et al., 2011). This showed that AHR is required for TCDD to alter the distribution of protons across the IMM. This increased membrane potential, however, did not translated into increased ATP production as ATP concentrations were the same in control and TCDD cells (Tappenden et al., 2011). This means that the increased number of protons in the IMS are not being used by ATP synthase to produce proportionally more ATP. TCDD exposure can also decrease maximum cellular respiration in an AHR-dependent manner (Park et al., 2013; Hwang et al., 2016). TCDD decreases mitochondrial efficiency to produce energy in a yet undetermined manner.

Ligands of AHR

While AHR can bind many environmental pollutants, the core structures of its ligands can be described as either polycyclic aromatic hydrocarbons (PAHs) or halogenated aromatic hydrocarbons (HAHs) (Poland & Knutson, 1982). These chemicals are almost exclusively produced accidentally during industrials combustion processes, but some can be produced by

high heat natural events like volcanic eruptions or fires (Karp et al., 2018). Many of the accidental contaminations involve chlorinated phenols that are used for production of herbicides and pesticides that are spread widely in the environment. These chemicals are persistent because they are resistant to degradation; very few bacteria can break them down, and the lipophilic nature makes them accumulate in the fat tissue of animals. TCDD, which is a HAH, is the most studied exogenous ligand of AHR. Food consumption is the main source of human exposure, and TCDD can be retained in the human body for extended periods of time with an estimated half-life of 7.1 years (Pirkle et al., 1989; Warner et al., 2014). As seen with the exposed industrial workers, a hallmark symptom of TCDD exposure in humans is chloracne which is the development of cysts and lesions due to increased keratinization of the skin (Caramaschi et al., 1981; Passarini et al., 2010). TCDD exposure has also been linked to immunosuppression (Baccarelli et al., 2002; Dornbos et al., 2016), metabolic syndrome(Uemura et al., 2009; Warner et al., 2013), and tumor promotion (Hooiveld et al., 1998; Pesatori et al., 2009). The International Agency for Research on Cancer (IARC) has classified TCDD as a human carcinogen since 1997. Mouse studies indicate that TCDD exposure can cause hepatic toxicity progressing to hepatic fibrosis (Nault et al., 2016; Pierre et al., 2014).

Exposure of AHR-null mice to TCDD does not result in the classic exposure symptoms (Fernandez-Salguero et al., 1996). This could imply that TCDD binding to AHR induces the expression of a gene that either metabolizes TCDD into a toxic form or induces/suppresses a developmental gene anachronistically. Chloracne commonly forms after human exposure, but it is rarely seen in animals (only occurring at high doses in the ears of rabbits and on hairless mice) (Greene et al., 2003). This gives more evidence that AHR-induced toxicity is a complicated process, involving multiple elements.

AHR has the ability to bind a variety of PAHs. 3-methylcholanthrene (3-MC) (Kouri et al., 1973; Poland & Glover, 1974) and benzo[a]pyrene (Vaziri & Faller, 1997) are two known exogenous ligands for AHR (Fig.1.3). Both chemicals are thought to be mutagenic, with 3-MC having the ability to cause mutations in rat lung (Maddox et al., 2008) and liver (Rihn et al., 2000) along with benzo[a]pyrene being able to form DNA adducts in mice (Mass et al., 1993; Zuo et al., 2014). The number of DNA adducts decreases in AHR null mice compared to controls after PAH exposure indicating that AHR binding plays a role in these chemicals altering DNA (Kondraganti et al., 2003).

While AHR is known primarily as a receptor that mediates responses to pollutants, environmental sensing might not be its endogenous role. It is possible that the pollutant ligands are just similar enough in structure to endogenous ligands to cause inappropriate activation of the AHR. Genetic loss of the AHR homolog in *C. elegans* causes alterations in neuronal development in the absence of exogenous ligand (Qin & Powell-Coffman, 2004). When the *spineless* gene (the AHR homolog in *Drosophila)* is deleted, the flies exhibit changes in leg and antenna morphology (Duncan et al., 1998). *Ahr-/-* mice have smaller livers and elevation of fatty deposits during some stages of early development (P. Fernandez-Salguero et al., 1995; Schmidt et al., 1996). It is interesting to note that the Warner et al. (2013) study only detected metabolic syndrome associated with TCDD exposure from the Seveso, Italy accident in the group of women who had been less than 12 years of age at the time of the exposure. This suggests that there might be endogenous substances acting through AHR to mediate certain developmental stages. Several groups of endogenous ligands have been proposed to bind to the AHR including heme metabolites, cholesterol-like molecules, and tryptophan metabolites (Fig 1.3).

Heme is an iron-containing tetrapyrrole that is used as a building block for multiple

molecules including hemoglobin, which is used to carry oxygen in the blood. Bilirubin and biliverdin are heme degradation products that induce AHR-dependent transcription and activity of CYP1A1 (Phelan et al., 1998; Sinal & Bend, 1997). AHR could be a sensor for red blood cell degradation or even liver health as that is the organ in which bilirubin is conjugated for excretion from the body.

Cholesterol is an essential molecule for humans to maintain cell membrane flexibility, make steroid hormones, and produce bile for fat absorption. TCDD decreases the expression of enzymes critical to cholesterol biosynthesis (Dornbos et al., 2019). TCDD exposure can also alter cholesterol levels in mouse serum (Angrish et al., 2013; Dornbos et al., 2019). The mechanism of action of this is still unknown, but 7-ketocholesterol can displace TCDD from AHR (Savouret et al., 2001). 7-ketocholestorel is a cytotoxic compound that can form when reactive oxygen species attack cholesterol. 7-ketocholesterol is thought to be involved in upregulating inflammatory pathways and elevation of disease states like atherosclerosis (Brown et al., 1997; Tani et al., 2018). AHR might play a role in the inflammation progression with 7-ketocholestorol-induced transcription.

AHR is predicted to bind dietary components, including tryptophan metabolites, which could be a means to sense microbiome changes. Tryptophan can be broken down into multiple intermediates including kynurenine and quinolinic acid (Fig. 1.2) (Heidelberger et al., 1949; Henderson et al., 1949). Quinolinic acid can be toxic or can be converted to nicotinamide adenine dinucleotide (NAD) (El-Deprawy et al., 1985; Henderson et al., 1949). Being able to react to the levels of tryptophan intermediates might be a way to protect from the buildup of toxic molecules or provide more energy producing components. There is evidence that kynurenine can activate AHR as demonstrated by AHR translocation to the nucleus and

induction of *Cyp1a1* and *Cyp1b1* after kynurenine exposure (Mezrich et al., 2010; Opitz et al., 2011). Kynurenine-AHR signaling has been suspected in immune responses including immune escape of tumors (Campesato et al., 2020; Y. Liu et al., 2017). The kynurenine-AHR pathway is thought to promote this escape by the generation of regulatory T cells (Tregs) which act to dampen the immune response (Campesato et al., 2020; Mezrich et al., 2010). It is still unknown why kynurenine would be an endogenous ligand for AHR, but it is at a branch point in tryptophan metabolism, where either kynurenic acid or 3-hydrozykynurenine (the precursor to quinolinic acid) could be produced (Fig. 1.2) (Titcomb & Tanumihardjo, 2019). AHR could be acting to sense either metabolic health of the cell or acting to influence immune response.

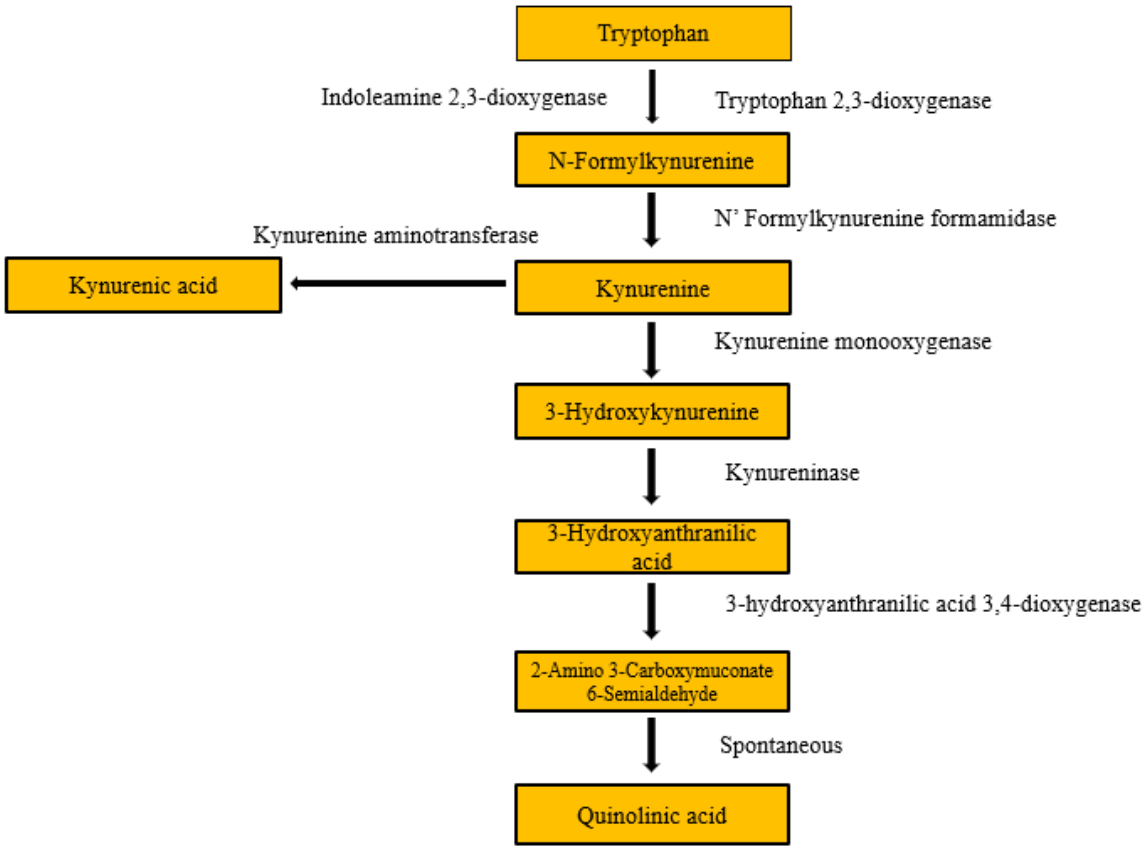

Figure 1.2 Kynurenine pathway

When the proposed ligands for the AHR are examined as a group, they share a large overlap of ligands for the translocator protein (TSPO). TSPO is known to be located in the outer mitochondrial membrane, so if the predicted intermembrane space localization of AHR is correct, it is possible that these two proteins might interact or share crosstalk in overlapping pathways.

TSPO as a conserved environmental sensor

TSPO was discovered when kidney, liver, and lung tissues were used as negative controls for diazepam binding in brain tissue experiments. Surprisingly, binding was still detected in all the negative controls (Braestrup & Squirest, 1977). Unlike the brain, however, the binding did not occur in the plasma membrane fraction but instead in the mitochondrial fraction (Braestrup & Squirest, 1977). Originally, the protein was called the peripheral-type benzodiazepine receptor (PBR) but the name of TSPO was suggested by Papadopoulos et al. (2006). This name would be a better fit because of the presence of the protein in organisms without a nervous system. TSPO homologs can be found in a wide range of organisms from bacteria (Yeliseev & Kaplan, 1995) to plants (Lindemann et al., 2004). The bacterial tryptophan-rich sensory protein (TspO) is localized to the outer membrane of the cell (Yeliseev & Kaplan, 1995) and mammalian TSPO is found predominantly in the outer membrane of mitochondria (Bernassau et al., 1993). There is evidence that the bacterial homolog in *Rhodobacter sphaeroides* can influence gene expression based on light and oxygen levels (Yeliseev & Kaplan, 1995). This could give some explanation as to why TSPO is located in the OMM if it was retained from bacterial endosymbiosis. TSPO has also been found in the plasma membranes of certain types of mammalian cells (Oke et al., 1992). TSPO has been proposed to be involved in many different pathways including apoptosis (Cui et al., 2021; Zeno et al., 2009) and redox homeostasis (Carayon et al., 1996; Guilarte et al.,

2016). TSPO appears to have multiple functions even between cell types.

TSPO contains five transmembrane α-helixes that extend through the OMM (Bernassau et al., 1993). TSPO precipitates with another OMM protein called the voltage-dependent anion channel (VDAC) suggesting that these two proteins might function as a complex (McEnery et al., 1992). Exposure to environmental stresses can cause the oligomerization of VDAC monomers into functional pores in the OMM (Keinan et al., 2010). It is predicted that calcium (Gincel et al., 2001), ATP (Rostovtseva & Colombini, 1996), cytochrome c (Shimizu et al., 1999), and even mitochondrial DNA (mitoDNA) (Keinan et al., 2010) can move through the OMM via this pore. The interaction of TSPO with VDAC leads to the hypothesis that TSPO might also play a role in controlling the movement of many elements into and out of mitochondria. The release of some of these substances like cytochrome c and mitoDNA results in apoptotic signaling for the cell.

Ligands of TSPO

Like the AHR, TSPO can bind a wide range of aromatic molecules. TSPO binds to manufactured benzodiazepines such as Ro5-4864 (7-chloro-5-(4-clorophenyl)-1-methyl-3H-1,4-benzodiazepin-2-one) (Schoemaker et al., 1981) and isoquinolines such as PK 11195 (1-(2-chlorophenyl)-N-methyl-N-(1-methyl-propyl)-3-isoquinoline carboxamide) (Fig 1.3) (Le Fur et al., 1983; Parola et al., 1991). Ro5-4864 has little ability to bind to neurons, (which express very little TSPO), but does bind to TSPO-containing glial cells indicating that TSPO does have a different selectivity from other benzodiazepine receptors in the brain (Gallager et al., 1981). Due to the increased infiltration of microglial cells into the brain during times of neural inflammation, PK 11195, via its ability to bind TSPO with high affinity, has been utilized in positron emission tomography (PET) for studying disease progression (Chen & Guilarte, 2008). The fact that

TSPO or TSPO-like proteins are found in such a variety of species suggests that it is likely that there are multiple endogenous ligands. Heme, cholesterol, and kynurenine, like AHR, have also been proposed to bind to TSPO.

Heme synthesis involves a pathway that occurs partially in mitochondria and partially in the cytosol, a process that requires transport of the intermediates. TSPO has been shown to bind porphyrins (Verma et al., 1987) and could play a role in that process by facilitating the passing of coproporphyrinogen back into mitochondria (Taketani et al., 1995). Examining TSPO-/- mice, Zhao et al. (2016) found that heme levels were not altered in the liver and spleen, but it was significantly higher in the bone marrow compared to controls. This indicates that TSPO might not be essential for heme synthesis but could have some influence in a cell-type specific manner.

TSPO is observed in many cell types but one type in which it is highly expressed is steroidogenic cells including those in the adrenal glands, pituitary glands, and testis (De Souza et al., 1985). TSPO has a cholesterol recognition amino acid consensus (CRAC) domain at the c-terminus of the protein that is essential for its binding to cholesterol (Li & Papadopoulos, 1998; Jamin et al., 2005). There is debate about whether TSPO is essential for the synthesis of steroids as the original hypothesis that it was required for transporting cholesterol into mitochondria (the rate limiting step) has been contradicted. It has been shown that knocking out TSPO does not affect the production of certain steroids like testosterone (Morohaku et al., 2014) and corticosterone (Fan et al., 2020; Tu et al., 2014). It is also intriguing that microglia, which contain high concentrations of TSPO, are known not to produce as many neurosteriods as astrocytes, which contain less TSPO (Germelli et al., 2021). Not all cells containing TSPO have the ability to synthesize steroids from cholesterol, leaving the possibility that TSPO might be involved in another pathway involving cholesterol.

If TSPO is similar to AHR in that it can respond to multiple endogenous aromatics, it might also bind dietary metabolites including those in the kynurenine pathway. Currently, there is no published data to indicate that tryptophan metabolites bind to TSPO, so these are ligands that needs to be investigated with TSPO.

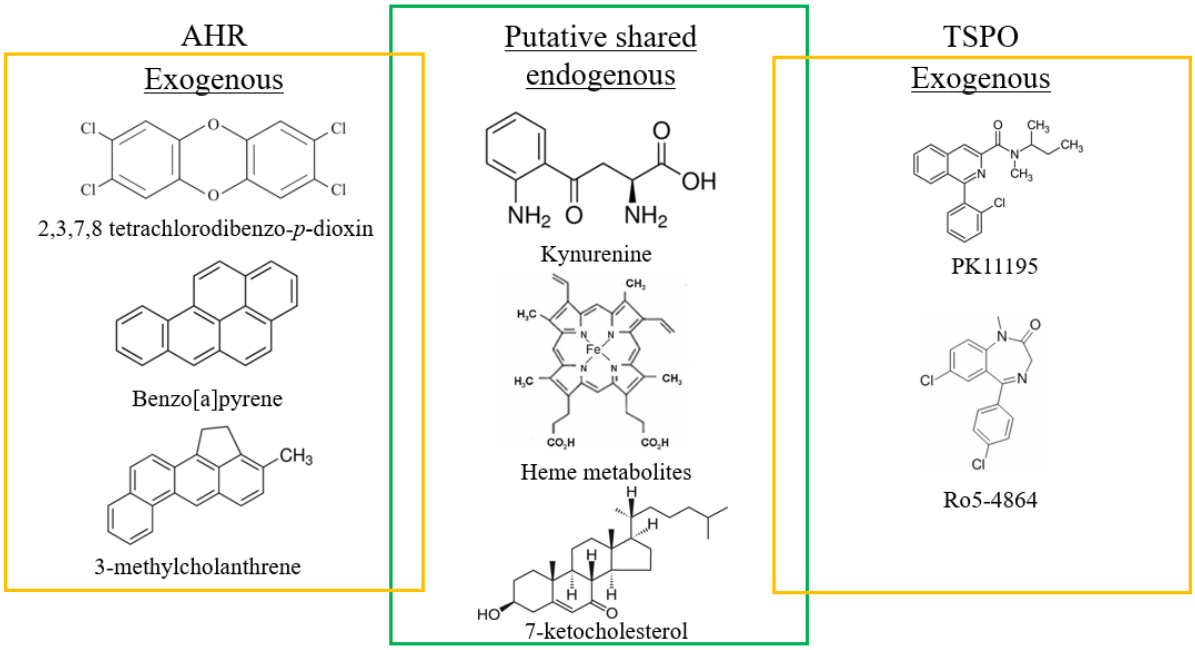

Figure 1.3 Putative ligands of AHR and TSPO

AHR and TSPO function as environmental sensors to help the cell maintain homeostatic levels, and both may influence cellular health. This leads to the possibility that they may also play a role in diseases in which environmental stress plays a role, such as Parkinson's disease.

Parkinson's disease

The symptoms of Parkinson's disease have long been observed in the human population, but physician Dr. James Parkinson was the first to describe them as one disease in 1817. Dr. Parkinson used observations of his patients along with strangers he just saw on the street to describe a disease that was very slow to develop, so slow that many people did not take real notice of the first signs. Dr. Parkinson included descriptions that involved shaking limbs,

severely bowed bodies, and difficulty walking (Parkinson, 2002). Since most of the evidence Dr. Parkinson had was just behavioral observations, he had little evidence for a biological cause of the disease. He postulated that the disease could originate in the spinal cord and progress to the brain or be related to rheumatoid arthritis which some of the patients also had. Today Parkinson's disease is the second most common neurodegenerative disease worldwide, and while progress has been made on describing the disease, the initiating cause is still unknown.

Arvid Carlsson's discovery in 1957 that dopamine was a major factor in movement was a major step forward in understanding Parkinson's (Carlsson et al., 1957). In 1960, Herbert Ehringer and Oleh Hornykiewicz would go on to find that dopamine levels were decreased in the postmortem brains of people with Parkinson's (Hornykiewicz, 2002). Parkinson's disease symptoms progress as nigrostriatal dopamine neurons, that project into the striatum, are lost (Bernheimer et al., 1973). A classic feature in the brains of Parkinson's patients is the accumulation of Lewy bodies in surviving dopamine neurons (Förstl & Levy, 1991). Lewy bodies are cytosolic structures that contain α-synuclein, ubiquitin, and neurofilaments (Pollanen et al., 1993). It is unclear if Lewy bodies contribute to disease progression or if they are protective for neurons.

Another major step in understanding Parkinson's disease development was made following the result of terrible accidents. In the early 80s, young adults began being admitted to hospitals with symptoms very similar to Parkinson's that had manifested very rapidly (Langston et al., 1983). The one thing that linked all of them together was that they all had recently used a new synthetic heroin (Langston, 2017). Testing revealed that the heroin had been contaminated with 1-methyl-4-phenyl-1,2,3,6- tetrahydropyridine (MPTP) by improper illegal production (Langston et al., 1983). One victim showed neuron degradation in the substantia nigra, similar to

Parkinson's (Langston et al., 1983). MPTP is not toxic until it is converted to 1-methyl-4-phenylpyridinium (MPP^+) by monoamine oxidase (Chiba et al., 1984), and then MPP^+ can be selectively up taken by dopaminergic neurons (Shen et al., 1985). It is further concentrated in mitochondria and inhibits the activity of complex I of the electron transport system (Ramsay et al., 1986, 1987). It is predicted that this inhibition decreases ATP production and increases ROS production eventually causing the death of the neurons. Through the study of MPTP, scientists were able to link mitochondrial function to Parkinson's disease. While most Parkinson's causes do not appear to be genetic, there are several gene mutations that have been linked to the disease including mutations in *Leucine-rich Repeat Kinase 2 (LRRK2).*

Leucine-rich repeat kinase 2 (LRRK2) involved in Parkinson's disease

Mutations in *LRRK2* are the most common causes of familiar Parkinson's disease. Alternatively called *PARK8, LRRK2* was first linked to familial parkinsonism by Funayama et al. (2002) through the study of genetic samples collected from a Japanese family. The linkage was further supported by Zimprich et al. (2004) using a total of twenty-one families. There is emerging evidence that even in sporadic causes having the mutation can increase the risk of developing the disease.

LRRK2 is a large protein consisting of 2,527 amino acids and seven predicted domains. It is multifunctional with a kinase domain, a GTPase domain, and several protein interaction regions (Fig. 1.4) (Mills et al., 2012). The G2019S mutation, which is a gain of kinase function, was found by Healy et al. (2008) to be present in 4% of familial PD cases and 1% of sporadic PD cases worldwide. Penetrance for G2019S in all population has been estimated to be 42.5% (95% confidence interval [CI]: 26.3%-65.8%) to age 80 (Lee et al., 2017). The low penetrance of the mutation suggests that environmental factors might also influence disease development.

Knocking the G2019S LRRK2 mutation into mice results in a larger degeneration of dopamine neurons after MPTP treatment (Novello et al., 2022). LRRK2 might not be the initiating factor for Parkinson's but its overactivity might decrease the cell's ability to deal with damage. Knocking out *Lrrk2* in mice protects against the loss of dopaminergic neurons due to bacterial mimic lipopolysaccharide (LPS) exposure (Daher et al., 2014), indicating that microglia and the immune response might come into play in the LRRK2-Parkinson's connection. LRRK2 has the ability to phosphorylate itself, and autophosphorylation is increased in G2019S mutants (West et al., 2005). So G2019S could also counterintuitively be a loss of function if phosphorylation decreases another activity of LRRK2.

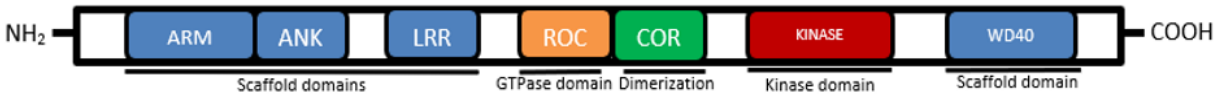

Figure 1.4 Structural domains of LRRK2. LRRK2 is a 286-kDa protein comprises multiple functional units including Armadillo (ARM), Ankyrin (ANK), leucine-rich repeat (LRR), Ras of complex proteins (ROC), C-terminal of Roc (COR), Kinase, and WD40. Image adapted from (Guaitoli et al., 2016).

The multiple domains of LRRK2 has led to numerous functions being postulated for the protein including the ability to phosphorylate Ras-related proteins including Rab8 and Rab10 (Ito et al., 2016; Steger et al., 2016), regulate calcium homeostasis (Cherra et al., 2013), and vesicle trafficking (Schreij et al., 2015). LRRK2 involvement with vesicles could range from synaptic transmission to surfactant secretion. Mouse *Lrrk2* knockouts have an increased abundance of lysosomal proteins in kidney cells (Fernandez-Salguero et al., 1996). LRRK2 is associated with the outer membrane of mitochondria but is not present inside of the organelle (West et al., 2005). LRRK2 is also associated with the Golgi network (Hatano et al., 2007). It is thought that LRRK2 might act in membrane remodeling through kinase activity and has been connected to mitophagy (Bonello et al., 2019). The multiple applications of LRRK2 implies that the protein is not just

active in brain cells.

LRRK2 outside of the central nervous system

LRRK2 kinase inhibitors are a class of drugs that many researchers hope can be used to slow the progression of Parkinson's disease due to many of the LRRK2 mutations being a gain of kinase function (Fuji et al., 2015). In early animal studies, however, abnormal phenotypes were observed. When primates were treated with LRRK2 kinase inhibitors, they developed enlarged lamellar bodies in alveolar type II cells (Fuji et al., 2015), a phenotype that was replicated in mouse *Lrrk2* knockouts (Herzig et al., 2011). The lamellar body formation was reversible after stopping the administration of the inhibitors in the primates, and it did not seem to result in any toxicity. Lamellar bodies are lysosomal-like structures that are made up of multiple membranes. In alveolar type II cells, they hold surfactant and transport it out to the plasma membrane to be released. This inhibitor effect showed that LRRK2 function was also involved in lung function. Normalized human mRNA expression data showed that *LRRK2* expression is higher in lung than in any brain region (Verma et al., 2021). LRRK2 also appears to influence immune responses in and outside of the brain. Decreases in LRRK2 make lung cells more susceptible to bleomycin-induced fibrosis as Tian et al., 2021, found that LRRK2-deficient mice had lower survival rate, increased macrophage lung infiltration, and increased collagen deposition. It is unknown if LRRK2 has different functions in each cell type or why it is more highly expressed in some cells than others.

Chemical exposure and Parkinson's

Since only about 10% of Parkinson's cases can directly be linked to a genetic cause, there must be environmental agents that cause the neurons to start to decline. While linkage is still controversial, many herbicides have been associated with Parkinson's in humans including

paraquat (Weed, 2021) and Agent Orange (2,4-D and 2,4,5-T but often contaminated with TCDD) (de la Monte & Goel, 2022). Rotenone, a pesticide, has been shown to cause Parkinson's like endpoints in animal studies (Betarbet et al., 2000; Johnson et al., 2018). Currently, there have been no definitive studies linking Parkinson's to Agent Orange exposure, but the U.S. Department of Veterans Affairs has decided that all veterans are eligible to receive compensation for Parkinson's symptoms because they list it as an "illness caused by Agent Orange exposure." There is evidence though that 2,4,5-T use in American applicators does increase risk for Parkinson's (Shrestha et al., 2020).

Paraquat has a very similar structure to MPP^+ (Fig. 1.5), a known complex I inhibitor, providing a base structure that might be close to a natural chemical that could interact with the electron transport system. Rotenone is also an inhibitor of complex I (Krueger et al., 1990).

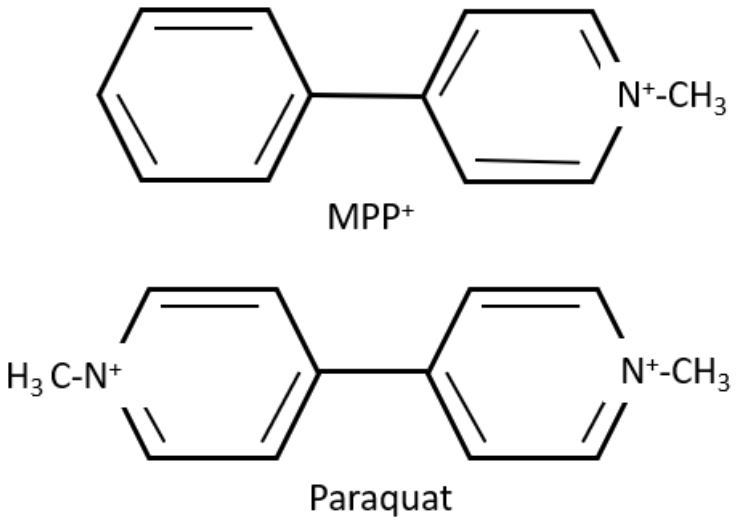

Figure 1.5 Structure of MPP^+ and paraquat

TCDD-contaminated chemicals being suspected environmental causes of Parkinson's is interesting because with many of the other chemicals being complex I inhibitors, it could be possible that TCDD could also hinder mitochondrial function in some way. AHR having similar

ligands to mitochondrial TSPO means TSPO could also be involved in mitochondrial health and disease states. Understanding the endogenous activity of AHR and TSPO might provide clues as to what goes wrong when the cell encounters too much of an exogenous chemical.

Overall research aim:

AHR and TSPO are two proteins that have been predicted to influence many pathways within cells, but a true endogenous function has not been established for either. The overlap of putative ligands and the prediction that some AHR might also be found in mitochondria led to the hypothesis that these proteins might have the ability to influence the expression or function of the other. This "crosstalk" could either be direct protein-to-protein interaction or indirect through transcriptional modulation or signaling pathways. This AHR-TSPO interaction could influence mitochondrial homeostasis and function. The majority of research described in this dissertation employed the use of CRISPR-generated AHR and TSPO knockout mouse cell lines to study the activity of each through loss of it. The goal of this research was to determine if AHR could be present in the intermembrane space mitochondria, if AHR and TSPO could impact similar genes or activity of the other, and how the activity of these two genes might affect the progression of neurodegenerative diseases. A majority of chapter 4 will analyze the influence of AHR and TSPO on LRRK2, a gene known to be mutated in some cases of Parkinson's disease. Understanding the crosstalk between these two environmental sensors might help to unravel how environmental toxicants could enhance degenerative disease development and progression.

Hypothesis: The aryl hydrocarbon receptor and translocator protein exhibit crosstalk that coordinates cellular homeostasis, that when disrupted can alter mitochondrial function.

Specific Aim 1: Determine the localization and influence of AHR in mitochondria

Transmission electron microcopy of untreated wild-type Hepa1c1c7 cells was used to try

to accurately determine in what region of the mitochondrion AHR could be located. The location of mito-AHR is important because it would provide assistance in determining with what proteins/components of the mitochondria it could be interacting. Electron transport complex assays were conducted on isolated mitochondria from AHR-sufficient (1C1C7) and AHR-deficient (C12) mouse liver cell lines to assess if the level of AHR in a cell had any influence over complex activity. This would help to determine how mito-AHR could impact the functioning of mitochondria.

Specific Aim 2: Characterize possible crosstalk between AHR and TSPO

CRISPR technology was used to create AHR and TSPO knockout mouse cell lines. RNA-sequencing and qRTPCR were used to compare the knockouts to wild-type cells to determine differentially expressed genes that could indicate interaction between the proteins. Genes that were altered between AHR-/- and wild-type and TSPO-/- and wild-type were analyzed for overlap. AHR ligand TCDD and TSPO ligand PK 11195 were used to analyze how the activity of one protein might affect the other.

Specific Aim 3: Investigate the influence of TSPO and AHR on factors involved in the development of neurodegenerative diseases, specifically LRRK2 and downstream effects

BV-2 and MLE-12 cells were used to analyze the RNA and protein levels of LRRK2 after CRISPR knockout of AHR and TSPO. Consequences of loss of LRRK2 were examined including lamellar bodies in MLE-12 cells and paraquat-induced toxicity. These studies could provide clues as to what influence AHR and TSPO have over LRRK2 and how that could be linked to the progression of Parkinson's.

CHAPTER 2: LOCALIZATION AND FUNCTION OF MITOCHONDRIAL AHR

This chapter contains a portion of a previously published data article in Data in Brief, Volume 8, pages 93-97 entitled "Data of enzymatic activities of the electron transport chain and ATP synthase complexes in mouse hepatoma cells following exposure to 2,3,7,8-tetrachlorodibenzo-p-dioxin (TCDD)."

Authors: Hye Jin Hwang[ab], Michelle Steidemann[cd], Taylor K. Dunivin[e], Mike Rizzo[cf], John J. LaPres[abc]

Affiliations: [a] Department of Biochemistry and Molecular Biology, Michigan State University, East Lansing, MI 48824, [b] Center for Mitochondrial Sciences and Medicine, Michigan State University, East Lansing, MI 48824, [c] Institute for Integrative Toxicology, Michigan State University, East Lansing, MI 48824, [d] Department of Pharmacology and Toxicology, Michigan State University, East Lansing, MI 48824, [e] Department of Microbiology and Molecular Genetics, Michigan State University, East Lansing, MI 48824, [f] Cell and Molecular Biology Graduate Program, Michigan State University, East Lansing, MI 48824.

Abstract

Traditionally, the aryl hydrocarbon receptor (AHR), is considered a cytosol-to-nucleus, ligand-activated, transcription factor. Previous research in the LaPres lab, however, indicates that a portion of the cellular pool of AHR might be located within mitochondria in the absence of ligand (Hwang et al., 2016; Tappenden et al., 2011). This evidence was based on fractionation studies which did not provide an actual image of AHR within intact mitochondria. In an attempt to visualize in what specific region of mitochondria AHR can be located, Hepa1c1c7 wild-type cells were fixed and stained with AHR primary antibody for transmission electron microscopy (TEM) analysis. TEM has the ability to provide high magnification images and is the gold standard in subcellular protein detection. Secondly, Tappenden et al. (2011) demonstrated that AHR could influence the efficiency of mitochondria, so the activity of the individual electron transport complexes was analyzed from cells that were deficient in AHR after TCDD treatment to determine how the AHR could affect the efficiency of cellular respiration. This chapter did not achieve all of its goals as the TEM images collected did not have fine enough resolution to

designate membrane structures, but AHR staining was observed in mitochondria. These results show that some portion of AHR can be found internally in mitochondria, but adjustments will have to be made to the collection and fixation of the cells to get nicely preserved native structure images. The electron transport complex activity assays showed no differences between AHR-sufficient and deficient cells after TCDD treatment. These assays were conducted using isolated mitochondria in artificial extracellular environments so this suggests that AHR might be affecting mitochondrial function based on interaction with the cytosol. This chapter places AHR inside of the mitochondria but it raises the question of with what AHR could be interacting in the mitochondria.

Results

Transmission electron microscopy of immunogold-labeled AHR in mitochondria of Hepa1c1c7 cells

In the attempt to get visual representation of a portion of AHR being located within mitochondria and specifically what compartment, wild-type untreated Hepa1c1c7 were fixed, embedded, stained with primary antibody for AHR, and then stained with gold-conjugated secondary. Lack of proper collection and fixation technique prevented the production of images with fine resolution of mitochondria ultrastructure. The double membranes of mitochondria could only be clearly distinguished in a few organelles, so it was hard to assign internal compartment regions. Of the few mitochondria that could be identified, several did contain gold secondary antibodies (Fig 2.1B-D). The average number of gold antibodies observed within one mitochondrion was approximately one to four. The antibodies often appeared to be in close proximity to an inner mitochondrial membrane. Negative controls, (not stained with primary antibody but with secondary), showed almost no nonspecific gold-secondary staining (Fig 2.1A).

One additional independent experiment was conducted with isolated mitochondria with similar results (Fig 2.2).

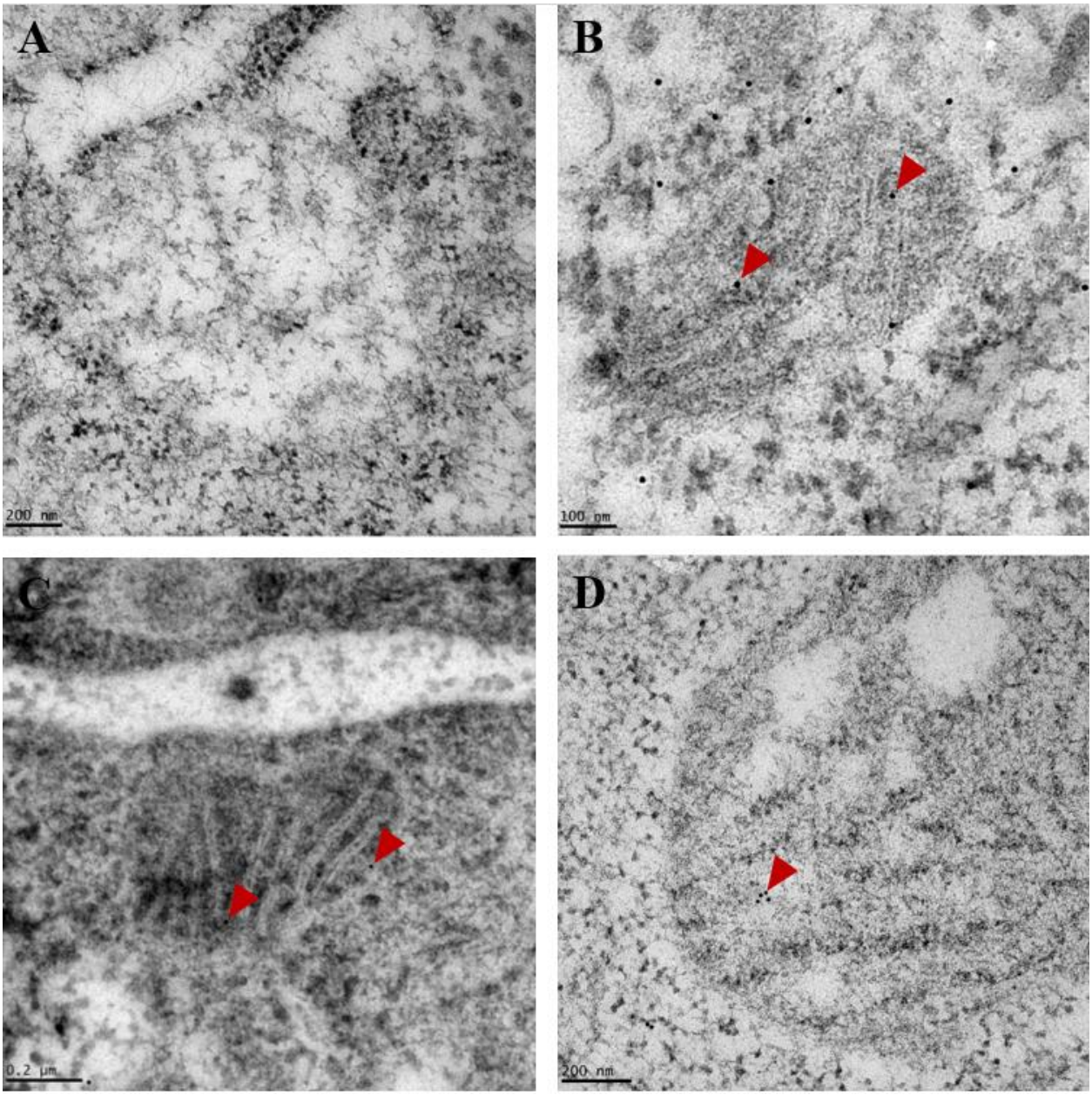

Figure 2.1 TEM images exhibiting a portion of AHR located within mitochondria. Exponentially growing wild-type Hepa1c1c7 cells were fixed in 4% paraformaldehyde and 1% glutaraldehyde. Samples were processed for transmission electron microscopy by The Center for Advanced Microscopy at MSU. Negative control lacking primary antibody (**A**). Grids incubated with rabbit polyclonal anti-AHR primary and 10 nM gold-conjugated anti-rabbit secondary (**B-D**). Red arrow indicates gold particle. Magnification A-B=40,000X, C =27,000X. D=50,000X. Scale bars A, C, D=200 nm. B=100 nm. Representative images from two independent experiments.

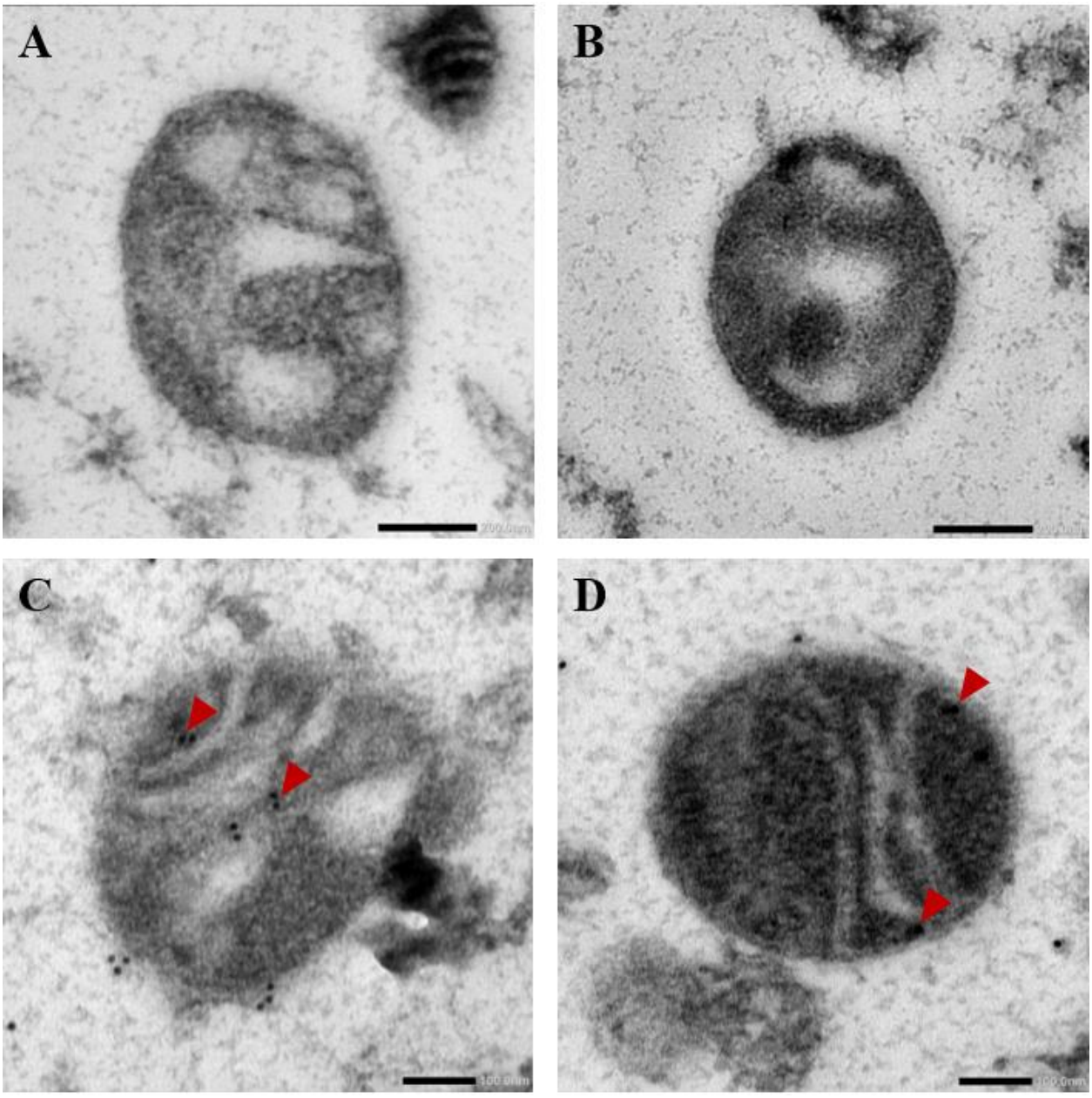

Figure 2.2 TEM images exhibiting a portion of AHR located within isolated mitochondria. Exponentially growing wild-type Hepa1c1c7 cells were collected and mitochondria isolated by differential centrifugation. Mitochondrial pellets were fixed in 4% paraformaldehyde and 1% glutaraldehyde. Samples were processed for transmission electron microscopy by The Center for Advanced Microscopy at MSU. Mitochondria negative controls lacking primary antibody (**A-B**). Mitochondria incubated with rabbit polyclonal anti-AHR primary and 10 nM gold-conjugated anti-rabbit secondary (**C-D**). Red arrow indicates gold particle. Magnification A-B=30,000X, C-D=50,000X. Scale bars A-B=200 nm. C-D=100 nm. Representative images from one independent experiment.

Enzymatic activities of electron transport complexes after TCDD treatment

With increased evidence for AHR in the mitochondria it was tested to see what effect AHR could have on the electron transport system activity. Isolated mitochondria from AHR-deficient mouse liver cell line (C12) were compared to mitochondria from AHR-sufficient mouse liver cell line (1C1C7, Hepa1c1c7) after TCDD treatment (30 nM) for 6 or 24 hours (Fig 2.3). Individual complex assays were conducted and normalized to citrate synthase activity which was the control for sample mitochondria integrity. The activity was then described as a fold change to the respective time and cell line DMSO control. The decrease of cellular AHR in C12 cells did not cause any significant changes in the activity in any of the complex assays compared to the 1C1C7 cells. In the complex I assay, the c12 cells had a 1.63-fold increase in activity over DMSO control at 6 hours after TCDD treatment while the 1C1C7 cells had a 1.20 decrease from DMSO control, but this was not significant (Fig. 2.3a). These fold changes remained similar at 24 hours with c12 having a 1.50-fold increase and 1C1C7 having a 1.14-fold decrease. At 6 hours post TCDD treatment, both cell types had a decrease in complex V activity (1C1C7 -1.29-fold, C12 -1.71-fold) but at 24 hours there was very little change in activity for either cell type (1C1C7 1.20-fold, C12 -1.02-fold) (Fig. 2.3f).

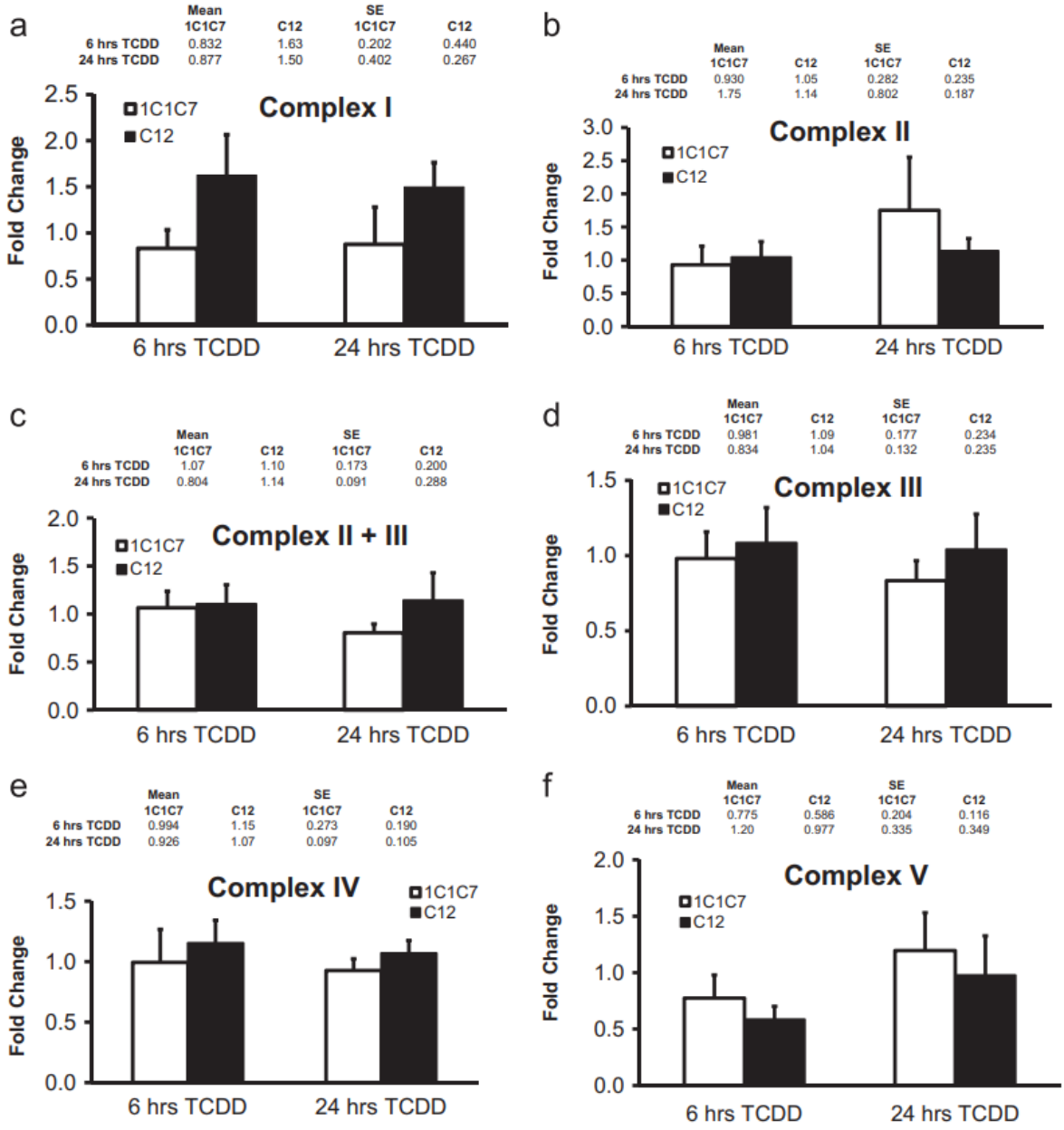

Figure 2.3 AHR deficiency does not alter electron transport complex activity after TCDD treatment. The activities of the ETC complexes were measured with isolated mitochondria from 1C1C7 and C12 cells exposed to TCDD (30 nM) or vehicle control DMSO (0.01%) for 6 and 24 hrs. The activity of each complex: Complex I (**a**), Complex II (**b**), Complex II+III (**c**), Complex III (**d**), Complex IV (**e**), and Complex V (**f**), was normalized against the activity of citrate synthase. The fold change was calculated by re-normalization of enzyme activity from cells exposed to time-matched vehicle control. Error bars represent standard error. Represents four independent experiments.

Discussion

Protease protection with digitonin extraction of mitochondria had previously shown that AHR could be located in the intermembrane space of mitochondria (Hwang et al., 2016). Transmission electron microscopy was chosen to provide evidence that AHR could be located within the IMS. Hepa1c1c7 cells were chosen as the specimens for the microscopic analysis because they express a large amount of AHR. TEM imaging of proteins in specific organelles is very challenging, requiring a balance between the level of fixing and epitope availability. Using Hepa1c1c7 cells increased the chances of detection based on overall number of targets available. It is, however, predicted that AHR is present in mitochondria of many different cell types as indicated by western blot detection, not just liver cells (data not shown). TEM was used because it offers much higher magnifications than light microscopy to be able to distinguish a more specific location of AHR.

Preliminary images of Hepa1c1c7 cells showed that organelles designated as mitochondria did contain staining for AHR protein, but the poor resolution of the images did not provide strong evidence for in what compartment. Much more optimization needs to be conducted to determine the correct fixative concentrations to use that maintains the structure of the mitochondrial components but also allows for the antibodies to recognize the epitopes. In the literature there are images of mitochondria where the inner and outer mitochondrial membranes are clearly defined but they also were not intended for immunogold labeling and could therefore be post-fixed with osmium tetroxide, which provides more maintenance of native ultrastructure. Even the process of collecting the cells needs to be improved to help maintain the cell structure or mitochondria.

There were only a few gold particles per mitochondrion, so this raises the question of if

the AHR is scarce in the mitochondria or if it was a result of incomplete staining. TEM images of mitochondria stained for glucocorticoid receptors appear to have a higher amount of gold-labeling (Psarra et al., 2005; Scheller et al., 2000). The lack of staining in the negative controls and the lack of overstaining does help with the assurance that the staining was specific and might truly represent mito-AHR. In future studies it will be useful to use Hepa1c1c7 cells that have had AHR knocked out in them using CRISPR/Cas9 system. This will help to determine if the primary antibody is specifically binding to AHR because many primary antibodies can still bind to proteins with similar epitopes. Dr. Hye Jin Hwang demonstrated in her MSU dissertation that the level of mito-AHR decreased after TCDD exposure similar to what occurs with the cytosolic pool, so it would be interesting to test what happens to the staining after TCDD treatment (Hwang, 2015). Chemicals that are known to induce different types of mitochondrial stress could also be used to see what happens to the level of mito-AHR.

While still not very specific, the TEM images did show mito-AHR. This furthers the importance of finding what AHR is doing in the mitochondria and what it could be interacting with. To see if AHR could specifically interact with one of the electron transport complexes, individual enzymatic assays were completed using isolated mitochondria. The C12 AHR-deficient mitochondria did not have any significant difference in activity compared to the 1C1C7 that have sufficient AHR after TCDD treatment for 6 or 24 hours. This implies that the AHR is affecting mitochondrial efficiency by some means other than directly through the electron transport system. These assays were conducted on isolated mitochondria in solutions that would not represent the normal cytosolic environment. AHR might function in altering composition of mitochondria and since the solutions had saturating substrates for the individual complexes, it could have less of an impact in these assays compared to whole cells in normal cell medium.

CHAPTER 3: CROSSTALK BETWEEN AHR AND TSPO

This chapter contains material from a paper that is submitted for publication and is in press entitled "Evidence for Crosstalk between the Aryl Hydrocarbon Receptor and the Translocator Protein in Mouse Lung Epithelial Cells"

Authors: Michelle M. Steidemann[a,b], Jian Liu[c], Kalin Bayes[d], Lizbeth P. Castro[e], Shelagh Ferguson-Miller[c], John J. LaPres[b,c]

Affiliations: [a] Department of Pharmacology and Toxicology, Michigan State University, East Lansing, MI 48824, [b] Institute for Integrative Toxicology, Michigan State University, East Lansing, MI 48824, [c] Department of Biochemistry and Molecular Biology, Michigan State University, East Lansing, MI 48824, [d] Department of Integrative Biology, Michigan State University, East Lansing, MI 48824, [e] Cell and Molecular Biology Graduate Program, University of Texas Southwestern Medical Center, Dallas, TX 75390

Abstract

Cellular homeostasis requires the use of multiple environmental sensors that can respond to a variety of endogenous and exogenous compounds. The AHR is classically known as a transcription factor that induces drug metabolizing enzymes when bound to toxicants such as TCDD, but the receptor has a growing number of putative endogenous ligands, such as tryptophan, cholesterol, and heme metabolites. Many of these compounds are also linked to TSPO, an outer mitochondrial membrane protein. Given that a portion of the cellular pool of the AHR has also been localized to mitochondria and the overlap in putative ligands, the hypothesis that crosstalk exists between the two proteins was tested. CRISPR/Cas9 was used to create knockouts for AHR and TSPO in a mouse lung epithelial cell line (MLE-12). WT, AHR-/-, and TSPO-/- cells were then exposed to AHR ligand (TCDD, 10 nm, 6 hrs), TSPO ligand (PK 11195, 100 nM, 6 hrs), or both and RNA-seq was performed. Expression of mitochondrial-related genes was altered more by loss of either AHR or TSPO than would have been expected just by chance. Some of the genes with altered expression included those that encode for components of the electron transport system and the mitochondrial calcium uniporter. Both proteins altered the activity of the other as AHR

loss caused the increased expression of TSPO at both the mRNA and protein level and loss of TSPO significantly increased the expression of classic AHR battery genes after TCDD treatment. This research provides evidence that AHR and TSPO participate in similar or overlapping pathways that contribute to mitochondrial homeostasis.

Results

The AHR and TSPO share putative endogenous ligands

Though the AHR is most known for its role in regulating the body's response to exogenous chemicals, such as TCDD, some progress has been made in determining possible endogenous ligands. These molecules include cholesterol (Savouret et al., 2001), heme and heme metabolites (Phelan et al., 1998), as well as tryptophan derivatives, such as kynurenine and 6-formylindolo[3,2-b] carbazole (FICZ) (Mezrich et al., 2010; Seok et al., 2018). Many of these same small molecules have also been reported to bind to TSPO, with the exception of tryptophan derivatives. To explore the possibility that kynurenine could also bind TSPO, fluorescence quenching binding experiments were performed by Dr. Jian Liu in the lab of Dr. Shelagh Ferguson-Miller. The results show that TSPO binds kynurenine in the high micromolar range and thus shares another putative endogenous ligand with AHR (Fig. 3.1). This further supports the possibility that some level of crosstalk exists in their signaling cascades.

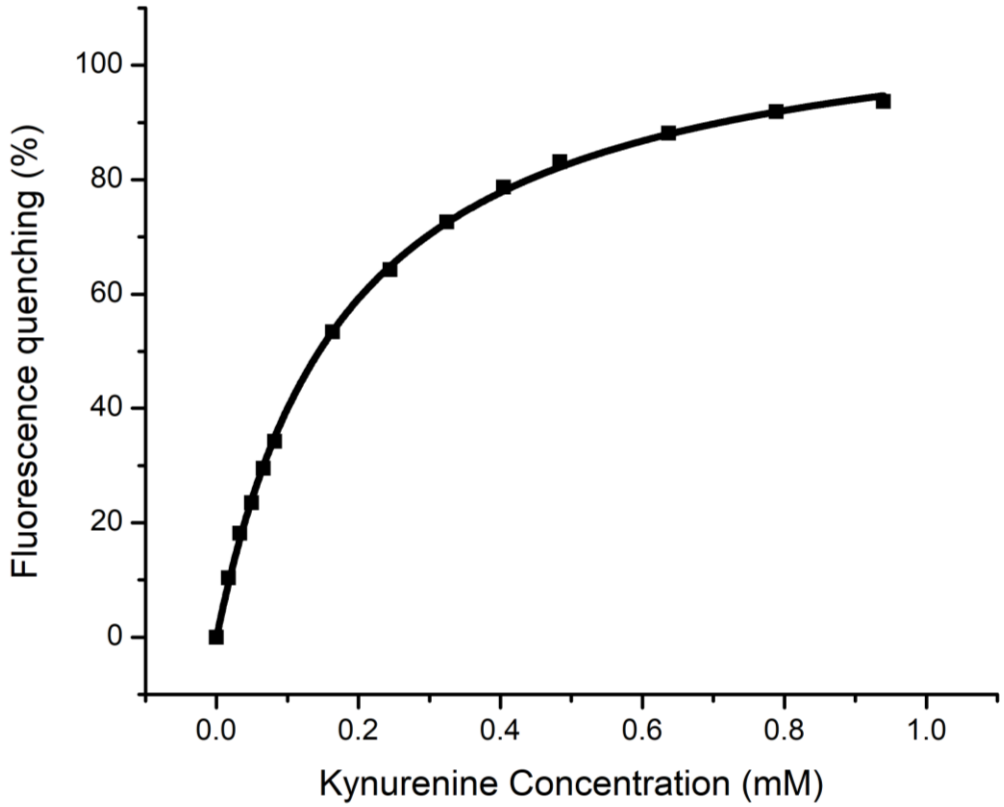

Figure 3.1 Binding curve of kynurenine with WT RsTSPO. Kynurenine dissociation constant K_d=0.172±0.011 (mM) is calculated from three repeated experiments as described in Material and Methods

Generation of AHR-/- and TSPO-/- mouse cell lines

Given that the AHR and TSPO share many putative endogenous ligands, it was hypothesized that some degree of crosstalk existed between the two proteins. To test this hypothesis, knockout cell lines were created in three murine cell lines for each protein via CRISPR/Cas9. BV-2 cells, (a microglial cell line)(Blasi et al., 1990), were used to model immune cells of the central nervous system. Hepa1c1c7, (a liver epithelium cell line)(Hankinson, 1979), was used to model cells that encounter orally absorbed toxicants. The mouse lung epithelial 12 (MLE-12) cell line (Wikenheiser et al., 1993), was used to model cells that would be exposed to inhaled toxicants (Table. 3.1).

Cell line	Background	Sex	Cell type	Immortalization	Reference
BV-2	C57BL/6	Female	Microglia	J2 retrovirus containing a v-*raf*/v-*myc* oncogene	Blasi et al., 1990
Hepa1c1c7	C57L/J	Female	Liver epithelial	Spontaneously developed	Hankinson, 1979
MLE-12	FVB/N	Female	Lung epithelial	Simian virus 40 large tumor antigen under the control of the promoter from the human surfactant c gene	Wikenheiser et al., 1993

Table 3.1 Description of mouse cell lines

Possible knockout candidates were isolated with puromycin selection and confirmed by western blot (Figs. 3.1, 3.2, 3.4). Hepa1c1c7 had one of each gene knockout cell line (AHR 1.4D and TSPO 2.2), the MLE-12 had one AHR-/- (G5) and three TSPO-/- lines (G10, 1.1G, and A8). One TSPO knockout (E6) was created in the BV-2 cell line (Table 3.2).

Cell line	ID	CRISPR construct
BV-2	E6	TSPO 2.2
Hepa1c1c7	AHR 1.4D	AHR 1.4
	TSPO 2.2	TSPO 2.2
MLE-12	G5	AHR 1.4
	G10	TSPO 1.1
	1.1G	TSPO 1.1
	A8	TSPO 2.2

Table 3.2 Description of CRISPR cell lines

Sanger sequencing was used to further confirm gene disruption and to try to determine

what gene editing had occurred. The BV-2 TSPO-/- 2.2 (E6) cell line contained two erroneous sequences with one beginning at the third base pair in the CRISPR region (Fig. 3.1A). It is difficult to know what the exact sequence is of each due to the overlap in the sequencing. The Hepa1c1c7 AHR-/- 1.4D cell line had a single cytosine deletion which caused a shift in the reading frame and premature stop codon (Fig. 3.2A). The resulting protein would be only 17 amino acids long. The Hepa1c1c7 TSPO-/- 2.2 cell line appeared to have two sequences present for the region (Fig. 3.2A). In at least one sequence an adenosine was incorrectly inserted toward the beginning of the CRISPR region. The MLE-12 AHR-/- 1.4 (G5) cells had a deletion of 12 nucleotides that began after the adenine in the start codon, essentially blocking any translation of AHR protein from occurring (Fig 3.3). The MLE-12 TSPO-/- 1.1 (G10) cells had a single cytosine incorrectly inserted into the sequence (Fig. 3.3). This caused a frame shift mutation that resulted in an early termination so that only a 35 amino acid protein would be translated. The MLE-12 TSPO-/- 2.2 (A8) sequence appears to have two sequences that both have a mistake in the reading frame, one starting at the third base (Fig. 3.3). This would produce two shortened but different TSPO fragments. The MLE-12 TSPO-/- 1.1 (1.1G) appears like it might have a guanine insertion and then two different sequences (Fig. 3.3). All of the Sanger sequencing for the knockout cell lines confirmed that they did have some form of disruption to the reading frame of the DNA that would have produced a shortened or no protein.

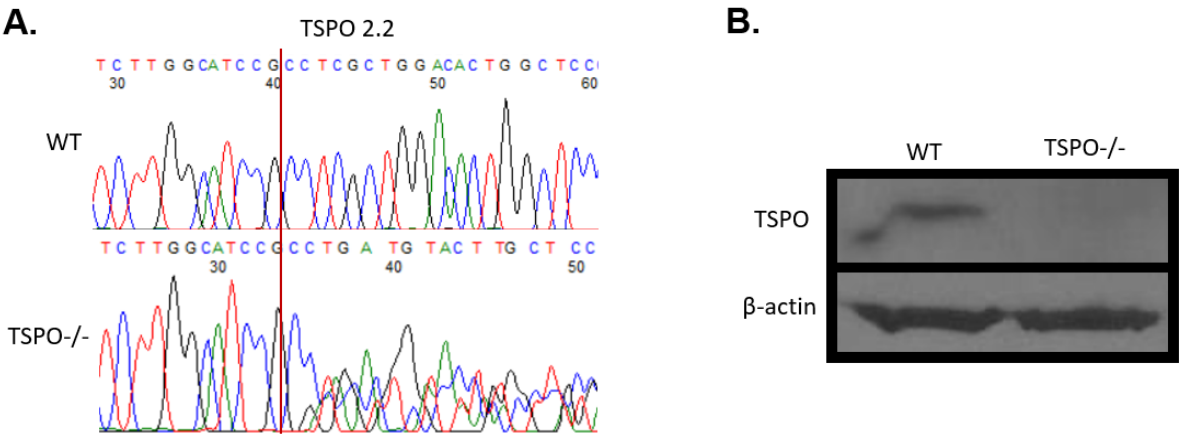

Figure 3.1 TSPO was knocked out at the genomic and protein level in BV-2 E6 TSPO-/- cell line using CRISPR. Genomic DNA was extracted from BV-2 cells using Qiagen DNeasy Blood & Tissue Kit, TSPO 2.2 CRISPR region was PCR amplified, and analyzed using Sanger Sequencing. Red line represents start of CRISPR target region (**A**). BV-2 cells were grown to exponential growth phase and then collected in RIPA buffer. Whole cell protein (150 µg) was separated by 15% SDS-PAGE. Protein was transferred to nitrocellulose membrane and probed for TSPO and β-actin (loading control) (**B**).

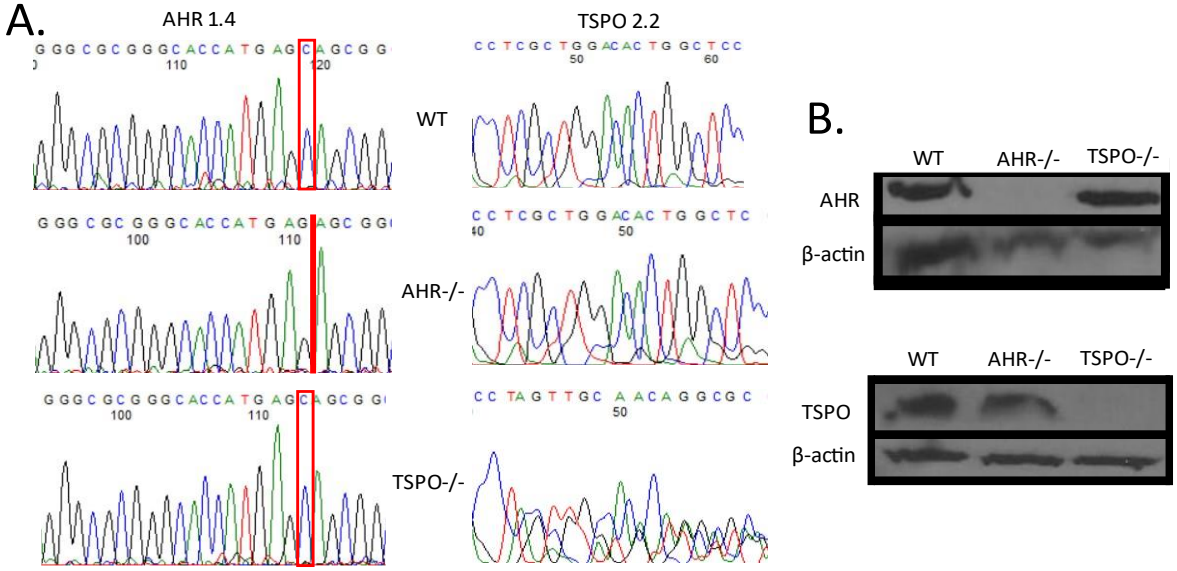

Figure 3.2 Confirmation of AHR and TSPO CRISPR knockout in Hepa1c1c7 cells. Genomic DNA was extracted from Hepa1c1c7 cells using Qiagen DNeasy Blood & Tissue Kit. CRISPR regions were amplified using specific primers and Q5 Polymerase PCR. PCR fragments were verified for size using gel electrophoresis and analyzed using Sanger Sequencing (**A**). Hepa1c1c7 cells were grown to exponential growth phase and then collected in RIPA buffer. Whole cell protein: 38 µg was separated by 8% SDS-PAGE for AHR and 150 µg was separated by 15% SDS-PAGE for TSPO. Protein was transferred to nitrocellulose membrane and probed for AHR, TSPO, and β-actin (loading control) (**B**).

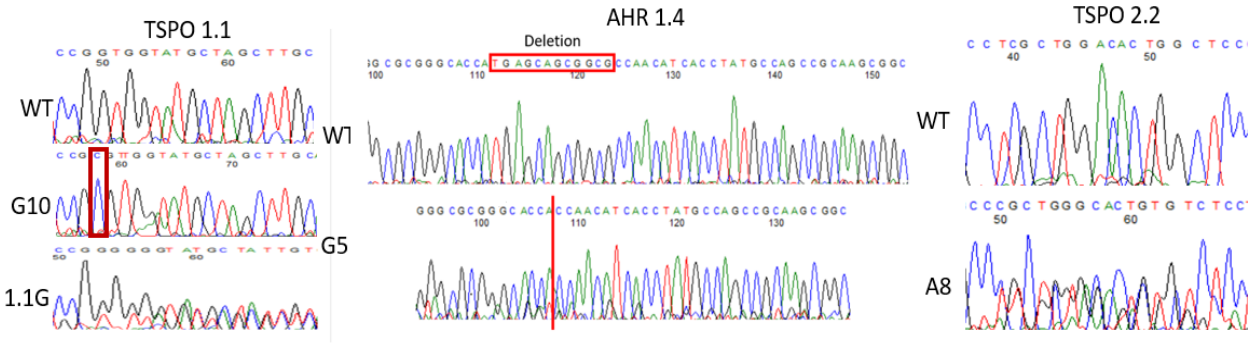

Figure 3.3 Confirmation of AHR and TSPO CRISPR knockout in MLE-12 cells. Genomic DNA was extracted from MLE-12 cells using Qiagen DNeasy Blood & Tissue Kit. CRISPR regions were amplified using specific primers and Q5 Polymerase PCR. PCR fragments were verified for size using gel electrophoresis and analyzed using Sanger Sequencing.

Characterization of MLE-12 AHR and TSPO knockout cell lines

To explore the possibility that the presence of either AHR or TSPO could affect the expression of the other, RNA-seq data was examined. *Tspo* mRNA was increased 1.30-fold in AHR-/- cells compared to wild-type (padj = 9.58E-07) (Fig. 3.4A). This increased expression was not altered upon exposure to the AHR ligand, TCDD (10 nM, 6 hrs) (data not shown). The level of *Tspo* mRNA decreased 1.88-fold in the TSPO-/- cells when compared to the AHR-/- cells (padj = 1.52E-29). It was also decreased 1.45-fold in TSPO-/- cells compared to wild-type cells (padj = 5.74E-10) (Fig. 3.4A). So, while the CRISPR process prevented whole TSPO protein synthesis, transcripts were still synthesized but at a lower level than non-transfected cells. Loss of TSPO did not change the expression of *Ahr* mRNA (Fig. 3.4A).

Since the level of mRNA does not always match protein concentration, the level of AHR and TSPO was analyzed through western blots (Fig. 3.4B-C). TSPO protein was completely absent from the TSPO-/- G10 and A8 CRISPR knockouts (Fig. 3.4B). AHR protein was also confirmed to not be present in AHR-/- cells (Fig. 3.4C). The level of TSPO increased about 2-fold in AHR-/- cells when compared to wild-type as calculated when using β-actin as a loading control ($p < 0.05$)

(Fig. 3.4D). This significant increase is similar to the increase in mRNA described above. The level of AHR in TSPO -/- cells was not significantly different when compared to wild-type cells (Fig. 3.4D). On average the AHR protein amount in TSPO -/- cells was about 90% of the wild-type. This result also agrees with the RNA-seq data which did not show a difference at the transcript level. The mRNA and protein expression data indicate that AHR pathways exhibit signaling crosstalk with TSPO, but AHR expression is not influenced by TSPO abundance.

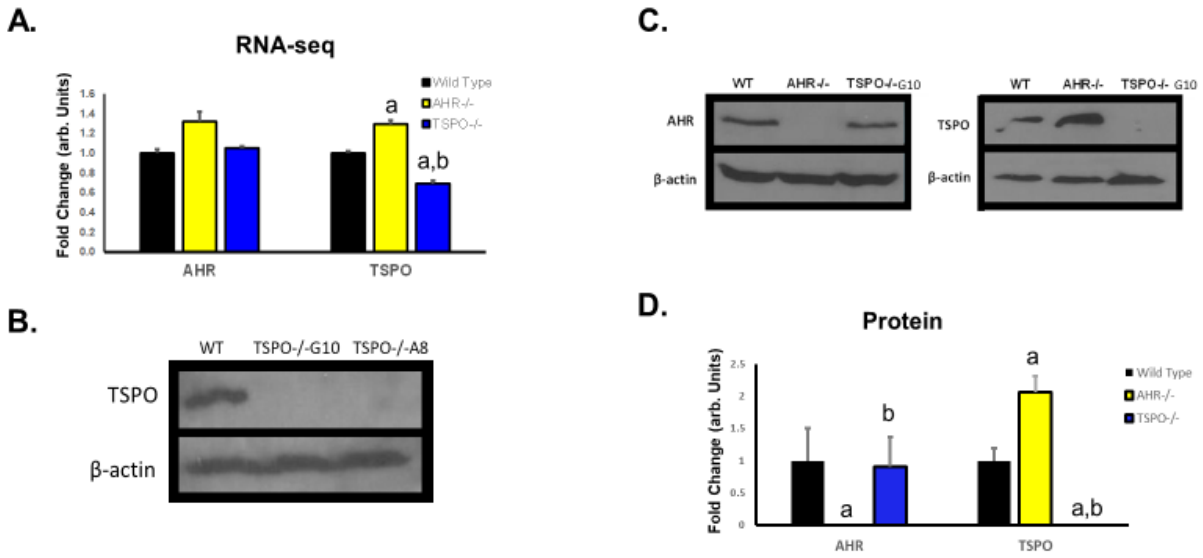

Figure 3.4 Analysis of RNA and protein expression of AHR and TSPO in wild-type (WT), AHR-/-, and TSPO-/- MLE-12 cells. RNAseq data were analyzed for the expression AHR and TSPO in wild type (WT), AHR-/-, and TSPO-/- G10 cells and shown relative to WT cells. a=significance from WT padj<0.05. b=significance from AHR-/- padj<0.05. n=3 (**A**). MLE-12s were grown to exponential growth phase and then collected in RIPA buffer. Whole cell protein (200 µg for AHR and 150 µg for TSPO) was separated by SDS-PAGE and protein was transferred to nitrocellulose and probed for AHR, TSPO, or β-actin (loading control). TSPO-/-G10 and A8 protein (**B**). AHR and TSPO expression of AHR-/- and TSPO-/- G10 (**C**)**.** Protein levels from C were normalized with loading control and then compared to WT levels. a=significance from WT padj<0.05. b=significance from AHR-/- padj<0.05. n≥3 (**D**).

To determine if the absence of either AHR or TSPO caused a change in proliferation, cell viability was analyzed using trypan blue cell counting and MTT viability assays over three days. For trypan blue measurements, cells were plated at a density of 40,000 cells per well in 6-well dishes and then live cells were counted. The growth for all cell lines was essentially the same

between initial plating and 71 hours with no significant differences (Fig. 3.5A). For the MTT assay cells were plated at a density of 1,334 cells per well in 96-well dishes and MTT assays were individually run for three days after plating. There was no significant difference in the conversion of MTT at any of the time points assayed (Fig.3.5B).

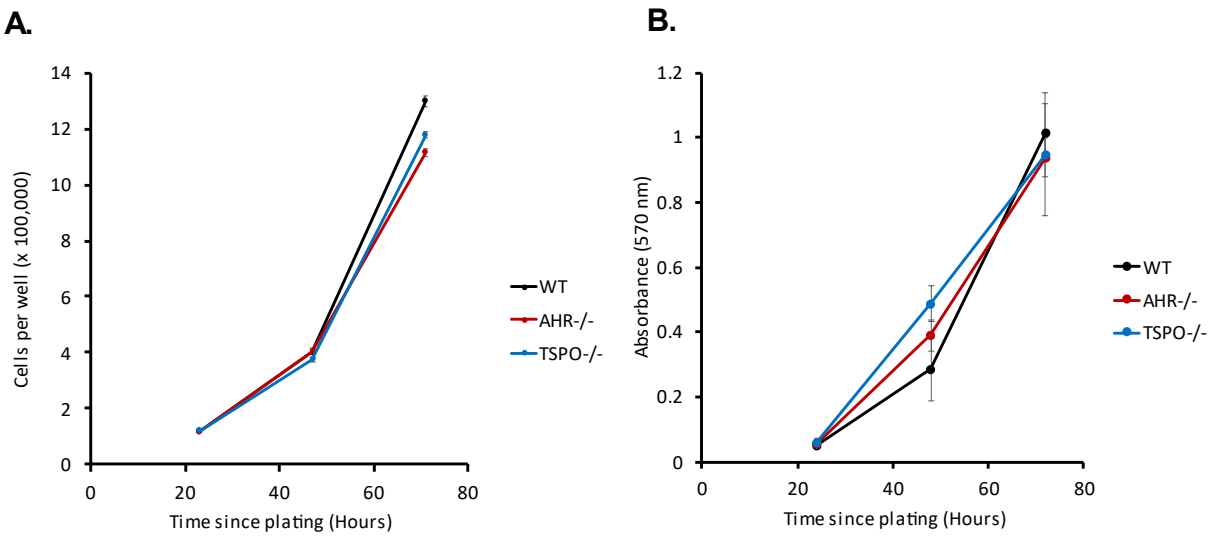

Figure 3.5 Growth curves of wild-type (WT), AHR-/-, and TSPO-/- MLE-12 cells. Cells were plated at an initial density of 40,000 cells per well in 6-well dishes. Two technical replicates were examined at each time point. Cells were removed from the well using 0.25% trypsin-1 mM EDTA, stained with 0.4% trypan blue, and counted using a hemacytometer. Represents four independent experiments. Error bars represent standard error **(A)** Cell were plated at an initial density of 1,334 cells per well in 96-well dish in technical triplicates. At each time point, medium was removed and replaced with 0.5 mg/ml MTT medium. After 1 hour incubation, MTT medium was removed and replaced with 100% DMSO. Absorbance was read at 570 nm. Represents three independent experiments. Error bars represent standard error (**B**).

Differential expression of genes in AHR-/- and TSPO-/- MLE-12 cell lines

The change in TSPO protein levels in the AHR-/- knockout cells suggests some level of crosstalk exists between the two proteins. To determine if this crosstalk has functional significance, RNA-seq was performed on RNA extracted from the three cell lines (i.e. WT, AHR-/-, and TSPO-/-) following treatment (6 hrs) of DMSO (0.003%) + ethanol (0.005%), TCDD (10 nM), PK11195

(100 nM), or TCDD + PK11195 (10 nM and 100 nM respectively). Globally, loss of AHR led to 1,125 differentially expressed genes (DEGs) when compared to WT cells (Fig. 3.6). In comparison, loss of TSPO led to 2,757 DEGs when compared to wild-type cells. Interestingly, there were 567 DEGs shared between these two groups. When AHR-/- cells were compared to TSPO-/- cells there were 3,041 DEGs between the two knockout cell lines. Of these, 729 were shared with the AHR-/- vs WT DEGs and 1,801 were shared with the TSPO-/- vs WT DEGs. Finally, a core set of 333 genes were different between all three comparisons. Included in this core set of genes was *Glutathione S-transferase kappa 1* (*Gstk1)* with expression that increased 3.88-fold in AHR-/- cells (padj=6.1E-12) compared to WT cells but decreased 171.29-fold in TSPO-/- cells when compared to WT cells (padj=1.9E-7). The *Gstk1* mRNA expression was decreased 664.43-fold (padj=3.12E-13) when TSPO-/- cells were compared to AHR-/- cells. *Gstk1* is a phase II drug-metabolizing enzyme that can localize to mitochondria. Another of these genes, *ATP binding cassette subfamily A member 1 (Abca1),* is used to transport cholesterol (which can be a ligand for both proteins) across the plasma membrane. It was increased 1.9–fold in AHR-/- cells (padj=3.6E-15) when compared to WT cells but decreased 1.57-fold in TSPO-/- cells (padj=4.0E-4) when compared to WT cells. It was decreased 3.07-fold when TSPO-/- cells were compared to AHR-/- cells (padj=2.15E-33). These data support the hypothesis that loss of AHR or TSPO affects a set of genes with functions that could imply crosstalk exists between the two proteins.

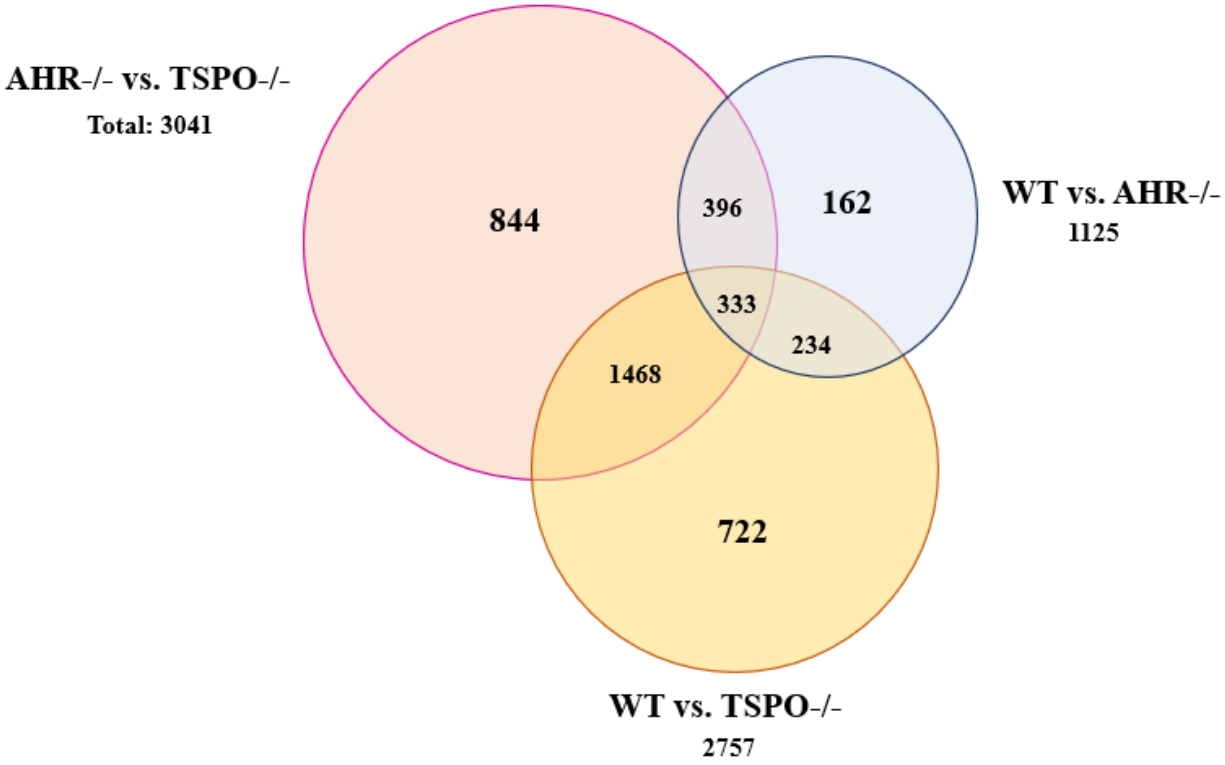

Figure 3.6 Differentially expressed genes between vehicle treated wild-type (WT), AHR-/-, and TSPO-/- MLE-12 cells. RNA was isolated from cells using TRIzol protocol and sequenced by Novogene. Genes were considered significantly changed if padj value was <0.05. Represents three biological replicates.

Identifying AHR target genes that are susceptible to TSPO-mediated alterations in expression in MLE-12 cells

The AHR regulates the expression of a core battery of genes. This group includes approximately 100 genes, including *Cyp1a1*, *Cyp1a2*, *Cyp1b1*, *AHR repressor* (*Ahrr*), and *NAD(P)H quinone dehydrogenase 1* (*Nqo1*) (Favreau & Pickett, 1991; Mimura et al., 1999; Pendurthi et al., 1993; Sutter et al., 1994; Xu et al., 2000). To determine if loss of TSPO could impact the expression of these genes, the RNA-seq data were analyzed in the three cells lines following exposure to TCDD (10 nM), PK11195 (100 nM) or TCDD + PK11195 (10 nM, 100 nM, respectively) for 6 hours. All five of these core AHR battery genes displayed increased expression in the wild type cells following exposure to TCDD; however, only *Cyp1b1* and *Nqo1* reached the

level of significance (Table 3.3). Their expression was not altered by PK11195 alone. Three of the five genes showed an increased expression in wild-type cells following co-exposure to TCDD and PK11195, with *Cyp1b1* and *Nqo1* again being significant but not when compared to cells just treated with TCDD. As expected, none of the genes displayed a change in expression following any treatment in the AHR-/- cells (Table 3.3) providing another layer of validation for AHR knockout. Finally, in the TSPO-/- cells, three of the five genes were significantly upregulated when treated with TCDD or TCDD + PK11195 when compared to control treated cells within cell type (Table 3.3). Interestingly, the loss of TSPO led to a significant increase in *Cyp1a1* and *Cyp1b1* when treated with TCDD or TCDD + PK11195 when compared to wild-type cells within respective treatment group (Table 3.3). These results suggest that TSPO plays a role in modulating the level of induction of some key AHR target genes.

	Wild Type			
	Control	TCDD	PK11195	TCDD+PK
Cyp1A1	0.0000	0.0943	0.0000	0.0471
Cyp1A2	0.0000	0.0288	0.0000	0.0000
Cyp1B1	43.6353	150.4421	45.3969	156.8090
AHRR	0.0016	0.0048	0.0000	0.0000
Nqo1	11.8222	25.3125	11.2235	24.6279

	AHR-/-			
	Control	TCDD	PK11195	TCDD+PK
Cyp1A1	0.0000	0.0000	0.0000	0.0000
Cyp1A2	0.0000	0.0233	0.0070	0.0000
Cyp1B1	40.8458	40.7283	40.2986	40.1564
AHRR	0.0015	0.0021	0.0000	0.0000
Nqo1	9.9061	10.0269	9.8448	9.6662

	TSPO-/-			
	Control	TCDD	PK11195	TCDD+PK
Cyp1A1	0.0000	0.5584	0.0000	0.5360
Cyp1A2	0.0000	0.0000	0.0000	0.0000
Cyp1B1	36.7047	216.0881	37.6043	218.0877
AHRR	0.0039	0.0000	0.0034	0.0121
Nqo1	11.0459	23.7388	11.0096	23.9986

Table 3.3 The impact of AHR and TSPO knockout on the expression of five AHR target genes in MLE-12 cells. Data were normalized and represented as fragments per kilobase per million mapped reads (fpkm). Green = padj < 0.05 compared to controls within the same cell type. Red = padj < 0.05 compared to control within cell type and compared to wild-type cells within treatment. Represents three biological replicates.

To determine the extent of TSPO's ability to modulate AHR-mediated transcription, global changes in expression were analyzed. To identify genes most susceptible to TSPO influence, TCDD-induced DEGs in wild-type cells were analyzed for influence of loss of TSPO and/or co-treatment with PK11195. Treatment with TCDD led to 91 DEGs in wild-type cells, 132 DEGs in the TSPO-/- cells, and 1 DEG in the AHR-/- cells (Fig. 3.7A and data not shown). Treatment with PK11195 led to 0 DEGs in the wild-type cells, 1 DEG in the TSPO-/- cells, and 7 DEGs in the AHR-/- cells (Data not shown). Exposing the cells to both chemicals concurrently led to 120 DEGs in the wild-type cells, 114 DEGs in the TSPO- /- cells, and zero DEGs in the AHR-/- cells (Fig. 3.7A and data not shown). Of the 91 DEGs identified in TCDD-treated WT cells, 29 of them were no longer significantly changed in the TCDD-treated TSPO-/- when compared to control TSPO-/-

cells (Fig. 3.7A). There were 70 additional genes that were significantly changed in the TCDD-treated TSPO-/- when compared to control TSPO-/- cells that were not in the TCDD-treated WT cells. These data suggest that approximately a third of AHR target genes are susceptible to TSPO-mediated crosstalk. To limit the number of false positives, the original 91 DEGs were also compared to the DEGs following TCDD+PK11195 co-treatment in WT cells. Co-treatment led to 32 of the 91 genes no longer being significantly altered. When this set is compared to the 29 impacted by the loss of TSPO, there are 13 genes that overlap (Fig. 3.7A-B). These genes represent the core genes regulated by the AHR that are susceptible to TSPO-mediated activity. Included in this group was *Dhrs3,* which is a short-chain dehydrogenase/reductase, which can catalyze reactions involving steroids and retinoids. This is of note since these compounds are predicted to be ligands for TSPO. *Dhrs3* expression had been previously noted to be altered upon TCDD exposure, and its promoter region contains DREs (Boverhof et al., 2005).

A.

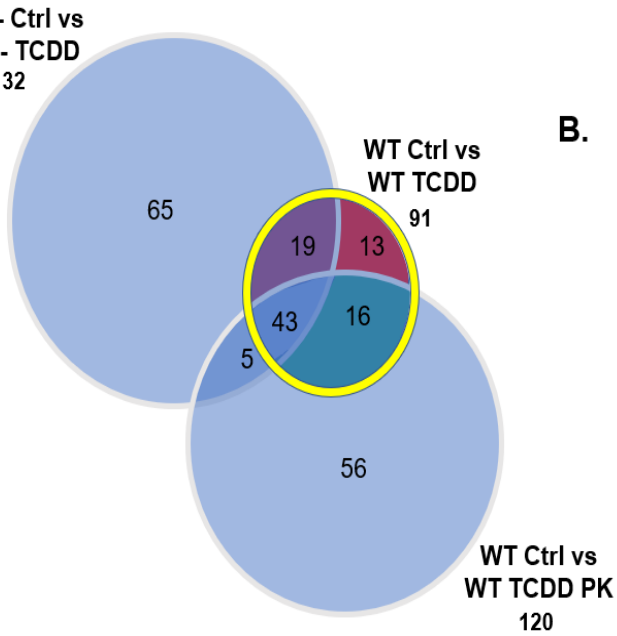

B.

name	Change	Gene description
Gm10358	-41.51	predicted gene 10358 GAPDH
Cacna1a	-1.25	calcium channel, voltage-dependent, P/Q type, alpha
Trp53bp2	-1.16	transformation related protein 53 binding protein 2
Flrt2	-1.15	fibronectin leucine rich transmembrane protein 2
Ahnak	1.19	AHNAK nucleoprotein (desmoyokin)
Gm28438	1.26	predicted gene 28438
Gm28437	1.36	predicted gene 28437
Lif	1.42	leukemia inhibitory factor
Arhgap45	1.65	Rho GTPase activating protein 45
Gsdme	1.67	gasdermin E
Dhrs3	1.90	dehydrogenase/reductase (SDR family) member 3
Padi1	2.20	peptidyl arginine deiminase, type I [Source:MGI
Gm22009	5.52	predicted gene, 22009 [Source:MGI

Figure 3.7 Differentially expressed genes between control, TCDD-treated, or TCDD+PK 11195-treated wild-type (WT) and TSPO-/- MLE-12 cells. RNAseq was performed on wild type (WT) and TSPO-/- cells following treatment with TCDD or TCDD + PK 11195 as described in Materials and Methods. Differentially expressed genes (padj < 0.05) in the three groups were compared (**A**). There were 13 genes that were significantly changed following TCDD treatment in WT cells that were not significantly altered in the TSPO-/- cells following similar treatment nor in the WT cells following co-treatment with TCDD + PK11195 (**B**). Represents three biological replicates.

Differential expression of mitochondrial genes in WT, AHR-/-, and TSPO-/- MLE-12 cells

Of the over 50,000 genes used in the RNA-seq dataset, 0.647% of the gene descriptions contained the word mitochondria. This percentage significantly increased to 1.33% for the list of DEGs when wild-type and AHR-/- cells were compared and to 1.92% for the list of DEGs between wild-type and TSPO-/- cells. This enrichment is not unexpected for a protein located in the outer mitochondrial membrane, such as TSPO, but it is for a nuclear transcription factor like AHR. The enrichment following loss of AHR supports the notion that the pool of AHR found within the mitochondria has functional significance (Hwang et al., 2016).

The RNA-seq data was also used to analyze changes in genes located in the mitochondrial genome. Out of the 13 protein-encoding mitochondrial genes, seven were slightly but significantly

upregulated in TSPO-/- cells and two were upregulated in AHR-/- cells (Fig. 3.8). *Nd3*, *Nd4l*, *Nd6*, *Co3*, and *Atp8* were the five genes that were not significantly altered in either of the knockout cell lines. *NADH dehydrogenase 4* (*Nd4),* a subunit of respiratory complex I, was the one gene that was upregulated by the loss of either AHR or TSPO. Loss of TSPO had a larger impact on mitochondrial-encoded genes than loss of AHR, however both demonstrated the ability to alter the expression of genes that encode key subunits of the electron transport system.

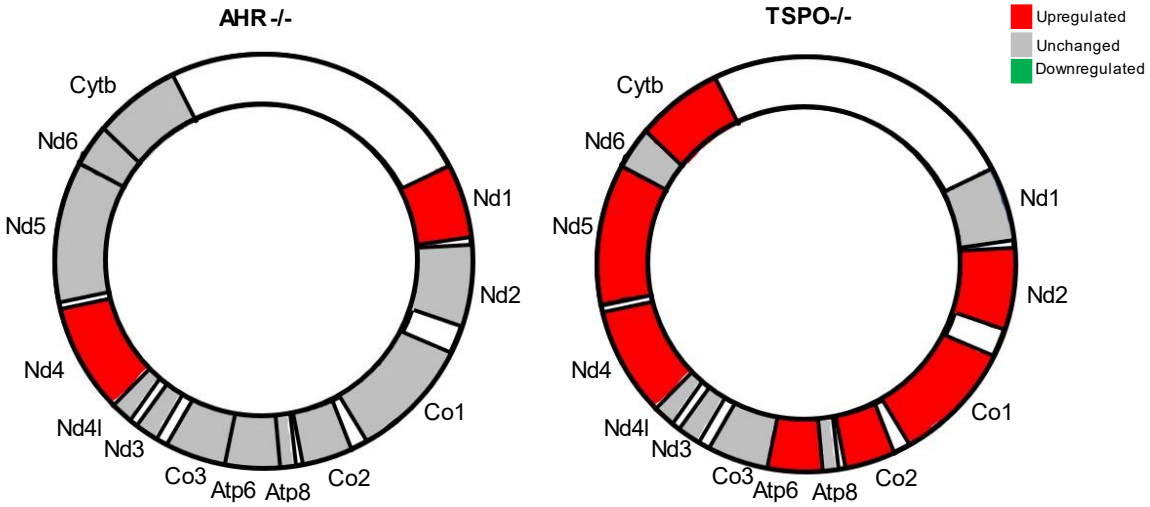

Figure 3.8 Mitochondrial encoded genes were upregulated in AHR-/- and TSPO-/- MLE-12 cells. Graphical representation of the 13 genes within the murine mitochondrial genome. RNA was isolated from untreated MLE-12 wild-type (WT), AHR-/-, and TSPO-/- cells using TRIzol protocol and sequenced by Novogene. Genes were designated as significantly upregulated or downregulated compared to WT if the padj < 0.05. Represents three biological replicates. Nd1, 2, 3, 4, 4L, 5, and 6 are components of electron transport complex I. Cytb is a component of complex III. Co1, 2, and 3 are components of complex IV. Atp6 and 8 are components of ATP synthase.

Mitochondrial calcium transport alterations in AHR and TSPO MLE-12 knockout cell lines

Mitochondrial-involved calcium homeostasis and signaling is essential for all cells and is tightly controlled. One way that calcium can enter the mitochondrial matrix is via the mitochondrial calcium uniporter (MCU). The MCU is a multiunit protein, and loss of either AHR or TSPO altered the expression of MCU components. For example, loss of either AHR or TSPO led to a drastic decrease of *Micu2* expression. *Micu2* expression was decreased 94.88-fold in the AHR-/- cells (padj=3.5E-05) and 94.08-fold in the TSPO -/- cells (padj=2.2E-05) compared to wild-type cells (Table 3.4).

	AHR-/-	TSPO-/-
Mcu	1.16	-1.28
Micu1	1.17	1.08
Micu2	-94.88	-94.08
Micu3	1.05	1.30
Smdt1	1.02	-1.06

Table 3.4 Differential expression of mitochondrial calcium importer genes in CRISPR knockout AHR-/- and TSPO-/- MLE-12 cells.
Red= increase padj < 0.05 compared to WT
Green=decrease padj <0.05 compared to WT

Loss of AHR caused an increase in expression of *Micu1* (1.17-fold, padj=1.7E-03) but this did not occur in TSPO-/- cells. Loss of TSPO caused a 1.3-fold (padj=3.0 E-02) increase in expression of *Micu3* but this did not occur in AHR-/- cells. *Mcu* was significantly decreased 1.28-

fold (padj=4.2E-04) in TSPO-/- and non-significantly increased 1.16-fold (padj=6.0E-02) in AHR-/-. The gene for the SMDT1 (aka EMRE) subunit was not significantly altered in either of the mutant cell lines. It is unclear how much loss of AHR or TSPO affects total calcium within the mitochondria, but it should be noted that there are mitochondrial exchangers that were not altered in either mutant cell line. *Letm1*, for example, encodes a Ca^{2+}/H^{+} antiporter located in the inner mitochondrial membrane that was not significantly changed in either AHR-/- or TSPO-/- mutants. Finally, treatment of WT, AHR-/- or TSPO-/- cells with TCDD, PK11195, or the combination of both did not alter the expression of any gene that encodes an MCU subunit.

Variation between cell types for RNA-seq differentially expressed genes

To determine if the changes in gene expression due to loss of AHR or TSPO was lung cell specific, the CRISPR AHR and TSPO knockouts of mouse liver cell line Hepa1c1c7 were used for comparison. RNA was collected from untreated MLE-12 and Hepa1c1c7 cells and analyzed using SYBR Green PCR protocol. Six DEGs from the MLE-12 RNA-seq data were compared: *Abca1*, *Gpr39*, *Gstk1*, *Micu2*, *Mt1*, and *Nfatc2* (Fig. 3.9). Expression of none of the genes was significantly altered in the Hepa1c1c7 cells while *Abca1*, *Gpr39*, *Gstk1*, *Micu2*, and *Nfatc2* were significantly altered in the MLE-12 in at least one cell type. *Gpr39* had a similar trend between cell types with a decrease of 1.4-fold (p=0.4106) in the AHR-/- and 1.5-fold (p=0.3293) in the TSPO-/- Hepa1c1c7 cells and a significant decrease of 16.4-fold (p<0.0001) in the AHR-/- and 12.6-fold (p<0.0001) in the TSPO-/- MLE-12 cells (Fig. 3.9B). *Metallothionein 1* (*Mt1*) expression followed a similar decreasing trend in both of the TSPO-/- cells, but it increased a nonsignificant 2.4-fold (p=0.2790) in Hepa1c1c7 AHR-/- and decreased a nonsignificant 2.0-fold (p=0.1137) in MLE-12 AHR-/- cells (Fig. 3.9E).

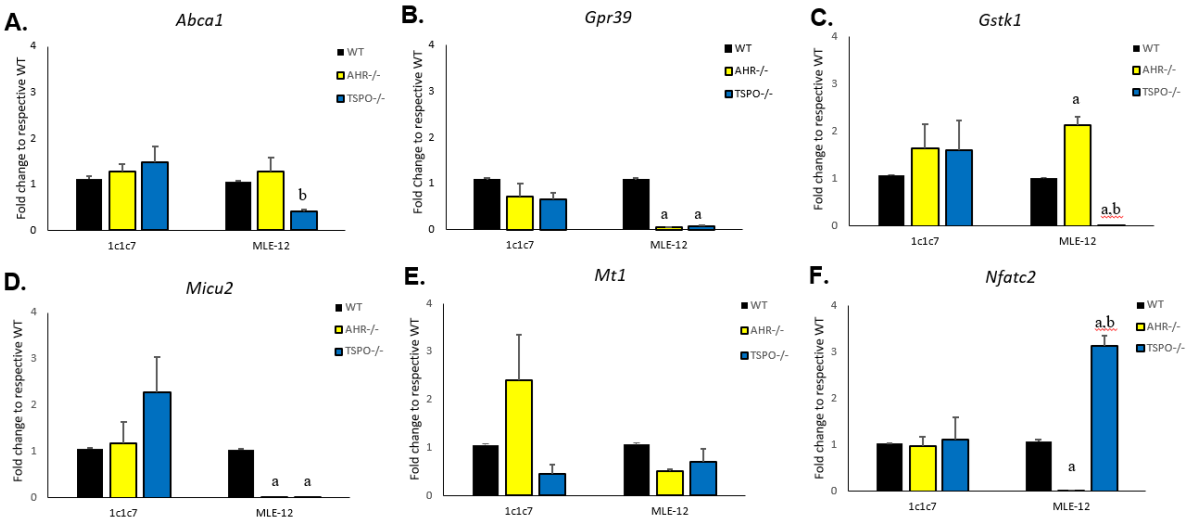

Figure 3.9 qRTPCR analysis of select DEGs from RNA-Seq show cell-cell variability. 1c1c7 and MLE-12 cells were grown in 6 well dishes in triplicates, collected in TRIzol, and RNA isolated according to manufacturer's protocol. cDNA was created using GoScript Reverse Transcriptase per manufacturer's protocol. qRTPCR was performed using SYBR Green MasterMix. Gene expression was normalized using the geometric mean of housekeeping genes, *Hprt*, *Actb,* and *18s*, and calculated using $\Delta\Delta C_T$ method. Final comparisons were made as fold change to the wild-type control. a=significance from WT $p<0.05$. b=significance from AHR-/- $p<0.05$. Represents three independent experiments.

Discussion

The proper maintenance and growth of biological cells is a complex process requiring multiple proteins and various signaling pathways. The cell needs to be able to respond quickly to both endogenous and exogenous signals to alter activity for survival. The AHR and TSPO are two ligand-binding proteins that influence many pathways. The goal of this research was to explore the possibility that these two previously unlinked proteins might participate in crosstalk. This postulation was based on the discovery that there is considerable overlap between putative ligands for AHR and TSPO, raising the potential for these proteins to work together in response to those ligands or to respond to similar microenvironments.

Through analysis of gene expression, it was determined that there were categories of genes that were influenced by loss of the proteins and/or exposure to known ligands, that implied an

overlap of functionality of the AHR and TSPO. For example, the expression level of TSPO mRNA and protein was increased in untreated AHR-/- cells compared to their wild-type counterparts. The increase in TSPO protein following the loss of AHR could be a mechanism to compensate for a function of the AHR that needs to be maintained. The exact mechanism that explains this link between AHR and TSPO levels is unknown; however, the AHR could modulate TSPO transcription directly or indirectly though activating another signaling pathway, such as mitochondria-to-nucleus stress signaling. Loss of TSPO, however, does not cause a similar increase in expression of AHR mRNA or protein. This might provide evidence against the AHR and TSPO working in the same physical pathway because the cell would normally be expected to try to make up for the loss of one step by altering the expression of others. The protein analysis supports TSPO somehow being involved downstream of AHR activity.

The AHR is classically associated with enhancing drug metabolizing enzymes to protect the cell from foreign toxicants. The alteration in TSPO expression after AHR elimination suggests that TSPO might also act in those processes. To examine this, RNA expression of the two major AHR-linked cytochrome P450s, *Cyp1a1* and *Cyp1b1*, was measured after TCDD (AHR ligand) treatment. It was found that the expression of both increased more in the TSPO-/- cells compared to the wild-type cells after 6 hours of TCDD exposure. This result indicates that either TSPO normally functions to dampen the expression of these P450 genes, or its loss indirectly allows for increased AHR activity. Interestingly, this TSPO-dependent increase in *Cyp1a1* and *1b1* did not occur for all known AHR target genes suggesting that the signaling interaction between the AHR and TSPO might be context or cell-type specific.

CYP1B1 metabolizes many endogenous molecules including estradiol (Hayes et al., 1996) and retinol (Chambers et al., 2007). These substrates for CYP1B1 might offer some clues as to

why TSPO could dampen its AHR-mediated expression. Both estradiol and retinoic acid can modulate TSPO expression and retinoic acid can bind TSPO (Chen et al., 2014; González-Blanco et al., 2021), directly linking their intracellular concentration to TSPO signaling. The ability of TSPO to modulate TCDD-induced *Cyp1a1* and *1b1* expression might also involve heme homeostasis. TSPO has been linked to regulating the concentration of other heme-dependent enzymes by acting as a source of heme for these molecules, such as NOX2 (Guilarte et al., 2016), so it could also provide this function for heme-containing P450s. The fact that other cytochrome P450s were not influenced by loss of TSPO (i.e., *Cyp1a2*) does not support this model, meaning that the *Cyp1a1* and *1b1* expression increase could be specific. The level of *Cyp1A2*, however, is much lower in MLE-12s and might not act as the same heme sink as the other two isoforms.

The current model of AHR biology has the receptor only in the cytosol of the cell when unbound or in the nucleus when bound by a ligand. Tappenden et al. (2011) and Hwang et al. (2016) have suggested that a portion of the AHR can be located in mitochondria, allowing for the hypothesis that the receptor could influence mitochondrial activity. The RNA-sequencing data also show that loss of either TSPO or AHR impacted a significantly larger number of mitochondrial-associated genes than would be expected just by chance. The AHR-/- cells having an enrichment of mitochondrial DEGs similar to a known mitochondrial protein strengthens the possibility of mito-AHR. Some of these genes were nuclear-encoded genes but some were mitochondrial-encoded. Of the mitochondrial-encoded genes altered by AHR and TSPO loss, all of them exhibited increased expression. The reason for this increase is unknown; however, the AHR can induce mitochondrial stress and decrease the organelle's oxidative phosphorylation efficiency (Tappenden et al., 2011). Directly linking AHR to maintenance of the expression of genes necessary for mitochondrial function, such as *Nd1* and *Nd4*, might be evidence of a way for the

cell to maintain proper cellular energetics following modulation of the receptor's activity.

The link between mitochondrial function and calcium signaling provides clues to the possible role of crosstalk between TSPO and AHR for cellular homeostasis. There are multiple calcium channels in mitochondria, and the mitochondrial calcium uniporter (MCU) is a major entrance for calcium into the mitochondrial matrix from the intermembrane space. The MCU is a 480 kDa transmembrane protein complex that varies in protein composition among species, but the core MCU protein is highly conserved (Baughman et al., 2011; Sancak et al., 2013). The other proteins comprising the murine MCU are the mitochondrial calcium uptake 1 (MICU1) (Perocchi et al., 2010), the mitochondrial calcium uptake 2 (MICU2) (Plovanich et al., 2013), and the single-pass membrane protein with aspartate rich tail 1 (SMDT1, aka EMRE) (Sancak et al., 2013) (Fig. 3.10). The MCU and SMDT1 proteins make up the transmembrane portion of MCU complex, and MICU1 and MICU2 are located on the intermembrane space side to control calcium entry (Csordás et al., 2013). It is currently proposed that at low intermembrane calcium levels, the MICU proteins act to prevent the entry of calcium ions into the matrix (Payne et al., 2017). At high intermembrane calcium levels, this inhibition is removed and allows for the increase of the matrix calcium level. The data showed that loss of both AHR and TSPO caused the expression of *Micu2* to decrease to an undetectable level within vehicle-treated MLE-12 cells. The location of AHR and TSPO could provide some clues as to why they influence expression of components in the MCU. Hwang et al. (2016) showed that a portion of the cellular pool of AHR is located within the intermembrane space, so it is possible that the receptor could physically interact with the MICU2 protein projecting into that region. TSPO is known to interact with VDAC in the outer membrane of mitochondria (McEnery et al., 1992), which functions to allow transport of molecules into the intermembrane space, including calcium. These calcium ions could then be funneled into the mitochondrial matrix

through the MCU. Gatliff et al. (2017) found that loss of TSPO caused an elevation of calcium uptake into mitochondria after ATP stimulation. This would match the proposal that TSPO limits calcium uptake through VDAC and supports the observation of the decrease in *Micu2* expression in TSPO-/- cells. The cells could be reacting to remove the inhibition of calcium flow into the MCU as a reaction to the higher concentration of calcium in the intermembrane space. The ability of AHR and TSPO to modulate the gene expression of components of the MCU is a possible mechanism for the two proteins to modulate mitochondrial function by regulating the entry of calcium into the matrix.

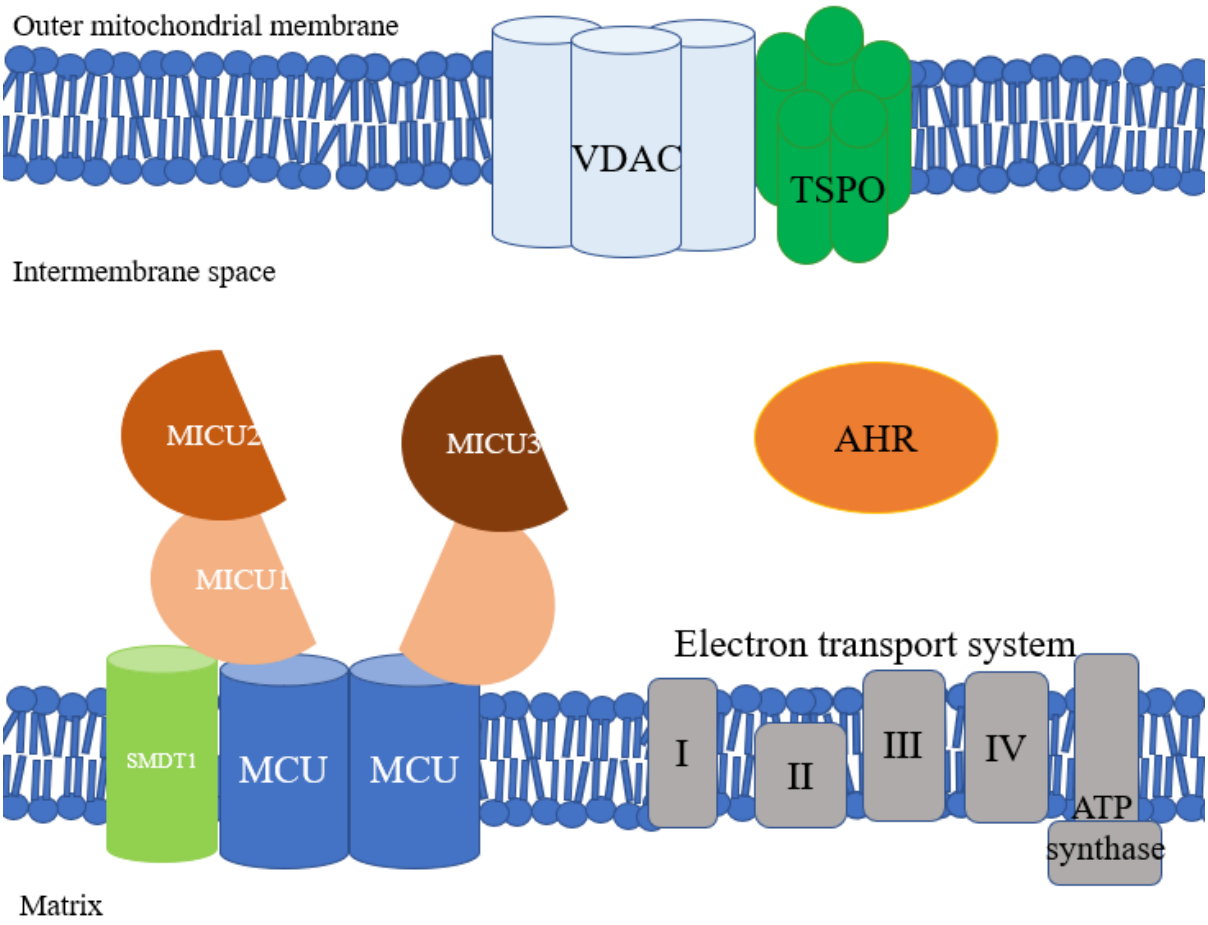

Figure 3.10 Proteins influenced by the possible crosstalk of AHR and TSPO in mitochondria. Voltage-dependent anion channel (VDAC) located in the outer mitochondrial membrane along with TSPO. The MCU complex partially in the inner mitochondrial membrane made up of mitochondrial calcium uniporter (MCU), mitochondrial calcium uptakes 1-3 (MICUs), and single-pass membrane protein with aspartate rich tail 1 (SMDT1). Proposed location of AHR located in intermembrane space.

Most functions of the AHR have been attributed to nuclear DNA binding, but a growing number of AHR-dependent outcomes have suggested that this might not be the only utility of the receptor. Independent of DNA binding, agonists of the receptor can still elicit effects including altering cholesterol synthesis proteins (Tanos et al., 2012)and cell cycle progress (Kohle et al., 1999). The AHR would also not be the first transcription factor receptor proposed to be located in mitochondria as the estrogen receptor (Cammarata et al., 2004; S.-H. Yang et al., 2004), glucocorticoid receptor (Psarra et al., 2005; Scheller et al., 2000), and thyroid receptor (Hashizume

& Ichikawa, 1982; Morrish et al., 2006) have all been detected there. There is even evidence that certain hormones have the ability to influence mitochondrial RNA synthesis including thyroid hormone (Barsano et al., 1977) and glucocorticoids (Van Itallie, 1992). The AHR could similarly act to modulate mitochondrial activity.

In an attempt to determine the level of cell-type specificity of these results, two additional CRISPR cell lines were created for AHR and TSPO knockouts in a mouse liver line (Hepa1c1c7). The RNA gene expression experiments comparing the MLE-12 and Hepa1c1c7 indicated that the functions of AHR and TSPO tend to vary between cell types. While cell lines have been immortalized, they still retain characteristics of their tissue of origin. It is possible that AHR and TSPO have different functions in lung cells versus liver cells due to the interaction with other cell-type specific protein expression. For example, ABCA1 is used to transport cholesterol out of the cell across the plasma membrane, and cholesterol regulation is most likely very different in the two tissues (Chen et al., 2022). For example, the liver is primarily a cholesterol producing organ, while this is not the case for the lung, and therefore the difference in expression patterns observed in the MLE12 vs. Hepa1c1c7 is understandable. *Gpr39* was the only gene analyzed that showed a similar expression pattern in both cell types. G-Protein Coupled Receptor 39 (GPR39) is classified as an orphan receptor, but zinc has been proposed to be an endogenous ligand (Holst et al., 2007). Currently no direct link has been established between AHR or TSPO and GPR39. GRP39, when overexpressed, has been found to prevent lipid accumulation and reduce mitochondrial stress in a liver cell model of nonalcoholic fatty liver disease (NAFLD) (Chen & Lou, 2022). Taken together, these findings might suggest that GPR39 is regulated in an AHR- and/or TSPO-dependent manner to maintain mitochondrial homeostasis. More studies across cell types will be needed to understand the complex relationship between AHR and TSPO.

The RNA-seq study described in chapter 3 provides evidence that AHR and TSPO are able to impact similar groups of genes that might indicate they participate in crosstalk. The direct pathway of this interaction is still not known but in the future experiments, like proximity ligation assays, could be conducted to see where and if AHR and TSPO have protein-protein interactions. It still needs to be understood if AHR and TSPO just have similar functions or if they have a more direct connection.

CHAPTER 4: INFLUENCE OF AHR AND TSPO ON PARKINSON'S GENE *LRRK2*

Abstract

More than ten million people in the world are currently living with Parkinson's, a disease which causes limb shaking and motor difficulties due to the progressive loss of dopaminergic neurons. Most cases are not strictly genetic but having mutations in certain genes including LRRK2 does increase the risk of developing the disease. While characterizing the CRISPR AHR-/- and TSPO-/- cells, it was discovered that in both BV-2 and MLE-12 cells loss of TSPO decreased the RNA and protein levels of LRRK2. AHR-/- cells were more variable, but they trended to have a decrease in LRRK2 protein. Attempts were made to measure downstream targets of LRRK2 kinase activity, but so far Western blots for phosphorylated proteins were unsuccessful. One MLE-12 cell line did exhibit enlarged vacuole-type structures which could be lamellar bodies like those observed in the LRRK2 kinase inhibitor animal studies. Understanding how AHR and TSPO interact normally with LRRK2 might help provide information for how LRRK2 mutations factor in the development of Parkinson's disease. Modulating the activity of AHR and TSPO could provide ways to help cells maintain cellular homeostasis and prevent mitochondrial dysfunction.

Results

TSPO-/- BV-2 have elongated cell bodies after 24-hour LPS treatment

Lipopolysaccharide (LPS) is used to induce activation of microglial cells because it is a molecule found in the outer membrane of Gram-negative bacteria, and cells react as if they are encountering an actual bacterium. Observations of mouse microglial BV-2 cells used in this lab showed that cells treated with LPS became elongated with polarized projections by 3 hours. After 24 hours, the projections shrank back and multiple shorter, bulbous projections formed.

Many of the TSPO-/- BV cells, however, still had elongated cell bodies after 24 hours of LPS treatment (Fig. 4.1D). The LPS-treated wild-type averaged 44 µM in length and the LPS-treated TSPO-/- E6 had an average length of 51 µM which was not significant from wild-type cells ($p=0.4484$).

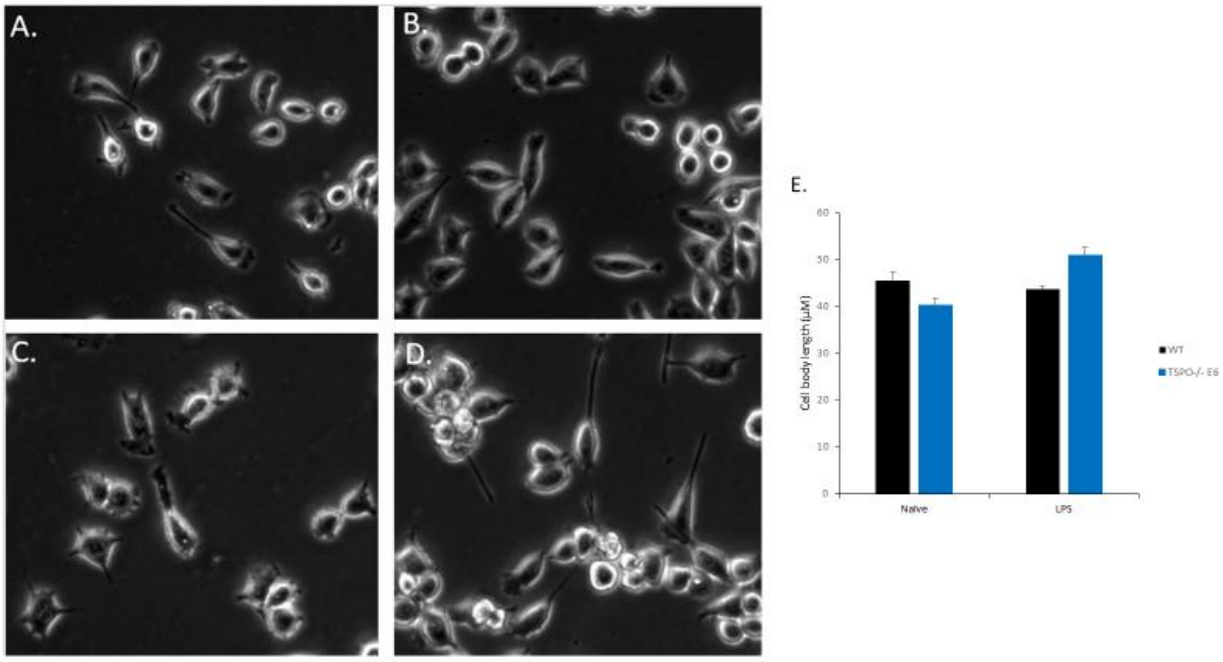

Figure 4.1 TSPO-/- BV-2 cells have non significantly elongated cell bodies 24 hours after LPS treatment. WT and TSPO-/- E6 BV-2 cells were plated at 60,000 cells per well and treated with 1 µg/ml LPS after 24 hours. Images were captured using Olympus Ix51 microscope and cell body length measured using MicroSuite Five after 24 hours. WT naïve (**A**). TSPO-/- E6 naïve (**B**). WT LPS (**C**). TSPO-/- E6 LPS (**D**). Graphical representation of length measurements. Error bars represent standard error (**E**) Represents three independent experiments.

LRRK2 Expression in BV-2 and MLE-12 CRISPR AHR-/- and TSPO-/- cells

In the attempt to discover why the BV-2 TSPO-/- cells remained elongated, a paper by Choi et al. (2015) was found with a supplementary video showing *Lrrk2* knockdown microglial cells with a sustained elongated polar phenotype like the activated TSPO-/- cells. It was proposed that TSPO might be interacting with LRRK2 in some way or be influencing the same movement/chemotaxis pathway. So, the expression levels of LRRK2 were compared in the available CRISPR knock out cells. According to the MLE-12 RNA-seq results, the level of *Lrrk2* decreased 7.19-fold (padj=3.2 E-08) in the vehicle G10 TSPO-/- compared to the vehicle wild-type cells (Table 4.1). The level of *Lrrk2* decreased 2.15-fold (padj=0.02) in the vehicle AHR-/- compared to the vehicle wild-type cells (Table 4.1). Treatment with TCDD (10nM, 6 hrs), PK 11195 (100 nM, 6hrs), or cotreatment did not significantly change the *Lrrk2* expression of MLE-12 wild-type, AHR-/-, or TSPO-/- cells.

	Lrrk2			
Cell type	Control	TCDD	PK 11195	TCDD+PK 11195
WT	0.2251	0.1721	0.2147	0.2497
AHR-/-	0.1048	0.0776	0.0910	0.0972
TSPO-/-	0.0323	0.0345	0.0321	0.0461

Table 4.1 Loss of AHR and TSPO results in the decreased expression of *Lrrk2* in MLE-12 cells. RNA was isolated from control, TCDD (10 nM, 6hrs), PK 11195 (100 nM, 6hrs), and TCDD+PK 11195 (10nM and 100 nM respectively, 6hrs) MLE-12 wild-type (WT), AHR-/-, and TSPO-/- cells using TRIzol protocol and sequenced by Novogene. Data were normalized and represented as fragments per kilobase per million mapped reads (fpkm). Red = padj < 0.05 compared to wild type cells within treatment. Represents three biological replicates.

To test the RNA-seq results, RNA was collected from untreated MLE-12 cells including the additional TSPO-/- A8 and analyzed using SYBR Green qRTPCR. The SYBR Green results supported the RNA-seq for both of the TSPO-/- cells. Expression of *Lrrk2* was decreased -368.60-fold ($p<0.001$) in TSPO-/- G10 cells and 167.28-fold ($p<0.001$) in TSPO-/- A8 cells (Fig. 4.2). Many of the cycle values were even undetected after 40 cycles, so the fold decrease could actually be larger. Expression of *Lrrk2* in AHR-/- cells had a significant 1.6-fold-increase ($p=0.0005$) over wild-type (Fig. 4.2).

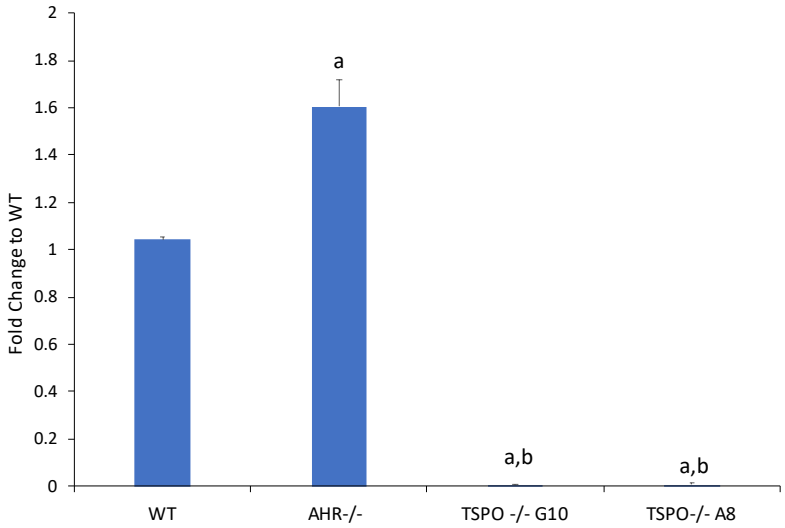

Figure 4.2 Knocking out TSPO in MLE-12 cells decreases the RNA expression of *Lrrk2* from wild-type (WT). MLE-12 cells were grown in 6-well dishes in triplicates, collected in TRIzol, and RNA isolated according to manufacturer's protocol. cDNA was created using GoScript Reverse Transcriptase per manufacturer's protocol. qRTPCR was performed using SYBR Green MasterMix. Gene expression was normalized using the geometric mean of housekeeping genes, *Hprt*, *Actb*, and *18s*, and calculated using $\Delta\Delta C_T$ method. Final comparisons were made as fold change to the wild-type control. Error bars represent standard error. a=significance from WT $p<0.05$. b= significance from AHR-/- $p<0.05$. Represents three independent experiments.

To examine LRRK2 at the protein level, whole cell extracts of untreated MLE-12 WT, AHR-/-, and TSPO-/- cells were collected and run on SDS-PAGE gels (Figs. 4.3,4.4). Similar to the RNA data, LRRK2 protein was decreased 5.8-fold ($p=0.0002$) in G10 TSPO-/- cells and 6.6-

fold (p=0.0002) in A8 TSPO-/- when compared the wild-type (Fig. 4.3B). In many of the trials, TSPO-/- had no detectable LRRK2. A third TSPO-/- MLE-12 cell line (1.1G) also showed very low levels of LRRK2 (Fig. 4.3C).

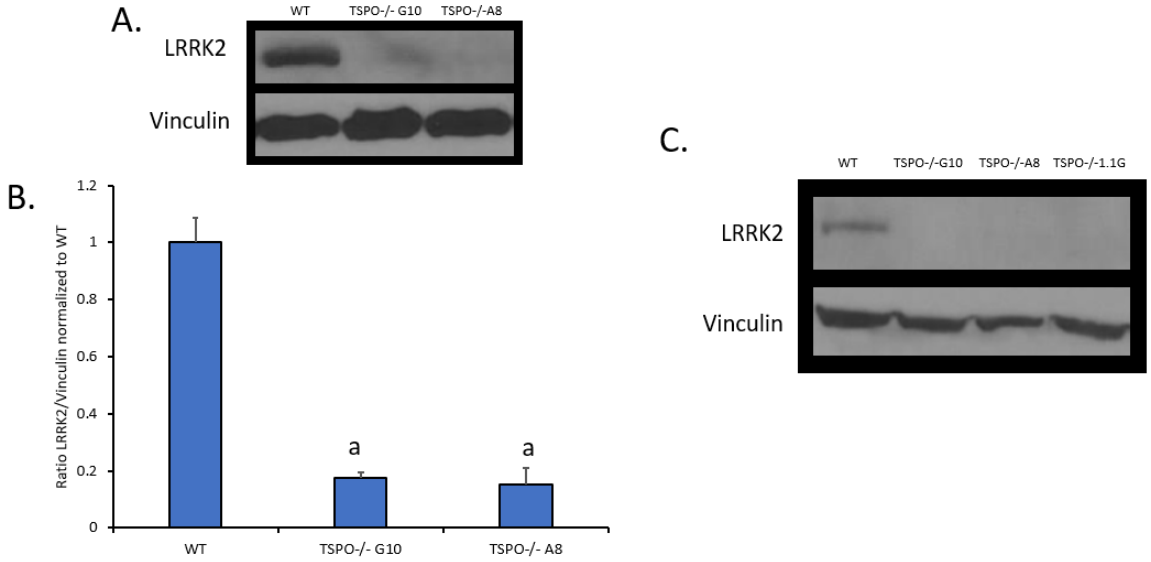

Figure 4.3 Knocking out TSPO in MLE-12 cells decreases the protein concentration of LRRK2. Exponentially growing wild-type (WT) ,TSPO-/- G10, and TSPO-/-A8 were collected in RIPA buffer. Whole cell protein (150 µg) was separated by SDS-PAGE and protein was transferred to nitrocellulose and probed for LRRK2 and Vinculin as loading control **(A).** Graphical representation of densitometry of blots described in A. Error bars represent standard error. a=significance from WT $p<0.05$. Represents three independent experiments. (**B**). Representative Western blot showing lack of LRRK2 in TSPO-/- 1.1G from one independent experiment (**C**).

Western blot analysis of LRRK2 in AHR-/- MLE-12 cells was variable (Fig.4.4). There were blots that showed no LRRK2 to blots that showed similar level of LRRK2 as the wild-type cells. Most blots showed LRRK2 in AHR-/- cells but less than wild-type cells. The cause for the variation has not been determined yet.

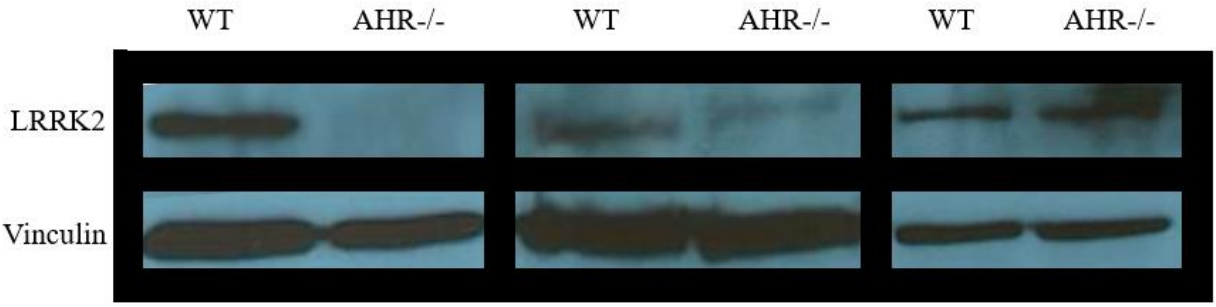

Figure 4.4 Level of LRRK2 protein varies in AHR-/- MLE-12 cells. Untreated wild-type (WT) and AHR-/- MLE-12 cells were collected in RIPA buffer and 80-100 µg of whole cell extract was run on 6% SDS-PAGE gel. Protein was transferred to nitrocellulose membrane and probed for LRRK2 and Vinculin (loading control). Represents three independent experiments.

Other cell types were also studied to determine if LRRK2 decrease was a cell line/type specific effect. It was found that the Hepa1c1c7 cells do not have detectable *Lrrk2* levels when analyzed with SYBR Green and Western Blot (data not shown).

BV-2 cells, however, did express LRRK2 protein. Based on Western blot trials, LRRK2 was decreased 10.2-fold in DMSO-treated (0.01%, 24 hrs) TSPO-/- BV-2 cells compared to DMSO-treated wild-type but not significantly ($p=0.529$) (Fig. 4.5B). Treatment with AHR ligand TCDD (30 nM, 24 hours) non significantly decreased LRRK2 expression 1.7-fold ($p=0.5179$) in wild-type cells compared to wild-type DMSO control (Fig. 4.5B). There was essentially no change in TSPO-/- cells between DMSO and TCDD-treated cells ($p>0.9999$). One trial was conducted testing exposure of BV-2 wild-type and TSPO-/- to TSPO ligand PK 11195 (0-200 nM, 0.01% ethanol control in all) for 24 hours but there appeared to be no large changes.

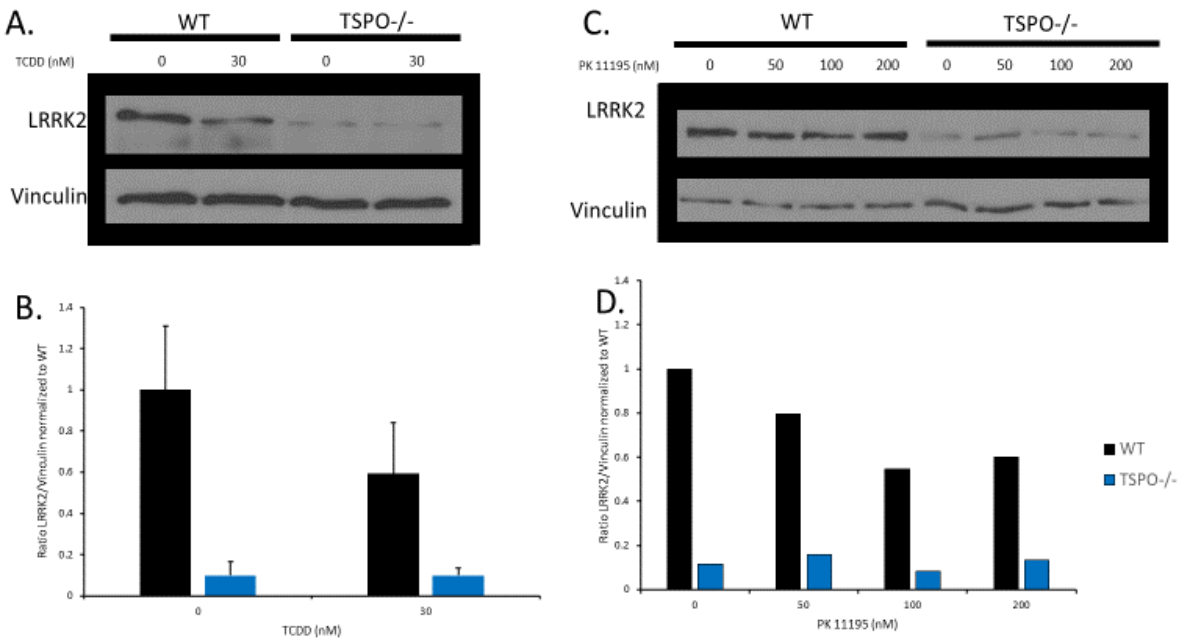

Figure 4.5 Knocking out TSPO in BV-2 cells trends to decreases protein concentration of LRRK2. Exponentially growing wild-type (WT) and TSPO-/- E6 BV-2 cells were exposed to 30 nM TCDD for 24 hours and then collected in RIPA buffer. Whole cell protein (100 µg) was separated by SDS-PAGE and protein was transferred to nitrocellulose and probed for LRRK2 and Vinculin as loading control (**A**). Graphical representation of densitometry from A. Error bars represent standard error. Represents three independent experiments (**B**). WT and TSPO-/- E6 cells were exposed to PK 11195 (0-200 nM, 0.01% ethanol) for 24 hours and then collected in RIPA buffer. Whole cell protein (150 µg) was separated by SDS-PAGE and protein was transferred to nitrocellulose and probed for LRRK2 and Vinculin as loading control (**C**)**.** Graphical representation of densitometry from C. Represents one independent experiment (**D**).

Lrrk1 is a homolog of *Lrrk2* found in both humans and mice, but previous knockout evidence shows that it functions more in bone maintenance (Xing et al., 2013). The expression of *Lrrk1* was not significantly different between the wild-type, AHR-/- or TSPO-/- in the RNA-seq experiment (data not shown).

Western blotting of phosphorylated LRRK2 targets including Ras-Related GTP-Binding Protein 10 (RAB10) and p38 Mitogen Activated Protein Kinase (p38 MAPK) were attempted but the phospho-proteins could not be detected even in positive controls, so better collection techniques will need to be used to maintain the phosphorylated state or try other antibodies.

Indication of lamellar bodies modifications in TSPO-/- cells

LRRK2 is suspected to be involved in lysosomal maintenance, and animal LRRK2 kinase inhibitor studies showed an increase in the size of lamellar bodies, a lysosomal-like organelle that transports surfactant in alveolar type II cells. In preliminary observations of MLE-12 TSPO-/- G10 cells, there appeared to be many cells that possessed clear circular bodies which might be lamellar bodies (Figs. 4.6C-D). The wild-type and AHR-/- do not have as many cells with these structures or as large (Figs.4.6A-B).

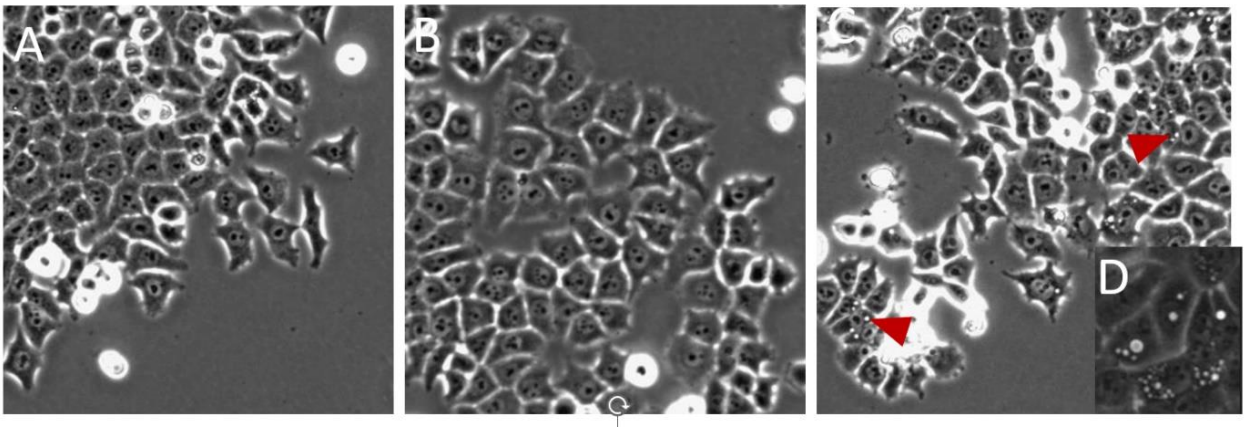

Figure 4.6 TSPO-/- G10 MLE-12 exhibit possible large lamellar bodies which are rarer in wild-type and AHR-/- cells. MLE-12 cells were plated for growth assay and images taken 72 hours after plating. Wild-type 20x(**A**). AHR-/-20x(**B**). TSPO-/-20x. Red arrows designate possible lamellar bodies (**C**). TSPO-/- 40x(**D**). Representative images.

To determine if TSPO-/- G10 cells had differential expression of lamellar body genes, the RNA-seq data was analyzed. It was found that the gene for *Surfactant associated protein b* (*Sftpb*) was increased 2.06-fold (padj=9.37E-09) over wild-type cells (Table 4.2). *Surfactant associated protein c* (*Sftbc*) was not significantly changed in the TSPO-/- cells. *ATP binding cassette subfamily a member 3 (Abca3)*, which is used to transport phospholipids into lamellar bodies, was increased 1.25-fold (padj=6.41E-06) compared to wild-type cells. Proteases *Cathepsin C (Ctsc)* and *Cathepsin H (Ctsh)* were increased 1.38 (padj=1.26E-12) and 1.24 (padj=6.35E-0.4) respectively. *Lysosomal associated membrane protein 1 (Lamp1)* was increased 1.13-fold (padj=4.99E-04). LAMP1 is not specific to lamellar bodies and total RNA would represent transcripts for protein destined for lysosomes.

Gene	TSPO-/- fold change to WT	padj
Abca3	1.25	6.41E-06
Ctsc	1.38	1.26E-12
Ctsh	1.24	6.35E-04
Lamp1	1.13	4.99E-04
Sftpb	2.06	9.37E-09
Sftbc	1.30	5.87E-01

Table 4.2 Expression of lamellar body genes increased in RNA-seq data in TSPO-/- G10 compared to WT.

TSPO-/- microglia trend to be more resistant to paraquat toxicity

Paraquat exposure has been suspected of being an environmental cause of Parkinson's symptoms. To characterize the impact of loss of TSPO on paraquat-induced toxicity, WT and TSPO-/- BV-2 cells were treated with paraquat (25, 50, or 100 µM, 24 hours). Mitochondrial dehydrogenase activity was measured with MTT assay to determine if paraquat could have an effect on immune cell viability. No significant differences were observed between the wild-type cells and TSPO-/- cells at any of the concentrations tested, but the TSPO-/- trended to have a higher percentage of respective control MTT conversion at all test concentrations (Fig. 4.7). At 25 µM paraquat, WT averaged 65% of respective untreated control and TSPO-/- averaged 122%. At 50 µM paraquat, WT averaged 46% and TSPO-/- averaged 109%. At 100 µM paraquat, WT averaged 18% and TSPO-/- averaged 68% (Fig 4.7).

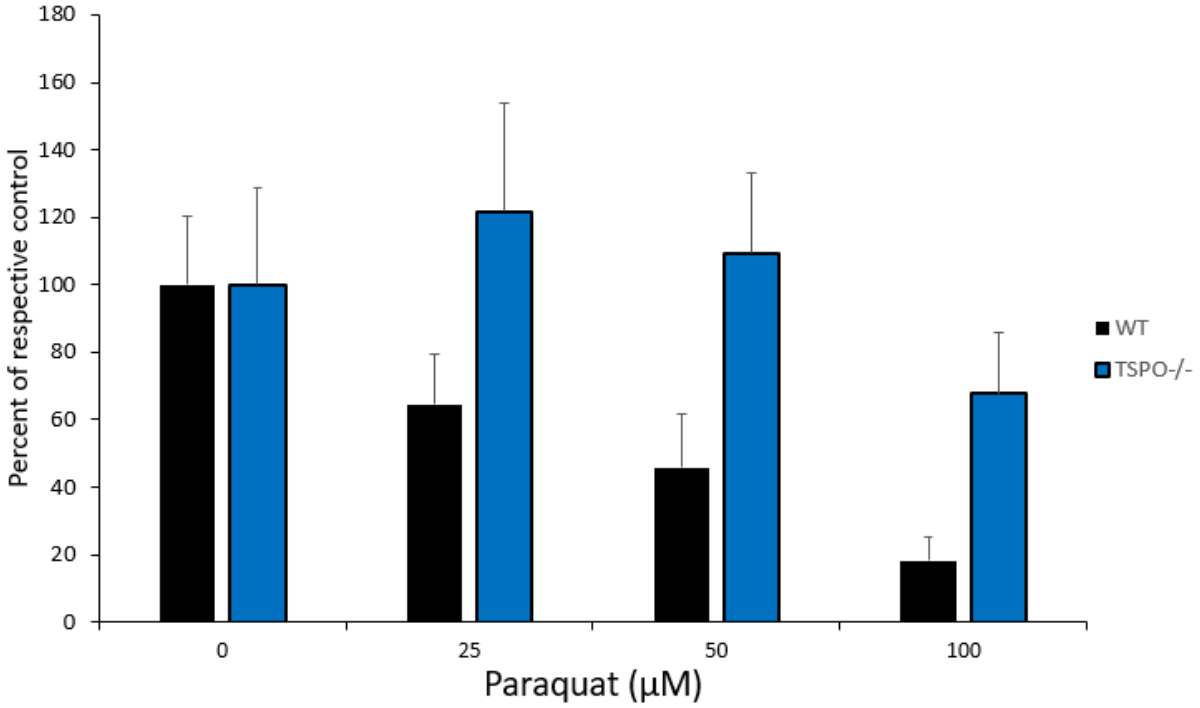

Figure 4.7 Paraquat-induced toxicity in WT and TSPO-/- E6 cells. Wild-type (WT) and TSPO-/- E6 BV-2 cells were plated at 3,000 cells per well in 96-well dish. After 24 hours, both were treated with 0-100 µM paraquat. After 24-hour incubation, medium was removed and replaced with MTT (0.5 mg/ml) for 1 hour. MTT medium was replaced with 100% DMSO and absorbance was read at 570 nM using a SpectraMax ABS Plus. Error bars represent standard error. Represents three to four independent experiments.

Discussion

Chapter 3 of this dissertation found that both AHR and TSPO could influence the expression of genes involved in modulating mitochondrial homeostasis. The next step was to determine what functional consequences result from loss of AHR and TSPO. After LPS-activation, TSPO-/- BV-2 cells remained elongated and failed to adopt the classic ameboid shape of the wild-type cells. A supplementary video from Choi et al. (2015) showed that *Lrrk2* knockdown microglia had a very similar phenotype with elongated polar processes. It was predicted that TSPO might affect the expression of LRRK2. The level of *Lrrk2* expression was checked first in the MLE-12 RNA-seq data and this provided confirmation with *Lrrk2* expression

dropping dramatically in TSPO-/- cells. This decrease was confirmed in three MLE-12 TSPO-/- cell lines (with two different CRISPR guide RNA regions) at the RNA and protein level. This decrease was confirmed in a second cell line in the TSPO-/- BV-2 cell line at the protein level.

Mutations in LRRK2 are some of the most common mutations found in familial Parkinson's disease cases. The role of this gene in Parkinson's progression is still largely unknown, so it will be crucial to find any genes that might influence or be influenced by LRRK2. Linking TSPO to the level of LRRK2 is an interesting find because it again connects LRRK2 to mitochondria and possibly to ligands of TSPO.

The location of TSPO embedded in the outer mitochondrial membrane allows for the protein to be able to interact with the cytosolic exterior and the intermembrane space. There are regions of the cell where the endoplasmic reticulum (ER) is located close to mitochondria, termed mitochondrial-associated membranes (MAMs). It is in these regions that substances are able to be shuttled between the ER and mitochondria including calcium (Szabadkai et al., 2006) and possibly heme (Guilarte et al., 2016; Loth et al., 2020). VDAC is known to bind to ER inositol 1,4,5-trisphosphate receptor (IP_3R) at MAMs to conduct calcium from the ER to mitochondria (Szabadkai et al., 2006). TSPO has been found to precipitate with VDAC, suggesting that these two proteins might work together, and forming this connection between the ER and mitochondria might be one of their co-functions. The kinase activity of LRRK2 has been proposed to be involved in the tethering of ER and mitochondrial outer membranes at MAMs (Toyofuku et al., 2020). So, there is a possibility that TSPO affects the amount of LRRK2 present at MAMs to modulate this connection. According to the RNA-seq data, loss of TSPO did not significantly alter the RNA level of *Vdac1* (-1.09-fold from WT, padj=0.08). This would suggest that if TSPO did have an effect on VDAC1 it would be through functional activity, not

abundance. There is evidence that LRRK2 might be involved with the movement of mitochondrial creatine kinase (MtCK) into the mitochondria, a translocation needed to influence the interaction of VDAC with adenine nucleotide translocase (ANT) (Cui et al., 2011). ANT is a protein located in the inner mitochondrial membrane that is thought to interact with VDAC to form the permeability transition pore complex (PTPC) that is involved in mitochondrial apoptotic signaling (Marzo et al., 1998). This postulation would suggest that LRRK2 could have the ability to influence the opening of the PTPC and mitochondrial apoptosis signaling. Influence over VDAC activity could give some reasoning for why loss of TSPO also causes a loss of LRRK2.

The level of LRRK2 in AHR-/- cells was much more variable. In the RNA-seq data, *Lrrk2* expression was significantly decreased in AHR-/- cells but in the qRTPCR data the level was significantly increased in AHR-/- cells. The two RNA studies did have different treatment of the control cells with the RNA-seq controls being exposed to vehicle levels of DMSO and EtOH and the qRTPCR studies just used cell culture medium. The percentage of DMSO (0.003%) and EtOH (0.005%) used should have been low enough to not cause any cell damage, but sometimes low levels of chemicals have unexpected effects on cellular systems. The cell densities could also have been slightly different between the experiments. The AHR findings could not be substantiated in BV-2 cells because of the current lack of a knockout in that cell type. There is also only one AHR knockout in the MLE-12 cells. Hepa1c1c7 cells could not be used because they did not have detectable LRRK2.

LRRK2 is proposed to have many functions but one phenotype observed in multiple species is an enlargement of lamellar bodies in lungs with kinase inhibition of LRRK2. The MLE-12 TSPO-/- G10 cells also contained more numerous vacuole-like structures that might be

lamellar bodies and had modest but significant increases in the expression of genes known to be constituents of lamellar bodies. It is not known exactly what action of LRRK2 causes the enlargement, but it is predicted that it could be decreased exocytosis. Knockout *Lrrk2* mice have decreased levels of surfactant c in their bronchoalveolar lavage fluid supporting the idea that less surfactant is being released from the cells (Araki et al., 2021). The A8 TSPO-/-, however, do not seem to match the phenotype of the G10. To determine if the TSPO-/- do or do not have enlarged lamellar bodies, quantitative fluorescent microscopic studies will need to be conducted with dyes that label lipids like Nile Red. This will help to determine what the structures are and if the TSPO A8 have any that are significantly larger than the wild-type cells.

It is also of note that *Nuclear factor of activated T cells 2 (Nfatc2)* expression was increased in both the RNA-seq (4.78-fold, padj= 3.02E-17) and qRTPCR (3.13-fold, $p<0.0001$) (Fig 3.9F) in the control TSPO-/- G10 cells compared to control wild-type cells. NFATC2 (or NFAT1 as protein) is a calcium-dependent transcription factor that is influenced by LRRK2 activity (Liu et al., 2011). Loss of LRRK2 causes the nuclear accumulation of NFAT1, and LRRK2 overexpression prevents the nuclear translocation after ionomycin-induced calcium influx (Liu et al., 2011). So, the increase in *Nfatc2* in the TSPO-/- cells might be in reaction to less LRRK2. The story is complicated though because *Nfatc2* expression decreases in AHR-/- cells according to RNA-seq (-33.56-fold, padj= 4.76E-06) and qRTPCR (-44.25-fold, $p=0.0031$) (Fig. 3.9F). The Hepa1c1c7 cells, which lack detectable LRRK2, did not have any differences between either of the knockouts and the wild-type cells in the qRTPCR trials (Fig. 3.9F).

The low penetrance of LRRK2 mutation for Parkinson's development implies that additional environmental agents might factor into causing the disease. Paraquat is a toxic herbicide that is still used worldwide. It has been suspected of being an environmental inducer of

Parkinson's disease, but this is still controversial (Weed, 2021). Paraquat does have a similar structure to MPP^+ (a known cause of Parkinson's symptoms in humans) but it appears that paraquat does not impact complex I like MPP^+ (Richardson et al., 2005). Paraquat exposure has been shown to increase the production of reactive oxygen species and activation of microglia (Xiao et al., 2022) but this has also been disputed (Klintworth et al., 2009). So, the nonsignificant maintenance of cell viability in TSPO-/- BV-2 cells compared to wild-type cells after paraquat exposure could be due to the TSPO-/- cells not being activated by the paraquat or by being more resistant to reactive oxygen species production. LPS-induced activation of BV-2 cells decreases the ability to convert MTT (data not shown) so the trend of wild-type having decreased MTT conversion would match an activation endpoint. Reactive oxygen species are also produced more by microglial cells after activation (Banati et al., 1993; Zhang et al., 2018). TSPO-/- cells failing to adopt the classic activated phenotype after LPS treatment supports a lack of activation. This study provides evidence that microglial activation may be involved in paraquat toxicity, and loss of TSPO can alter that.

This chapter found that both AHR and TSPO could influence the expression of LRRK2, a protein associated with mitochondrial dynamics and a strong link to Parkinson's disease. A specific measure of LRRK2 activity will need to be developed to understand what the consequence of its loss is along with TSPO and AHR. It will be crucial to understand how AHR and TSPO normally interact with LRRK2 to get a better understanding of what happens during the development of Parkinson's disease.

CHAPTER 5: CONCLUSIONS

Specific Aim 1: Determine the localization and influence of AHR in mitochondria

Transmission electron microscopy provided evidence that AHR is located inside of mitochondria, but lack of image quality prevented any concrete spatial designation. Future studies will be required to increase the resolution of the images and use of AHR-/- cells will provide more support for specific binding. It would also be interesting to look at the TSPO-/- cells to see the impact on mito-AHR.

Individual electron transport complex assays with AHR-deficient cells did not show any change in enzyme activity after TCDD treatment from AHR-sufficient. This implies that AHR impact on mitochondria might not be through direct impact on electron transport complexes. Quantitative fluorescent studies could be conducted in the future to measure aspects of mitochondrial health like mitochondrial density, membrane potential, and reactive oxygen species production per cell along with ligand treatment.

Specific Aim 2: Characterize possible crosstalk between AHR and TSPO

CRISPR/Cas9 technology was used to create AHR and TSPO knockouts in several mouse cell lines. RNA-sequencing was conducted on MLE-12 knockouts and differences were observed when the AHR -/- and TSPO -/- cells were compared to WT controls. Differentially expressed genes included a significant number of mitochondrial genes, such as those used for calcium transport, and also AHR battery genes in TSPO-/- cells. The next step for determining the interaction of AHR and TSPO will be to test how close they come together physically with experiments such as a proximity ligation assay. Double mutants (AHR-/-TSPO-/-) could be made using CRISPR to compare DREs to the single mutants DREs.

Specific Aim 3: Investigate the influence of TSPO and AHR on factors involved in the development of neurodegenerative diseases specifically LRRK2 and downstream effects

Chapter 4 provided evidence that loss of TSPO in both mouse lung and microglial cell lines resulted in a drastic decrease in LRRK2 RNA and protein expression. The loss of AHR did not produce as clear results, as LRRK2 concentration varied at both the RNA and protein level between trials. Future experiments will need to determine functional consequences of the loss of LRRK2 including phosphorylation analysis of known LRRK2 targets. The interaction of LRRK2 and TSPO will also need to be further scrutinized to determine how direct of an interaction it is or if it is just reactionary. Different proposed ligands of TSPO could be used to see what effect they have on LRRK2 expression. Studying LRRK2 knockouts or G2019S gain of kinase mutants would be informative based on what happens to levels of TSPO in them.

Conclusion

Currently it is estimated that 60,000 to 95,000 adults, ages 45 and older, will be diagnosed with Parkinson's disease each year in North America (Willis et al., 2022). Traditionally, the most common form of medical remedy for Parkinson's is adding back dopamine to patients with dopamine precursor levo-3,4- dihydroxy-phenylalanine (levodopa, L-Dopa) (Cotzias et al., 1969). While levodopa can help with the motor symptoms, it does not prevent the further degeneration of dopaminergic neurons. As a result of this, patients can have periods where their symptoms return before their next dose because they have progressively fewer neurons to receive the dopamine (Ahlskog & Muenter, 2001). That is why it would be highly valuable to find druggable targets that would prevent the further degradation of neurons. The finding that AHR and TSPO are involved in modulating mitochondrial homeostasis and LRRK2 abundance could offer new disease targets with AHR or TSPO ligands.

CHAPTER 6: MATERIALS AND METHODS

Cell Culture

Mouse microglial (BV-2) cells were grown in Dulbecco's Modified Eagle Medium: Nutrient Mixture F-12 (Thermo Fisher Scientific, Waltham, MA) supplemented with fetal bovine serum (9.7%, Hyclone, Fisher Scientific, Waltham, MA), penicillin/streptomycin (100 units/mL penicillin, 100 µg/mL of streptomycin, Thermo Fisher Scientific, Waltham, MA), and L-glutamine (2 mM, Thermo Fisher Scientific, Waltham, MA). Mouse hepatoma Hepa1c1c7 cells were grown in Dulbecco's Modified Eagle Medium (Thermo Fisher Scientific, Waltham, MA) supplemented with Cosmic Calf Serum (8.9%, Hyclone, Fisher Scientific, Waltham, MA), penicillin/streptomycin (100 units/mL penicillin, 100 µg/mL of streptomycin, Thermo Fisher Scientific, Waltham, MA), and MEM sodium pyruvate solution (0.89 mM, Atlanta Biologicals, Flowery Branch, GA). Mouse hepatoma Hepac12 cells were grown in Dulbecco's Modified Eagle Medium (Thermo Fisher Scientific, Waltham, MA) supplemented with Cosmic Calf Serum (8.9%, Hyclone, Fisher Scientific, Waltham, MA), and MEM sodium pyruvate solution (0.89 mM, Atlanta Biologicals, Flowery Branch, GA). Mouse lung epithelial type II cell line 12 (MLE-12) cells were grown in Dulbecco's Modified Eagle Medium: Nutrient Mixture F-12 (Thermo Fisher Scientific, Waltham, MA) supplemented with fetal bovine serum (2%, Hyclone, Fisher Scientific, Waltham, MA), Insulin-Transferrin-Sodium selenite liquid medium supplement (1.0 mg/ml-0.55 mg/ml-0.5 µg/ml, Sigma-Aldrich, St. Louis, MO), hydrocortisone (10 nM, Sigma-Aldrich, St. Louis, MO), β-estradiol (10 nM, Sigma-Aldrich, St. Louis, MO), HEPES (10 mM, Sigma-Aldrich, St. Louis, MO), L-glutamine (2 mM, Thermo Fisher Scientific, Waltham, MA), and penicillin/streptomycin (100 units/mL penicillin, 100 µg/mL of streptomycin, Thermo Fisher Scientific, Waltham, MA). Cells were grown in a NAPCO 8000 incubator (Thermo Fisher Scientific, Waltham, MA) at 37°C and 5% CO_2.

Mitochondrial fractionation

Mitochondria were isolated from Hepa1c1c7 using protocols adapted from (Frezza et al., 2007; T. T. Yang et al., 2009). Cells were washed with cold phosphate buffered saline (PBS) (4°C) and scraped off of the plates using cell scraper in mitochondrial buffer B (250 mM sucrose, 20 mM HEPES, 1 mM EDTA, 1 mM EGTA, 1 mM dithiothreitol (DTT), and 0.2 mM phenylmethylsulfonyl fluoride (PMSF). Each sample was then homogenized with 100 strokes in a 7 ml Dounce tissue grinder (Wheaton, Millville, NJ) on ice. Insoluble material was removed by centrifugation (400 x g for 10 min at 4°C). The supernatant was cleared by centrifugation (10000 x g for 10 min at 4°C). The pellet was resuspended in mitochondrial buffer B. Insoluble material was removed by centrifugation (2000 x g for 10 min at 4°C). The supernatant was cleared by centrifugation (9000 x g for 10 min at 4°C). The pellet was resuspended in mitochondrial buffer B and the previous step repeated. The pellet was resuspended in mitochondrial buffer B.

Transmission electron microscopy (TEM)

Mouse liver hepatoma cell line (Hepa1c1c7) cells or isolated mitochondria were fixed with 4% electron microscopy (EM) grade paraformaldehyde (Electron Microscopy Sciences, Hatfield, PA) and 1% EM grade glutaraldehyde (Electron Microscopy Sciences, Hatfield, PA). After fixation, samples were embedded by Dr. Alicia Withrow in The Center for Advanced Microscopy at Michigan State University. Samples were stained with rabbit polyclonal anti-AHR (BML-SA210-0100, Enzo Life Sciences, Inc., Farmingdale, NY) at 1/5 and 1/10 dilution. Samples were counterstained with Goat-anti-rabbit IgG (H&L) 10 nM EM Grade secondary (Electron Microscopy Sciences, Hatfield, PA). Cells were visualized using a JEOL 1400 Flash (JEOL USA, Inc., Peabody, MA) using 27,000-50,000X magnification.

Electron Transport Complex Assays

The activities of the individual ETC complexes, ATP synthase and citrate synthase were determined as previously described with slight modifications (Barrientos et al., 2009). Each enzyme solution was prepared by suspension of mitochondrial pellets either in a hypotonic buffer [25 mM KPO4 (pH 7.4) and 5 mM MgCl2] for citrate synthase, complex I, complex II, complex IV, and complex V or in mitochondrial buffer A for complex II+III and complex III. After three cycles of freezing/thawing, protein concentration was determined using a Bradford Assay protocol and bovine serum albumin standards (Sigma-Aldrich, St. Louis, MO). Absorbance was read at 595 nm using SpectraMax ABS Plus (Molecular Devices, LLC, San Jose, CA). The enzyme activities were determined at 37 °C for complex I and V and at 30 °C for the other ETC complexes and citrate synthase. The enzyme activity was calculated by (Δabs/min)×(total assay volume)/[ε×(mitochondrial volume)×(mitochondrial concentration)] with units of micromoles per min per milligram (ε: extinction coefficient). The enzymatic activity was calculated as a ratio, dividing each activity in micromoles per min per milligram protein by the citrate synthase activity. The absorbance for each enzymatic activity was measured using a SpectraMax M2 spectrophotometer (Molecular Devices, Sunnyvale, CA). Cytochrome c was bovine heart cytochrome c.

Citrate Synthase Assay: 5 µg of each enzyme solution was incubated with citrate synthase buffer [50 mM KPO4 (pH 7.4), and 0.1 mM DTNB] containing 100 µM acetyl CoA, in a cuvette for 5 min. The change of absorbance was measured at 412 nm for 2 min for reference. After addition of 100 µM oxaloacetate, the change in absorbance at 412 nm was recorded for 3 min. Enzyme activity was calculated with ε for the thionitrobenzoate anion (13.6 mM^{-1} cm^{-1}).

Complex I Assay: 50 µg of each enzyme solution was mixed with complex I buffer [50

mM KPO4 (pH 7.4), 140 µM NADH, 1 mM KCN, 10 µM antimycin A, 0.1% BSA, and 50 µM DCPIP] with 1% ethanol and 50 µM Coenzyme Q1 (CoQ1) in a cuvette. The change in absorbance at 340 nm was recorded for 3 min. Reference was measured in the presence of 2.5 µM rotenone (dissolved in ethanol). Enzyme activity was calculated with ε for the NADH (6.22 mM^{-1} cm^{-1}).

Complex II assay: 10 µg of each enzyme solution was incubated with complex II buffer [50 mM KPO4 (pH 7.4), 10 mM succinate, 1 mM KCN, 2.5 µM rotenone, and 10 µM antimycin A] for 10 min in a cuvette. After addition of 50 µM DCPIP, the change in absorbance at 600 nm was recorded for 2 53 min for reference. The change in absorbance at 600 nm was then recorded for 3min in the presence of 50 µM CoQ1. Enzyme activity was calculated with ε for the DCPIP (19.1 mM^{-1} cm^{-1}). Complex II+III assay 10 µg of each enzyme solution was incubated with complex II+III buffer [50 mM KPO4 (pH 7.4), 10 mM succinate, 1 mM KCN, 2.5 µM rotenone, 0.1% BSA, 0.075% EDTA, and 1 mM ATP] in a cuvette for 5 min. Upon addition of 32 µM cytochrome c, absorbance at 550 nm was recorded for 5 min. The reference was measured in the absence of cytochrome c. Enzyme activity was calculated with ε for the reduced cytochrome c (19.6 mM^{-1} cm^{-1}).

Complex III assay: 5 µg of each enzyme solution was mixed with complex III buffer [50 mM KPO4 (pH 7.4), 1 mM n-dodecyl maltoside, 1 mM KCN, 2.5 µM rotenone, and 0.1% BSA] with 100 µM decylbenzolquinol and 30 µM cytochrome c in a cuvette. The change in absorbance at 550 nm was recorded for 3 min. Cytochrome c was fully reduced at the end of the measurement with dithionite. The reference was measured without enzyme solution. Enzyme activity was calculated with ε for the reduced cytochrome c (19.6 mM^{-1} cm^{-1}).

Complex IV Assay: Reduced cytochrome c was prepared using sodium dithionite. 10 µg

of each enzyme solution was mixed with complex IV buffer [40 mM KPO4 buffer (pH 6.8), 0.5% Tween 80, and 0.4 mg/mL reduced cytochrome c] in a cuvette. The change in absorbance at 550 nm was recorded for 2 min. 5 mM potassium ferricyanide was added to fully oxidized cytochrome c at the end of the measurement. The reference was measured without enzyme solution. Enzyme activity was calculated with ε for the reduced cytochrome c (19.6 mM^{-1} cm^{-1}).

Complex V Assay: Complex V buffer [40 mM Tris-HCO3 (pH 8.0), 1 mM EGTA, 5 mM MgCl2, 0.2 mM NADH, 2.5 mM phosphoenolpyruvate, 0.5 µM antimycin A, 15 µM CCCP, 50 µg/mL lactate dehydrogenase, and 50 µg/mL pyruvate kinase] was incubated with 2.5 mM ATP for 2 min in a cuvette. After 10 µg of each enzyme solution was added to the above mixture, the change in absorbance at 340 nm was recorded for 5 min. The reference was measured in the presence of 2 µM oligomycin for 5min. Enzyme activity was calculated with ε for the NADH (6.22 mM^{-1} cm^{-1}).

Kynurenine Binding Assay

The kynurenine binding affinity to wild-type *Rhodobacter spheroids* TSPO (RsTSPO) was measured by tryptophan fluorescence quenching assay as previously described (Li et al., 2013). 2.5 µM purified RsTSPO WT protein (in 20mM Tris pH 8.0, 150mM NaCl, 0.20% DM, 2mM TCEP) was titrated with increasing amounts of kynurenine dissolved in DMSO, at room temperature. The quenching curve was measured by a fluorescence scan from 290 to 400 nm (excitation at 285 nm) on an Agilent Eclipse® fluorescence spectrometer (Agilent, Santa Clara, CA). Control experiments were also performed to evaluate the absorption and emission of ligands as well as buffers and solvents. The dissociation constant Kd was calculated by fitting the binding curve with Hill equations.

CRISPR Knockout Cell Generation

The genes coding for AHR and TSPO were knocked out in BV-2, Hepa1c1c7, and MLE-12 cells using CRISPR/Cas9 protocol based on Ran et al. (2013). Guide oligos were ligated into pSpCas9 (BB)-AA-Puro.

Guide oligo primers for *Ahr* 1.4 were:

Forward 5'-CACCGGGCGCGGGCACCATGAGCAG-3'

Reverse 5'-AAACCTGCTCATGGTGCCCGCGCCC-3'.

Guide oligo primers for *Tspo* 1.1 were:

Forward 5'-AAACCCGGTGGTATGCTAGCTTGCC-3'

Reverse 5'-CACCGGCAAGCTAGCATACCACCGG-3'

Guide oligo primers for *Tspo* 2.2 were:

Forward 5'- AAACCCTCGCTGGACACTGGCTCCC-3'

Reverse 5'- CACCGGGAGCCAGTGTCCAGCGAGG-3'

Plasmids were transfected into cells using Lipofectamine 2000 (Thermo Fisher Scientific, Waltham, MA) based on manufacturer's protocol. Potential knockout cells were selected using puromycin (5 µg/ml). After three days cells were diluted to a density of one cell per well in a 96-well dish and then clonally expanded. Gene knockout was confirmed through Western blotting and characterized using Sanger sequencing.

Western Blot

Whole cells were collected in radio-immunoprecipitation assay (RIPA) lysis buffer (50 mM Tris-HCl, 150 mM NaCl, 1% Igepal, 1mM EDTA, 0.25% Na-deoxycholate) supplemented with cOmplete™, Mini Protease Inhibitor Cocktail (Sigma-Aldrich, St. Louis, MO). Protein concentration was determined using a Bradford Assay protocol with Pierce Detergent Compatible

Bradford Assay Reagent (Thermo Fisher Scientific, Waltham, MA) and bovine serum albumin standards (Sigma-Aldrich, St. Louis, MO). Absorbance was read at 595 nm using SpectraMax ABS Plus (Molecular Devices, LLC, San Jose, CA). 150 µg of whole cell protein for TSPO and 200 µg for AHR (37.5 µg for Hepa1c1c7) was separated on a 15% sodium dodecyl sulfate−polyacrylamide gel for TSPO and an 8% gel for AHR. For LRRK2, 100 µg of BV-2 whole cell protein and 150 µg of MLE-12 whole cell protein was separated on a 6% sodium dodecyl sulfate−polyacrylamide gel. Proteins were transferred to Amersham Protran 0.2 NC nitrocellulose membrane (GE Healthcare Life Sciences, Chicago, IL) using Trans-Blot Semi-Dry Transfer Cell (Bio-Rad Laboratories, Hercules, CA). The membranes were stained with the following primary antibodies: rabbit polyclonal anti-AHR (BML-SA210-0100, Enzo Life Sciences, Inc., Farmingdale, NY), rabbit monoclonal anti-LRRK2 (ab133474, Abcam, Cambridge, UK), and rabbit monoclonal anti-TSPO (ab109497, Abcam, Cambridge, UK). Anti-β-actin mouse monoclonal (sc-47778, Santa Cruz Biotechnology, Inc., Dallas, TX) was used as the loading control for AHR and TSPO. Anti-Vinculin rabbit monoclonal (13901S, Cell Signaling Technology, Danvers, MA) was used as the loading control for LRRK2. The membranes were then labeled with either horseradish peroxidase (HRP) conjugated mouse anti-rabbit secondary (sc-2357, Santa Cruz Biotechnology, Inc., Dallas, TX) or HRP-conjugated mouse IgGκ light chain binding protein (sc-516102, Santa Cruz Biotechnology, Inc., Dallas, TX) according to host of primary antibody. Super Signal West Femto Maximum Sensitivity Substrate (Thermo Fisher Scientific, Waltham, MA) or Pierce™ ECL Western Blotting Substrate (Thermo Fisher Scientific, Waltham, MA) was used to visualize bands. Densitometry analysis was conducted using ImageJ (National Institutes of Health, Bethesda, MA). Bands were normalized to respective loading control and compared to wild-type controls.

DNA Sequencing

DNA was isolated from wild-type and CRISPR knockouts of BV-2, Hepa1c1c7, and MLE-12 cells using Dneasy Blood & Tissue Kit (Qiagen, Hilden, Germany). DNA was amplified using Q5 High-Fidelity DNA Polymerase (New England Biolabs, Ipswich, MA) according to the manufacturer's protocol. The annealing temperatures for the polymerase chain reaction (PCR) were 67^{o}C for AHR 1.4 and 71^{o}C for TSPO 1.1 and 2.2.

PCR primers for *Ahr* 1.4 were:

Forward 5'-GAGTCTCCTCTGTCGCCCGC -3'

Reverse 5'-CCGTCACTCACGTTTTCT -3'

PCR primers for *Tspo* 1.1 were:

Forward 5'-GCCGTGGGCCTCACTCTGGTGC-3'

Reverse 5'-CTACCCCATGGCTGAATACAGTGTGC-3'

PCR primers for *Tspo* 2.2 were:

Forward 5'-GGAGCCTACTTTGTACGTGGC-3'

Reverse 5'-GATTCCAGGGGCAACAGAGCACAGC-3'

The PCR fragments were confirmed with 2% agarose gel electrophoresis and then sequenced using Sanger Sequencing 96 capillary electrophoretic ABI 3730xl platform at the Michigan State University Research Technology Support Facility Genomics Core. Sequences were visualized as chromatograms using FinchTV Version 1.4.0 (Geospiza Inc., Seattle, WA).

Trypan Blue cell growth curves

MLE-12 cells were plated at 40,000 cells per well in a 6-well dish. At each time point cells were removed from duplicate wells using trypsin solution (trypsin 0.25%, Atlanta Biologicals, Flowery Branch, GA; 1 mM EDTA; Hank's Balanced Salts, Sigma-Aldrich, St. Louis, MO). Cells

were stained with trypan blue solution (0.4%, Sigma-Aldrich, St. Louis, MO) and counted using Bright-Line hemacytometer (Reichert, Buffalo, NY). Cell density was determined at approximately 23, 47, and 71 hours after plating.

MTT Cell Growth Curves

MLE-12 cells were plated at a density of 1,334 cells per well in a 96-well dish in technical triplicates. At 24, 48, and 72 hours after plating, old medium was removed and replaced with cell culture medium containing thiazolyl blue tetrazolium bromide (MTT) (0.5 mg/ml, Sigma-Aldrich, St. Louis, MO). Cells were incubated with MTT medium for 1 hour in 37°C incubator. After incubation MTT medium was removed and replaced with dimethyl sulfoxide (DMSO) (100%, Sigma-Aldrich, St. Louis, MO). Plates were wrapped in aluminum foil and agitated (25^{o}C, 5 minutes). Absorbance was read at 570 nm using a FLUOstar Omega (BMG Labtech, Ortenberg, Germany). Wells without cells served as blanks and their average absorbance was subtracted from sample well absorbances.

Novogene RNA-Sequencing (RNA-seq)

Wild-type, AHR-/-, and TSPO-/- G10 MLE-12 cells were treated with either DMSO (0.003%) and ethanol (0.005%), 2,3,7,8-tetrachlorodibenzo-ρ-dioxin (TCDD, 10 nM) and ethanol (0.005%), 1-(2-chlorophenyl)-N-methyl-N-(1-methyl-propyl)-3-isoquinoline carboxamide (PK11195, 100 nM, Cayman Chemicals, Ann Arbor, MI) and dimethyl sulfoxide (DMSO, 0.003%), or TCDD (10 nM) and PK11195 (100 nM) for 6 hours. Three biological replicates were conducted consisting of one technical replicate each. Cells were collected using TRIzol Reagent (Thermo Fisher Scientific, Waltham, MA) and RNA was isolated using protocol based on manufacturer's guide.

RNA concentration was determined using Qubit fluorometer (Thermo Fisher Scientific,

Waltham, MA) and RNA quality was assessed by the MSU Genomics Core using an Agilent 2100 Bioanalyzer. All samples had to have a purity ≥ 6.8. RNA samples were sequenced, and the data analyzed by Novogene (Sacramento, CA) using Illumina PE150 technology. Genes that had an adjusted p-value of ≤0.05 were considered to be differentially expressed.

Quantitative Real-Time Polymerase Chain Reaction (qRTPCR)

MLE-12 and Hepa1c1c7 cells were plated at density of 85,000 cells/well in 6 well dishes in technical triplicates. The cells were allowed to grow for approximately 48 hours before being collected using TRIzol Reagent (Thermo Fisher Scientific, Waltham, MA). RNA was isolated using protocol based on manufacturer's guide. Complimentary DNA (cDNA) was generated using GoScript Reverse Transcriptase (Promega, Madison, WI) with a c1000 Touch Thermocycler (Bio-Rad Laboratories, Hercules, CA). Samples were analyzed using SYBR Green PCR Master Mix (Applied Biosystems, Thermo Fisher Scientific, Waltham, MA) in QuantStudio 3 Real-Time PCR System (Applied Biosystems, Thermo Fisher Scientific, Waltham, MA). Primers used are listed in Table 6.1. Gene expression was normalized using the geometric mean of housekeeping genes, *Hprt*, *Actb,* and *18s*, and calculated using $\Delta\Delta C_T$ method. Final comparisons were made as fold change to the wild-type control.

Gene	Forward Primer	Reverse Primer	Reference
Abca1	TGAAGCCTGTCCAGGAGTTC	ATGACAAGGAGGATGGAAGC	
Actb	TGTTACCAACTGGGACGACA	GGGGTGTTGAAGGTCTCAAA	
Gpr39	AGTGAGGAGAGCCGGACAG	CAGTCATGTTTGGGTTTTGC	(Egerod et al., 2011)
Gstk1	AGGTTCCCCTCAACATACCC	TGGTTGCTCCATGCTTACAG	(Wang et al., 2018)
Hprt	GCTTACCTCACTGCTTTCCG	ATCGCTAATCACGACGCTGG	
Lrrk2	CAGCTTCAGAAGGGACAAGG	AAGGCTGCGTTCTCAGGATA	
Micu2	TGGAGCACGACGACGGAGAGTA	GCCAGCTTCTTGACCAGTGT	(Zaglia et al., 2017)
Mt1	GGCTGTCCTCTAAGCGTCAC	GAGTCTTACCGGTGGAGCAG	
Nfatc2	CTTTCAGATGGGAATAAACGTC	TCCTACTCACATAGCAACAGCA	(Chen et al., 2011)
Sftpb	CTTGTCCTCCGATGTTCCAC	GGCCTGGTTGATCACAGACT	
18s	TCGTATTGCGCCGCTAGAGGT	GGGTCATGGGAATAACGCCGC	

Table 6.1 Primer Sequences (5′-3′) used for SYBR Green qRTPCR

BV-2 LPS treatment and cell body length measurements

BV-2 cells were plated at 60,000 cells per 6-well dish. After 24 hours, cells were treated with lipopolysaccharide (LPS) (1 µg/ml, Sigma-Aldrich, St. Louis, MO) for another 24 hours. Cells were visualized using Olympus Ix51 microscope (Olympus, Center Valley, PA). Three images of each cell type and treatment were taken after 24 hours and 45 cells were measured using MicroSuite Five (Olympus, Center Valley, PA).

Paraquat toxicity MTT Assay

BV-2 wild-type and TSPO-/- E6 cells were plated at a density of 3,000 cells per well in a 96-well dish in technical triplicates. Approximately 24 hours after plating, cells were treated with 0-100 µM of paraquat. After 24-hour paraquat incubation, old medium was removed and replaced with cell culture medium containing thiazolyl blue tetrazolium bromide (MTT) (0.5 mg/ml, Sigma-Aldrich, St. Louis, MO). Cells were incubated with MTT medium for 1 hour in 37°C incubator. After incubation, MTT medium was removed and replaced with dimethyl sulfoxide (DMSO) (100%, Sigma-Aldrich, St. Louis, MO) to dissolve the formazan crystals. Plates were wrapped in aluminum foil and put on shaker at room temperature for 5 minutes. Absorbance was read at 570 nm using a SpectraMax ABS Plus (Molecular Devices, LLC, San Jose, CA). Blank wells were measured that did not have any cells but all of the solution changes and subtracted from sample well absorbances.

Statistics

Statistical analyses were performed using Astatsa, MiniTab Version 21.2 (MiniTab LCC, State College, PA) and Prism Version 9.5.1 (GraphPad Software, San Diego, CA). Grubb's test was employed to detect outliers ($p<0.05$). Differences across treatment groups were assessed with one-way or two-way analysis of variance (ANOVA) with a Tukey's pairwise post hoc test

with $p < 0.05$ considered significant.

REFERENCES

Ahlskog, J. E., & Muenter, M. D. (2001). Frequency of levodopa-related dyskinesias and motor fluctuations as estimated from the cumulative literature. *Movement Disorders*, *16*(3), 448–458. https://doi.org/10.1002/mds.1090

Anderson, S., Bankier, A. T., Barrell, B. G., De Bruijn, M. H. L., Coulson, A. R., Drouin, J., Eperon, I. C., Nierlich, D. P., Roe, B. A., Sanger, F., Schreier, P. H., Smith, A. J. H., Staden, R., & Young, I. G. (1981). Sequence and organization of the human mitochondrial genome. *Nature*, *290*(6), 457–465.

Angrish, M. M., Dominici, C. Y., & Zacharewski, T. R. (2013). TCDD-Elicited effects on liver, serum, and adipose lipid composition in C57BL/6 mice. *Toxicological Sciences*, *131*(1), 108–115. https://doi.org/10.1093/toxsci/kfs277

Araki, M., Ito, K., Takatori, S., Ito, G., & Tomita, T. (2021). BORCS6 is involved in the enlargement of lung lamellar bodies in Lrrk2 knockout mice. *Human Molecular Genetics*, *30*(17), 1618–1631. https://doi.org/10.1093/hmg/ddab146

Baccarelli, A., Mocarelli, P., Patterson, D. G., Bonzini, M., Pesatori, A. C., Caporaso, N., & Landi, M. T. (2002). Immunologic effects of dioxins: New results from Seveso and comparison with other studies. *Environmental Health Perspectives*, *110*, 1169–1173. http://ehpnet1.niehs.nih.gov/docs/2002/110p1169-1173baccarelli/abstract.html

Banati, R. B., Gehrmann, J., Schubert, P., & Kreutzberg, G. W. (1993). Cytotoxicity of microglia. *Glia*, *7*(1), 111–118. https://doi.org/10.1002/glia.440070117

Barrientos, A., Fontanesi, F., & Díaz, F. (2009). Evaluation of the mitochondrial respiratory Chain and oxidative phosphorylation system using polarography and spectrophotometric enzyme assays. In *Current Protocols in Human Genetics* (Issue SUPPL.63). Blackwell Publishing Inc. https://doi.org/10.1002/0471142905.hg1903s63

Barsano, C. P., Degroot, L. J., & Getz, G. S. (1977). The Effect of Thyroid Hormone on in Vitro Rat Liver Mitochondrial RNA Synthesis. *Endocrinology*, *100*(52), 52–60. https://academic.oup.com/endo/article/100/1/52/3043585

Baughman, J. M., Perocchi, F., Girgis, H. S., Plovanich, M., Belcher-Timme, C. A., Sancak, Y., Bao, X. R., Strittmatter, L., Goldberger, O., Bogorad, R. L., Koteliansky, V., & Mootha, V. K. (2011). Integrative genomics identifies MCU as an essential component of the mitochondrial calcium uniporter. *Nature*, *476*(7360), 341–345. https://doi.org/10.1038/nature10234

Bell, D. R., & Poland, A. (2000). Binding of aryl hydrocarbon receptor (AhR) to AhR-interacting protein: The role of hsp90. *Journal of Biological Chemistry*, *275*(46), 36407–36414. https://doi.org/10.1074/jbc.M004236200

Bernassau, J. M., Reversat, J. L., Ferrara, P., Caput, _F D, & Lefur, G. (1993). A 3D model of the peripheral benzodiazepine receptor and its implication in intra mitochondrial cholesterol transport. *Journal of Molecular Graphics*, *11*, 236–244.

Bernheimer, H., Birkmayer, W., Hornykiewicz, O., Jellinger, K., & Seitelberger, F. (1973). Brain Dopamine and the Syndromes of Parkinson and Huntington Clinical, Morphological and Neurochemical Correlations*. *Journal of the Neurological Sciences*, *20*, 41–455.

Betarbet, R., Sherer, T., MacKenzie, G., Garcia-Osuna, M., Panov, A., & Greenamyre, J. (2000). Chronic systemic pesticide exposure reproduces features of Parkinson's disease. *Nature Neuroscience*, *3*(12), 1301–1306.

Bibb, M. J., Van Etten, R. A., Wright, C. T., Walberg, M. W., & Clayton, D. A. (1981). Sequence and Gene Organization of Mouse Mitochondrial DNA. *Cell*, *26*, 167–180.

Blasi, E., Barluzzi, R., Bocchini, V., Mazzolla, R., & Bistoni, F. (1990). Immortalization of murine microglial cells by a v-raf/v-myc carrying retrovirus. *Journal of Neuroimmunology*, *27*, 229–237.

Bonello, F., Hassoun, S. M., Mouton-Liger, F., Shin, Y. S., Muscat, A., Tesson, C., Lesage, S., Beart, P. M., Brice, A., Krupp, J., Corvol, J. C., & Corti, O. (2019). LRRK2 impairs PINK1/Parkin-dependent mitophagy via its kinase activity: Pathologic insights into Parkinson's disease. *Human Molecular Genetics*, *28*(10), 1645–1660. https://doi.org/10.1093/hmg/ddz004

Boverhof, D. R., Burgoon, L. D., Tashiro, C., Chittim, B., Harkema, J. R., Jump, D. B., & Zacharewski, T. R. (2005). Temporal and dose-dependent hepatic gene expression patterns in mice provide new insights into TCDD-mediated hepatotoxicity. *Toxicological Sciences*, *85*(2), 1048–1063. https://doi.org/10.1093/toxsci/kfi162

Braestrup, C., & Squirest, R. F. (1977). Specific benzodiazepine receptors in rat brain characterized by high-affinity [3H] diazepam binding (affinity binding/diazepam/anxiolytic activity/brain membranes/regional distribution). *Biochemistry*, *74*(9), 3805–3809.

Brown, A. J., Leong, S.-L., Dean, R. T., & Jessup, W. (1997). 7-Hydroperoxycholesterol and its products in oxidized low density lipoprotein and human atherosclerotic plaque. *Journal of Lipid Research*, *38*, 1730–1745.

Cammarata, P. R., Chu, S., Moor, A., Wang, Z., Yang, S. H., & Simpkins, J. W. (2004). Subcellular distribution of native estrogen receptor α and β subtypes in cultured human lens epithelial cells. *Experimental Eye Research*, *78*(4), 861–871. https://doi.org/10.1016/j.exer.2003.09.027

Campesato, L. F., Budhu, S., Tchaicha, J., Weng, C. H., Gigoux, M., Cohen, I. J., Redmond, D., Mangarin, L., Pourpe, S., Liu, C., Zappasodi, R., Zamarin, D., Cavanaugh, J., Castro, A. C., Manfredi, M. G., McGovern, K., Merghoub, T., & Wolchok, J. D. (2020). Blockade of the AHR restricts a Treg-macrophage suppressive axis induced by L-Kynurenine. *Nature Communications*, *11*(1). https://doi.org/10.1038/s41467-020-17750-z

Caramaschi, F., Del Corno, G., Favaretti, C., Giambelluca, S. E., Montesarchio, E., & Fara, G. M. (1981). Chloracne Following Environmental Contamination by TCDD in Seveso, Italy. *International Journal of Epidemiology*. https://academic.oup.com/ije/article/10/2/135/658836

Carayon, P., Portier, M., Dussossoy, D., Bord, A., Petitprgtre, G., Canat, X., Le Fur, G., & Casellas, P. (1996). Involvement of Peripheral Benzodiazepine Receptors in the Protection of Hematopoietic Cells Against Oxygen Radical Damage. *Blood*, *8*, 3170–3178.

Carlsson, A., Lindqvist, M., & Magnusson, T. (1957). 3,4-Dihydroxyphenylalanine and 5-hydroxy-tryptophan as reserpine antagonists. *Nature*, *180*, 1200–1200.

Carter, C. D., Kimbrough, R. D., Liddle, J. A., Cline, R. E., Zack, M. M., Barthel, W. F., Koehler, R. E., & Phillips, P. E. (1975). Tetrachlorodibenzodioxin: An Accidental Poisoning Episode in Horse Arenas. *Source: Science*, *188*(4189), 738–740.

Carver, L. A., Lapres, J. J., Jain, S., Dunham, E. E., & Bradfield, C. A. (1998). Characterization of the Ah receptor-associated protein, ARA9. *Journal of Biological Chemistry*, *273*(50), 33580–33587. https://doi.org/10.1074/jbc.273.50.33580

Chambers, D., Wilson, L., Maden, M., & Lumsden, A. (2007). RALDH-independent generation of retinoic acid during vertebrate embryogenesis by CYP1B1. *Development*, *134*(7), 1369–1383. https://doi.org/10.1242/dev.02815

Chen, C., Kuo, J., Wong, A., & Micevych, P. (2014). Estradiol modulates translocator protein (tspo) and steroid acute regulatory protein (StAR) via Protein Kinase A (PKA) signaling in hypothalamic astrocytes. *Endocrinology*, *155*(8), 2976–2985. https://doi.org/10.1210/en.2013-1844

Chen, L., Zhao, Z. W., Zeng, P. H., Zhou, Y. J., & Yin, W. J. (2022). Molecular mechanisms for ABCA1-mediated cholesterol efflux. *Cell Cycle*, *21*(11), 1121–1139. https://doi.org/10.1080/15384101.2022.2042777

Chen, M. K., & Guilarte, T. R. (2008). Translocator protein 18 kDa (TSPO): Molecular sensor of brain injury and repair. *Pharmacology and Therapeutics*, *118*(1), 1–17. https://doi.org/10.1016/j.pharmthera.2007.12.004

Chen, Q., & Lou, Y. (2022). G protein-coupled receptor 39 alleviates mitochondrial dysfunction and hepatocyte lipid accumulation via SIRT1/Nrf2 signaling. *Journal of Bioenergetics and Biomembranes*. https://doi.org/10.1007/s10863-022-09953-4

Chen, W., Zhang, X., Siu, R. K., Chen, F., Shen, J., Zara, J. N., Culiat, C. T., Tetradis, S., Ting, K., & Soo, C. (2011). Nfatc2 is a primary response gene of nell-1 regulating chondrogenesis in ATDC5 cells. *Journal of Bone and Mineral Research*, *26*(6), 1230–1241. https://doi.org/10.1002/jbmr.314

Cherra, S. J., Steer, E., Gusdon, A. M., Kiselyov, K., & Chu, C. T. (2013). Mutant LRRK2 elicits calcium imbalance and depletion of dendritic mitochondria in neurons. *American Journal of Pathology*, *182*(2), 474–484. https://doi.org/10.1016/j.ajpath.2012.10.027

Chiba, K., Trevor, A., & Castagnoli, N. (1984). Metabolism of the neurotoxic tertiary amine, MPTP, by brain monoamine oxidase. *Biochemical and Biophysical Research Communications*, *120*(2), 574–578.

Choi, I., Kim, B., Byun, J. W., Baik, S. H., Huh, Y. H., Kim, J. H., Mook-Jung, I., Song, W. K., Shin, J. H., Seo, H., Suh, Y. H., Jou, I., Park, S. M., Kang, H. C., & Joe, E. H. (2015). LRRK2 G2019S mutation attenuates microglial motility by inhibiting focal adhesion kinase. *Nature Communications*, *6*. https://doi.org/10.1038/ncomms9255

Cotzias, G., Papavasiliou, P., & Gellene, R. (1969). Modification of Parkinsonism-Chronic treatment with L-Dopa. *The New England Journal of Medicine*, *280*(7), 337–345.

Csordás, G., Golenár, T., Seifert, E. L., Kamer, K. J., Sancak, Y., Perocchi, F., Moffat, C., Weaver, D., De la Fuente, S., Bogorad, R., Koteliansky, V., Adijanto, J., Mootha, V. K., & Hajnóczky, G. (2013). MICU1 controls both the threshold and cooperative activation of the mitochondrial Ca2+ uniporter. *Cell Metabolism*, *17*(6), 976–987. https://doi.org/10.1016/j.cmet.2013.04.020

Cui, J., Yu, M., Niu, J., Yue, Z., & Xu, Z. (2011). Expression of leucine-rich repeat kinase 2 (LRRK2) inhibits the processing of uMtCK to induce cell death in a cell culture model system. *Bioscience Reports*, *31*(5), 429–437. https://doi.org/10.1042/BSR20100127

Cui, Y., Liang, Y., Ip, M. S. M., & Mak, J. C. W. (2021). Cigarette smoke induces apoptosis via 18 kDa translocator protein in human bronchial epithelial cells. *Life Sciences*, *265*. https://doi.org/10.1016/j.lfs.2020.118862

D E Souza, E. B., H Anholt, R. R., M Murphy, K. M., Snyder, S. H., & Kuhar, M. J. (1985). Peripheral-Type Benzodiazepine Receptors in Endocrine Organs: Autoradiographic Localization in Rat Pituitary, Adrenal, and Testis*. *Endocrinology*, *116*(2), 567–572. https://academic.oup.com/endo/article/116/2/567/2538985

Daher, J. P. L., Volpicelli-Daley, L. A., Blackburn, J. P., Moehle, M. S., & West, A. B. (2014). Abrogation of α-synuclein -mediated dopaminergic neurodegeneration in LRRK2-deficient rats. *Proceedings of the National Academy of Sciences of the United States of America*, *111*(25), 9289–9294. https://doi.org/10.1073/pnas.1403215111

De Abrew, K. N., Kaminski, N. E., & Thomas, R. S. (2010). An integrated genomic analysis of aryl hydrocarbon receptor-mediated inhibition of B-cell differentiation. *Toxicological Sciences, 118*(2), 454–469. https://doi.org/10.1093/toxsci/kfq265

de la Monte, S., & Goel, A. (2022). Agent Orange reviewed: Potential role in peripheral neuropathy and neurodegeneration. *Journal of Military and Veterans' Health*, *30*(2), 17–26.

Denison, M. S., Fisher, J. M., & Whitlock, J. P. (1988). The DNA recognition site for the dioxin-Ah receptor complex. Nucleotide sequence and functional analysis. *Journal of Biological Chemistry*, *263*(33), 17221–17224. https://doi.org/10.1016/s0021-9258(19)77819-3

Detmer, S. A., & Chan, D. C. (2007). Functions and dysfunctions of mitochondrial dynamics. *Nature Reviews Molecular Cell Biology*, *8*(11), 870–879. https://doi.org/10.1038/nrm2275

Dornbos, P., Crawford, R. B., Kaminski, N. E., Hession, S. L., & LaPres, J. J. (2016). The influence of human interindividual variability on the low-dose region of dose-response curve induced by 2,3,7,8-tetrachlorodibenzo-p-dioxin in primary B Cells. *Toxicological Sciences*, *153*(2), 352–360. https://doi.org/10.1093/toxsci/kfw128

Dornbos, P., Jurgelewicz, A., Fader, K. A., Williams, K., Zacharewski, T. R., & LaPres, J. J. (2019). Characterizing the Role of HMG-CoA Reductase in Aryl Hydrocarbon Receptor-Mediated Liver Injury in C57BL/6 Mice. *Scientific Reports*, *9*(1). https://doi.org/10.1038/s41598-019-52001-2

Duncan, D. M., Burgess, E. A., & Duncan, I. (1998). Control of distal antennal identity and tarsal development in Drosophila by spineless-aristapedia, a homolog of the mammalian dioxin receptor. *Genes & Development*, *12*, 1290–1303. www.genesdev.org

Egerod, K. L., Jin, C., Petersen, P. S., Wierup, N., Sundler, F., Holst, B., & Schwartz, T. W. (2011). β-cell specific overexpression of GPR39 protects against streptozotocin-induced hyperglycemia. *International Journal of Endocrinology*, *2011*. https://doi.org/10.1155/2011/401258

El-Deprawy, S. R., Boegman, R. J., Jhamandas, K., & Beninger, R. J. (1985). The neurotoxic actions of quinolinic acid in the central nervous system1. *Canadian Journal of Physiology and Pharmacology*, *64*, 369–375.

Environmental Protection Agency. (n.d.). *1983 Press Release: Joint federal/state action taken to relocate Times Beach residents*. Epa.Gov.

Fan, J., Campioli, E., Sottas, C., Zirkin, B., & Papadopoulos, V. (2020). AMhR2-Cre–mediated global TSPO knockout. *Journal of the Endocrine Society*, *4*(2). https://doi.org/10.1210/jendso/bvaa001

Favreau, L. V, & Pickett, C. B. (1991). Transcriptional regulation of the Rat NAD(P)H: Quinone reductase gene. *The Journal of Biological Chemistry*, *266*(7), 4556–4561.

Ferguson-Miller, S., & Babcock, G. T. (1996). Heme/Copper Terminal Oxidases. *Chemical Reviews*, *96*(7), 2889–2907. https://pubs.acs.org/sharingguidelines

Fernandez-Salguero, P. M., Hilbert, D. M., Rudikoff, S., Ward, J. M., & Gonzalez, F. J. (1996). Aryl-hydrocarbon Receptor-Deficient Mice Are Resistant to 2,3,7,8-Tetrachlorodibenzo-p-dioxin-Induced Toxicity. *Toxicology and Applied Pharmacology*, *140*, 173–179.

Fernandez-Salguero, P., Pineau, T., Hilbert, D. M., Mcphail, T., Lee, S. S. T., & Kimura, S. (1995). Immune system impairment and hepatic fibrosis in mice lacking the dioxin-binding Ah receptor. *Science*, *268*. http://www.sciencemag.org.proxy2.cl.msu.edu/

Förstl, H., & Levy, R. (1991). F. H. Lewy on Lewy bodies, parkinsonism and dementia. *International Journal of Geriatric Psychiatry*, *6*(11), 757–766. https://doi.org/10.1002/gps.930061102

Frezza, C., Cipolat, S., & Scorrano, L. (2007). Organelle isolation: Functional mitochondria from mouse liver, muscle and cultured filroblasts. *Nature Protocols*, *2*(2), 287–295. https://doi.org/10.1038/nprot.2006.478

Fuji, R. N., Flagella, M., Baca, M., Baptista, M. A. S., Brodbeck, J., Chan, B. K., Fiske, B. K., Honigberg, L., Jubb, A. M., Katavolos, P., Lee, D. W., Lewin-Koh, S.-C., Lin, T., Liu, X., Liu, S., Lyssikatos, J. P., O'mahony, J., Reichelt, M., Roose-Girma, M., … Watts, R. J. (2015). Effect of selective LRRK2 kinase inhibition on nonhuman primate lung. *Science Translational Medicine*, *7*. https://www.science.org

Funayama, M., Hasegawa, K., Kowa, H., Saito, M., Tsuji, S., & Obata, F. (2002). A new locus for Parkinson's Disease (PARK8) maps to chromosome 12p11.2-q13.1. *Annals of Neurology*, *51*(3), 296–301. https://doi.org/10.1002/ana.10113

Gallager, D. W., Mallorga, P., Oertel, W., Henneberry, R., & Tallman, J. (1981). [3H] Diazepam binding in mammalian central nervous system: A pharmacological characterization. *The Journal of Neuroscience*, *1*(2), 218–225.

Gatliff, J., East, D. A., Singh, A., Alvarez, M. S., Frison, M., Matic, I., Ferraina, C., Sampson, N., Turkheimer, F., & Campanella, M. (2017). A role for TSPO in mitochondrial Ca2+ homeostasis and redox stress signaling. *Cell Death and Disease*, *8*(6). https://doi.org/10.1038/cddis.2017.186

Germelli, L., Pozzo, E. Da, Giacomelli, C., Tremolanti, C., Marchetti, L., Wetzel, C. H., Barresi, E., Taliani, S., Settimo, F. Da, Martini, C., & Costa, B. (2021). De novo neurosteroidogenesis in human microglia: Involvement of the 18 kda translocator protein. *International Journal of Molecular Sciences*, *22*(6), 1–24. https://doi.org/10.3390/ijms22063115

Gincel, D., Zaid, H., & Shoshan-Barmatz, V. (2001). Calcium binding and translocation by the voltage-dependent anion channel : a possible regulatory mechanism in mitochondrial function. *Biochem. J*, *358*, 147–155.

González-Blanco, L., Bermejo-Millo, J. C., Oliveira, G., Potes, Y., Antuña, E., Menéndez-Valle, I., Vega-Naredo, I., Coto-Montes, A., & Caballero, B. (2021). Neurogenic potential of the 18-kda mitochondrial translocator protein (TSPO) in pluripotent p19 stem cells. *Cells*, *10*(10). https://doi.org/10.3390/cells10102784

Greene, J. F., Hays, S., & Paustenbach, D. (2003). Basis for a proposed reference dose (RfD) for dioxin of 1-10 pg/kg-day: A weight of evidence evaluation of the human and animal studies. *Journal of Toxicology and Environmental Health - Part B: Critical Reviews*, *6*(2), 115–159. https://doi.org/10.1080/10937400306470

Guaitoli, G., Raimondi, F., Gilsbach, B. K., Gómez-Llorente, Y., Deyaert, E., Renzi, F., Li, X., Schaffner, A., Jagtap, P. K. A., Boldt, K., Von Zweydorf, F., Gotthardt, K., Lorimer, D. D., Yue, Z., Burgin, A., Janjic, N., Sattler, M., Versées, W., Ueffing, M., … Gloeckner, C. J. (2016). Structural model of the dimeric Parkinson's protein LRRK2 reveals a compact architecture involving distant interdomain contacts. *Proceedings of the National Academy of Sciences of the United States of America*, *113*(30), E4357–E4366. https://doi.org/10.1073/pnas.1523708113

Guilarte, T. R., Loth, M. K., & Guariglia, S. R. (2016). TSPO Finds NOX2 in Microglia for Redox Homeostasis. *Trends in Pharmacological Sciences*, *37*(5), 334–343. https://doi.org/10.1016/j.tips.2016.02.008

Hankinson, O. (1979). Single-step selection of clones of a mouse hepatoma line deficient in aryl hydrocarbon hydroxylase (carcinogen/benzo[alpyrene-resistant clones/stability/fluctuation test). *Cell Biology*, *76*(1), 373–376. https://www.pnas.org

Hashizume, K., & Ichikawa, K. (1982). Localization of 3,5,3'-L-Triiodothyronine Receptor in Rat Kidney Mitochondrial Membranes. *Biochemical and Biophysical Research Communications*, *106*(3), 920–926.

Hatano, T., Kubo, S. ichiro, Imai, S., Maeda, M., Ishikawa, K., Mizuno, Y., & Hattori, N. (2007). Leucine-rich repeat kinase 2 associates with lipid rafts. *Human Molecular Genetics*, *16*(6), 678–690. https://doi.org/10.1093/hmg/ddm013

Hatefi, Y., Haavik, A. G., & Griffiths, D. E. (1962a). Studies on the Electron Transfer System. *The Journal of Biological Chemistry*, *237*(5), 1681–1685.

Hatefi, Y., Haavik, A. G., & Griffiths, D. E. (1962b). Studies on the Electron Transfer System. *Journal of Biological Chemistry*, *237*(5), 1676–1680. https://doi.org/10.1016/s0021-9258(19)83761-4

Hayes, C. L., Spinkt, D. C., Spinkt, B. C., Caot, J. Q., Walker, N. J., & Sutter, T. R. (1996). 17B8-Estradiol hydroxylation catalyzed by human cytochrome P450 1B1. *Medical Sciences, 93*, 9776–9781.

Healy, D. G., Falchi, M., O'sullivan, S. S., Bonifati, V., Durr, A., Bressman, S., Brice, A., Aasly, J., Zabetian, C. P., Goldwurm, S., Ferreira, J. J., Tolosa, E., Kay, D. M., Klein, C., Williams, D. R., Marras, C., Lang, A. E., Wszolek, Z. K., Berciano, J., … Wood, N. W. (2008). Articles Phenotype, genotype, and worldwide genetic penetrance of LRRK2-associated Parkinson's disease: a case-control study. *Lancet Neurology*, *7*, 583–590. https://doi.org/10.1016/S1474

Heidelberger, Charles., Gullberg, M. E., Morgan, Agnes. Fay., & Lepkovsky, Samuel. (1949). Tryptophan metabolism. *Journal of Biological Chemistry*, *179*(1), 143–150. https://doi.org/10.1016/S0021-9258(18)56821-6

Henderson, L. M., Ramasarma, G. B., & Johnson, B. C. (1949). Quinolinic acid metabolism IV. Urinary excretion by man and other mammals as affected by the ingestion of tryptophan. *The Journal of Biochemical Chemistry*, *181*(2), 731–738.

Herzig, M. C., Kolly, C., Persohn, E., Theil, D., Schweizer, T., Hafner, T., Stemmelen, C., Troxler, T. J., Schmid, P., Danner, S., Schnell, C. R., Mueller, M., Kinzel, B., Grevot, A., Bolognani, F., Stirn, M., Kuhn, R. R., Kaupmann, K., Van der putten, P. H., … Shimshek, D. R. (2011). LRRK2 protein levels are determined by kinase function and are crucial for kidney and lung homeostasis in mice. *Human Molecular Genetics*, *20*(21), 4209–4223. https://doi.org/10.1093/hmg/ddr348

Hites, R. A. (2011). Dioxins: An overview and history. *Environmental Science and Technology*, *45*(1), 16–20. https://doi.org/10.1021/es1013664

Holst, B., Egerod, K. L., Schild, E., Vickers, S. P., Cheetham, S., Gerlach, L. O., Storjohann, L., Stidsen, C. E., Jones, R., Beck-Sickinger, A. G., & Schwartz, T. W. (2007). GPR39 signaling is stimulated by zinc ions but not by obestatin. *Endocrinology*, *148*(1), 13–20. https://doi.org/10.1210/en.2006-0933

Hooiveld, M., J Heederik, D. J., Kogevinas, M., Boffetta, P., Needham, L. L., Patterson, D. G., & Bas Bueno, H. (1998). Second Follow-up of a Dutch Cohort Occupationally Exposed to Phenoxy Herbicides, Chlorophenols, and Contaminants. *American Journal of Epidemiology*, *147*(9), 891–901. https://academic.oup.com/aje/article/147/9/891/68169

Hornykiewicz, O. (2002). Dopamine miracle: From brain homogenate to dopamine replacement. *Movement Disorders*, *17*(3), 501–508. https://doi.org/10.1002/mds.10115

Hwang, H. J. (2015). *The role of the aryl hydrocarbon receptor in 2,3,7,8-tetrachlorodibenzo-p-dioxin-induced mitochondrial dysfunction in mouse hepatoma cells*.

Hwang, H. J., Dornbos, P., Steidemann, M., Dunivin, T. K., Rizzo, M., & LaPres, J. J. (2016). Mitochondrial-targeted aryl hydrocarbon receptor and the impact of 2,3,7,8-tetrachlorodibenzo-p-dioxin on cellular respiration and the mitochondrial proteome. *Toxicology and Applied Pharmacology*, *304*, 121–132. https://doi.org/10.1016/j.taap.2016.04.005

Ikuta, T., Eguchi, H., Tachibana, T., Yoneda, Y., & Kawajiri, K. (1998). Nuclear Localization and Export Signals of the Human Aryl Hydrocarbon Receptor*. *The Journal of Biological Chemistry*, *273*, 2895–2904. http://www.jbc.org

Ito, G., Katsemonova, K., Tonelli, F., Lis, P., Baptista, M. A. S., Shpiro, N., Duddy, G., Wilson, S., Ho, P. W. L., Ho, S. L., Reith, A. D., & Alessi, D. R. (2016). Phos-Tag analysis of Rab10 phosphorylation by LRRK2: A powerful assay for assessing kinase function and inhibitors. *Biochemical Journal*, *473*(17), 2671–2685. https://doi.org/10.1042/BCJ20160557

Johnson, M. E., Stringer, A., & Bobrovskaya, L. (2018). Rotenone induces gastrointestinal pathology and microbiota alterations in a rat model of Parkinson's disease. *NeuroToxicology*, *65*, 174–185. https://doi.org/10.1016/j.neuro.2018.02.013

Karp, A. T., Behrensmeyer, A. K., & Freeman, K. H. (2018). Grassland fire ecology has roots in the late Miocene. *Proceedings of the National Academy of Sciences of the United States of America*, *115*(48), 12130–12135. https://doi.org/10.1073/pnas.1809758115

Keinan, N., Tyomkin, D., & Shoshan-Barmatz, V. (2010). Oligomerization of the Mitochondrial Protein Voltage-Dependent Anion Channel Is Coupled to the Induction of Apoptosis. *Molecular and Cellular Biology*, *30*(24), 5698–5709. https://doi.org/10.1128/mcb.00165-10

Klintworth, H., Garden, G., & Xia, Z. (2009). Rotenone and paraquat do not directly activate microglia or induce inflammatory cytokine release. *Neuroscience Letters*, *462*(1), 1–5. https://doi.org/10.1016/j.neulet.2009.06.065

Köhle, C., & Bock, K. W. (2007). Coordinate regulation of Phase I and II xenobiotic metabolisms by the Ah receptor and Nrf2. *Biochemical Pharmacology*, *73*(12), 1853–1862. https://doi.org/10.1016/j.bcp.2007.01.009

Kohle, C., Gschaidmeier, H., Lauth, D., Topell, S., Zitzer, H., & Bock, K. W. (1999). 2,3,7,8-Tetrachlorodibenzo-p-dioxin (TCDD)-mediated membrane translocation of c-Src protein kinase in liver WB-F344 cells. *Archives of Toxicology*, *73*, 152–158.

Kondraganti, S. R., Fernandez-Saluguero, P., Gonzalez, F. J., Ramos, K. S., Jiang, W., & Moorthy, B. (2003). Polycyclic aromatic hydrocarbon-inducible DNA adducts: Evidence by 32P-postlabeling and use of knockout mice for AH receptor-independent mechanisms of metabolic activation in vivo. *International Journal of Cancer*, *103*(1), 5–11. https://doi.org/10.1002/ijc.10784

Kouri, R. E., Rerrle, H., & Whitmire, C. E. (1973). Evidence of a Genetic Relationship Between Susceptibility to 3-Methyl-cholanthrene-Induced Subcutaneous Tumors and Inducibility of Aryl Hydro-carbon Hydroxylase 1,2. *Journal of the National Cancer Institute*, *51*, 197–200. https://academic.oup.com/jnci/article/51/1/197/886137

Krueger, M., Singer, T., Casida, J., & Ramsay, R. (1990). Evidence that the blocade of mitochondrial respiration by the neurotoxin 1-methhyl-4-phenylpyridinium (MPP+) involves binding at the same site as the respiratory inhibitor, rotenone. *Biochemical and Biophysical Research Communications*, *169*(1), 123–128.

Langston, J. W. (2017). The MPTP story. *Journal of Parkinson's Disease*, *7*, S11–S19. https://doi.org/10.3233/JPD-179006

Langston, J. W., Ballard, P., Tetrud, J. W., & Irwin, I. (1983). Chronic Parkinsonism in Humans due to a Product of Meperidine-Analog Synthesis. *Science*, *25*, 979–980.

Le Fur, G., Perrier, M. L., Vaucher, N., Imbault, F., Flamier, A., Benavides, J., Uzan, A., Renault, C., Dubroeucq, M. C., & Gueremy, C. (1983). Peripheral benzodiazepine binding sites: Effect of PK 11195, 1-(2-chlorophenyl)-n-methyl-n-(1-methylpropyl)-3-isoquinolinecarbocamide. I. In vitro studies. *Life Sciences*, *32*, 1839–1847.

Li, F., Xia, Y., Meiler, J., & Ferguson-Miller, S. (2013). Characterization and modeling of the oligomeric state and ligand binding behavior of purified translocator protein 18 kDa from Rhodobacter sphaeroides. *Biochemistry*, *52*(34), 5884–5899. https://doi.org/10.1021/bi400431t

Li, H., & Papadopoulos, V. (1998). Peripheral-Type Benzodiazepine Receptor Function in Cholesterol Transport. Identification of a Putative Cholesterol Recognition/Interaction Amino Acid Sequence and Consensus Pattern*. *Endocrinology*, *139*, 4991–4997. https://academic.oup.com/endo/article/139/12/4991/2991254

Lindemann, P., Koch, A., Degenhardt, B., Hause, G., Grimm, B., & Papadopoulos, V. (2004). A Novel Arabidopsis thaliana Protein is a Functional Peripheral-Type Benzodiazepine Receptor. *Plant Cell Physiol*, *45*(6), 723–733. https://academic.oup.com/pcp/article/45/6/723/1857399

Liu, Y., Liang, X., Yin, X., Lv, J., Tang, K., Ma, J., Ji, T., Zhang, H., Dong, W., Jin, X., Chen, D., Li, Y., Zhang, S., Xie, H. Q., Zhao, B., Zhao, T., Lu, J., Hu, Z. W., Cao, X., … Huang, B. (2017). Blockade of IDO-kynurenine-AhR metabolic circuitry abrogates IFN-γ-induced immunologic dormancy of tumor-repopulating cells. *Nature Communications*, *8*. https://doi.org/10.1038/ncomms15207

Liu, Z., Lee, J., Krummey, S., Lu, W., Cai, H., & Lenardo, M. J. (2011). The kinase LRRK2 is a regulator of the transcription factor NFAT that modulates the severity of inflammatory bowel disease. *Nature Immunology*, *12*(11), 1063–1070. https://doi.org/10.1038/ni.2113

Loth, M. K., Guariglia, S. R., Re, D. B., Perez, J., de Paiva, V. N., Dziedzic, J. L., Chambers, J. W., Azzam, D. J., & Guilarte, T. R. (2020). A Novel Interaction of Translocator Protein 18 kDa (TSPO) with NADPH Oxidase in Microglia. *Molecular Neurobiology*, *57*(11), 4467–4487. https://doi.org/10.1007/s12035-020-02042-w

Ma, Q., & Whitlock, J. P. (1997). A Novel Cytoplasmic Protein That Interacts with the Ah Receptor, Contains Tetratricopeptide Repeat Motifs, and Augments the Transcriptional Response to 2,3,7,8-Tetrachlorodibenzo-p-dioxin*. *The Journal of Biological Chemistry*, *272*, 8878–8884. http://www-jbc.stanford.edu/jbc/

Maddox, C., Wang, B., Kirby, P. A., Wang, K., & Ludewig, G. (2008). Mutagenicity of 3-methylcholanthrene, PCB3, and 4-OH-PCB3 in the lung of transgenic BigBlue® rats. *Environmental Toxicology and Pharmacology*, *25*(2), 260–266. https://doi.org/10.1016/j.etap.2007.10.021

Marzo, I., Brenner, C., Zamzami, N., Jurgensmeier, J., Susin, S., Vieira, H., Prevost, M.-C., Xie, X., Matsuyama, S., Reed, J., & Kroemer, G. (1998). Bax and adenine nucleotide translocator cooperate in the mitochondrial control of apoptosis. *Science*, *281*, 2027–2031.

Mass, M. J., Ross, J. A., Nesnow, S., Jeffers, A. J., Nelson, G., Galati, A. J., & Stoner, G. D. (1993). Ki-ras oncogene mutations in tumors and DNA adducts formed by benz[j]aceanthrylene and benzo[a]pyrene in the lungs of strain A/J mice. *Molecular Carcinogenesis*, *8*(3), 186–192. https://doi.org/10.1002/mc.2940080309

McEnery, M. W., Snowman, A. M., Trifilettit, R. R., & Snyder, S. H. (1992). Isolation of the mitochondrial benzodiazepine receptor: Association with the voltage-dependent anion channel and the adenine nucleotide carrier. *Biochemistry*, *89*, 3170–3174.

Meyer, B. K., & Perdew, G. H. (1999). Characterization of the AhR-hsp90-XAP2 core complex and the role of the immunophilin-related protein XAP2 in AhR stabilization. *Biochemistry*, *38*(28), 8907–8917. https://doi.org/10.1021/bi982223w

Meyer, B. K., Pray-Grant, M. G., Vanden Heuvel, J. P., & Perdew, G. H. (1998). Hepatitis B Virus X-Associated Protein 2 Is a Subunit of the Unliganded Aryl Hydrocarbon Receptor Core Complex and Exhibits Transcriptional Enhancer Activity. *Molecular and Cellular Biology*, *18*(2), 978–988.

Mezrich, J. D., Fechner, J. H., Zhang, X., Johnson, B. P., Burlingham, W. J., & Bradfield, C. A. (2010a). An Interaction between Kynurenine and the Aryl Hydrocarbon Receptor Can Generate Regulatory T Cells. *The Journal of Immunology*, *185*(6), 3190–3198. https://doi.org/10.4049/jimmunol.0903670

Mezrich, J. D., Fechner, J. H., Zhang, X., Johnson, B. P., Burlingham, W. J., & Bradfield, C. A. (2010b). An Interaction between Kynurenine and the Aryl Hydrocarbon Receptor Can Generate Regulatory T Cells. *The Journal of Immunology*, *185*(6), 3190–3198. https://doi.org/10.4049/jimmunol.0903670

Mills, R. D., Mulhern, T. D., Cheng, H. C., & Culvenor, J. G. (2012). Analysis of LRRK2 accessory repeat domains: Prediction of repeat length, number and sites of Parkinson's disease mutations. In *Biochemical Society Transactions* (Vol. 40, Issue 5, pp. 1086–1089). https://doi.org/10.1042/BST20120088

Mimura, J., Ema, M., Sogawa, K., & Fujii-Kuriyama, Y. (1999). Identification of a novel mechanism of regulation of Ah (dioxin) receptor function. *Genes & Development*, *13*, 20–25. www.genesdev.org

Morohaku, K., Pelton, S. H., Daugherty, D. J., Butler, W. R., Deng, W., & Selvaraj, V. (2014). Translocator protein/peripheral benzodiazepine receptor is not required for steroid hormone biosynthesis. *Endocrinology*, *155*(1), 89–97. https://doi.org/10.1210/en.2013-1556

Morrish, F., Buroker, N. E., Ge, M., Ning, X. H., Lopez-Guisa, J., Hockenbery, D., & Portman, M. A. (2006). Thyroid hormone receptor isoforms localize to cardiac mitochondrial matrix with potential for binding to receptor elements on mtDNA. *Mitochondrion*, *6*(3), 143–148. https://doi.org/10.1016/j.mito.2006.04.002

Nambu, J. F., Lewis, J. 0, Wharton, K. A., & Crews, S. T. (1991). The Drosophila single-minded gene encodes a Helix-Loop-Helix protein that acts as a master regulator of CNS midline development. *Cell*, *67*, 1157–1167.

Nass, M., & Nass, S. (1963). Intramitochondrial fibers with DNA characteristics I. Fixation and electron staining reactions. *The Journal of Cell Biology*, *19*, 593–611. http://rupress.org/jcb/article-pdf/19/3/593/1358594/593.pdf

Nault, R., Fader, K. A., Ammendolia, D. A., Dornbos, P., Potter, D., Sharratt, B., Kumagai, K., Harkema, J. R., Lunt, S. Y., Matthews, J., & Zacharewski, T. (2016). Dose-dependent metabolic reprogramming and differential gene expression in TCDD-elicited hepatic fibrosis. *Toxicological Sciences*, *154*(2), 253–266. https://doi.org/10.1093/toxsci/kfw163

Novello, S., Mercatelli, D., Albanese, F., Domenicale, C., Brugnoli, A., D'Aversa, E., Vantaggiato, S., Dovero, S., Murtaj, V., Presotto, L., Borgatti, M., Shimshek, D. R., Bezard, E., Moresco, R. M., Belloli, S., & Morari, M. (2022). In vivo susceptibility to energy failure parkinsonism and LRRK2 kinase activity. *Neurobiology of Disease*, *162*. https://doi.org/10.1016/j.nbd.2021.105579

Nukaya, M., & Bradfield, C. A. (2009). Conserved genomic structure of the Cyp1a1 and Cyp1a2 loci and their dioxin responsive elements cluster. In *Biochemical Pharmacology* (Vol. 77, Issue 4, pp. 654–659). https://doi.org/10.1016/j.bcp.2008.10.026

Ohnishi, T., Ohnishi, S. T., & Salerno, J. C. (2018). Five decades of research on mitochondrial NADH-quinone oxidoreductase (complex I). *Biological Chemistry*, *399*(11), 1249–1264. https://doi.org/10.1515/hsz-2018-0164

Oke, B., Suarez-Quian, C., Riond, J., Ferrara, P., & Papadopoulos, V. (1992). Cell surface localization of the peripheral-type benzodiazepine receptor (PBR) in adrenal cortex. *Molecular and Cellular Endocrinology*, *87*, 6.

Opitz, C. A., Litzenburger, U. M., Sahm, F., Ott, M., Tritschler, I., Trump, S., Schumacher, T., Jestaedt, L., Schrenk, D., Weller, M., Jugold, M., Guillemin, G. J., Miller, C. L., Lutz, C., Radlwimmer, B., Lehmann, I., Von Deimling, A., Wick, W., & Platten, M. (2011). An endogenous tumour-promoting ligand of the human aryl hydrocarbon receptor. *Nature*, *478*(7368), 197–203. https://doi.org/10.1038/nature10491

Palade, G. (1952). The fine structure of mitochondria. *The Anatomical Record*, *114*(3), 427–451. https://doi.org/10.1002/ar.1091140304

Papadopoulos, V., Baraldi, M., Guilarte, T. R., Knudsen, T. B., Lacapère, J. J., Lindemann, P., Norenberg, M. D., Nutt, D., Weizman, A., Zhang, M. R., & Gavish, M. (2006). Translocator protein (18 kDa): new nomenclature for the peripheral-type benzodiazepine receptor based on its structure and molecular function. *Trends in Pharmacological Sciences*, *27*(8), 402–409. https://doi.org/10.1016/j.tips.2006.06.005

Park, W. H., Jun, D. W., Kim, J. T., Jeong, J. H., Park, H., Chang, Y. S., Park, K. S., Lee, H. K., & Pak, Y. K. (2013). Novel cell-based assay reveals associations of circulating serum AhR-ligands with metabolic syndrome and mitochondrial dysfunction. *BioFactors*, *39*(4), 494–504. https://doi.org/10.1002/biof.1092

Parkinson, J. (2002). An Essay on the Shaking Palsy Member of the Royal College of Surgeons. *J Neuropsychiatry Clin Neurosci*, *14*(2).

Parola, A. L., Stump, D. G., Pepper, D. J., Krueger, K. E., Regan, J. W., & Laird II, H. E. (1991). *Cloning and Expression of a Pharmacologically Unique Bovine Peripheral-type Benzodiazepine Receptor Isoquinoline Binding Protein*. *266*(21), 14082–14087.

Passarini, B., Infusino, S. D., & Kasapi, E. (2010). Chloracne: Still cause for concern. *Dermatology*, *221*(1), 63–70. https://doi.org/10.1159/000290694

Payne, R., Hoff, H., Roskowski, A., & Foskett, J. K. (2017). MICU2 Restricts Spatial Crosstalk between InsP3R and MCU Channels by Regulating Threshold and Gain of MICU1-Mediated Inhibition and Activation of MCU. *Cell Reports*, *21*(11), 3141–3154. https://doi.org/10.1016/j.celrep.2017.11.064

Pendurthi, U. R., Okino, S. T., & Tukey, R. H. (1993). Accumulation of the Nuclear Dioxin (Ah) Receptor and Transcriptional Activation of the Mouse Cyp1a-1 and Cyp1a-2 Genes. *Archives of Biochemistry and Biophysics*, *306*(1), 65–69.

Perdew, G. H. (1988). Association of the Ah receptor with the 90-kDa heat shock protein. *Journal of Biological Chemistry*, *263*(27), 13802–13805. https://doi.org/10.1016/s0021-9258(18)68314-0

Perocchi, F., Gohil, V. M., Girgis, H. S., Bao, X. R., McCombs, J. E., Palmer, A. E., & Mootha, V. K. (2010). MICU1 encodes a mitochondrial EF hand protein required for Ca2+ uptake. *Nature*, *467*(7313), 291–296. https://doi.org/10.1038/nature09358

Pesatori, A. C., Consonni, D., Rubagotti, M., Grillo, P., & Bertazzi, P. A. (2009). Cancer incidence in the population exposed to dioxin after the "seveso accident": Twenty years of follow-up. *Environmental Health: A Global Access Science Source*, *8*(1). https://doi.org/10.1186/1476-069X-8-39

Phelan, D., Winter, G. M., Rogers, W. J., Lam, J. C., & Denison, M. S. (1998). Activation of the Ah Receptor Signal Transduction Pathway by Bilirubin and Biliverdin. *Archives of Biochemistry and Biophysics*, *357*(1), 155–163.

Pierre, S., Chevallier, A., Teixeira-Clerc, F., Ambolet-Camoit, A., Bui, L. C., Bats, A. S., Fournet, J. C., Fernandez-Salguero, P., Aggerbeck, M., Lotersztajn, S., Barouki, R., & Coumoul, X. (2014). Aryl hydrocarbon receptor-dependent induction of liver fibrosis by dioxin. *Toxicological Sciences*, *137*(1), 114–124. https://doi.org/10.1093/toxsci/kft236

Pirkle, J. L., Wolfe, W. H., Patterson, D. G., Needham, L. L., Michalek, J. E., Miner, J. C., Peterson, M. R., & Phillips, D. L. (1989). Estimates of the half-life of 2, 3, 7, 8-tetrachlorodibenzo-p-dioxin in vietnam veterans of operation ranch hand. *Journal of Toxicology and Environmental Health*, *27*(2), 165–171. https://doi.org/10.1080/15287398909531288

Plovanich, M., Bogorad, R. L., Sancak, Y., Kamer, K. J., Strittmatter, L., Li, A. A., Girgis, H. S., Kuchimanchi, S., De Groot, J., Speciner, L., Taneja, N., OShea, J., Koteliansky, V., & Mootha, V. K. (2013). MICU2, a Paralog of MICU1, Resides within the Mitochondrial Uniporter Complex to Regulate Calcium Handling. *PLoS ONE*, *8*(2). https://doi.org/10.1371/journal.pone.0055785

Poland, A., & Glover, E. (1974). Comparison of 2,3,7,8-tetrachlorodibenzo-p-dioxin, a potent inducer of aryl hydrocarbon hydroxylase, with 3-methylcholantrene. *Molecular Pharmacology*, *10*, 349–359.

Poland, A., & Knutson, J. C. (1982). 2,3,7,8-tetraxholodibenzo-p-dioxin and related halogenated aromatic hydrocarbons: Examination of the mechanism of toxicity. *Ann. Rev. Pharmacol. Toxicol*, *22*, 517–554. www.annualreviews.org

Pollanen, M., Dickson, D., & Bergeron, C. (1993). Pathology and biology of the Lewy body. *Journal of Neuropathology and Experimental Neurology*, *52*, 183–191.

Powell-Coffman, J. A., Bradfield, C. A., & Wood, W. B. (1998). Caenorhabditis elegans orthologs of the aryl hydrocarbon receptor and its heterodimerization partner the aryl hydrocarbon receptor nuclear translocator. *Biochemistry*, *95*, 2844–2849. www.pnas.org.

Probst, M. R., Reisz-Porszasz, S., Agbunag, R. V., Ong, M. S., & Hankinson, O. (1993). Role of the Aryl Hydrocarbon Receptor Nuclear Translocator Protein in Aryl Hydrocarbon (Dioxin) Receptor Action. *Molecular Pharmacology*, *44*(3), 511–518.

Prochaska, H. J., & Talalay, P. (1988). Regulatory Mechanisms of Monofunctional and Bifunctional Anticarcinogenic Enzyme Inducers in Murine Liver. *Cancer Research*, *48*, 4776–4782. http://aacrjournals.org/cancerres/article-pdf/48/17/4776/2958437/cr0480174776.pdf

Psarra, A. M. G., Solakidi, S., Trougakos, I. P., Margaritis, L. H., Spyrou, G., & Sekeris, C. E. (2005). Glucocorticoid receptor isoforms in human hepatocarcinoma HepG2 and SaOS-2 osteosarcoma cells: Presence of glucocorticoid receptor alpha in mitochondria and of glucocorticoid receptor beta in nucleoli. *International Journal of Biochemistry and Cell Biology*, *37*(12), 2544–2558. https://doi.org/10.1016/j.biocel.2005.06.015

Qin, H., & Powell-Coffman, J. A. (2004). The Caenorhabditis elegans aryl hydrocarbon receptor, AHR-1, regulates neuronal development. *Developmental Biology*, *270*(1), 64–75. https://doi.org/10.1016/j.ydbio.2004.02.004

Racker, E. (1964). A reconstituted system of oxidative phosphoylation. *Biochemical and Biophysical Research Communications*, *14*(1), 75–78.

Ramsay, R. R., Kowal, A. T., Johnson, M. K., Salach, J. I., And, ?, & Singer, T. P. (1987). The Inhibition Site of MPP+, the Neurotoxic Bioactivation Product of 1-Methyl-4-phenyl-1,2,3,6-tetrahydropyridine is near the Q-Binding Site of NADH Dehydrogenase'. *Archives of Biochemistry and Biophysics*, *259*(2), 645–649.

Ramsay, R. R., Salach, J. I., & Singer, T. P. (1986). Uptake of the neurotoxin 1-methyl-4-phenylpyridine (MPP+) by mitochondria and its relation to the inhibition of the mitochondrial oxidation of NAD+-linked substrates by MPP+. *Biochemical and Biophysical Research Communications*, *134*(2), 743–748.

Ran, F. A., Hsu, P. D., Wright, J., Agarwala, V., Scott, D. A., & Zhang, F. (2013). Genome engineering using the CRISPR-Cas9 system. *Nature Protocols*, *8*(11), 2281–2308. https://doi.org/10.1038/nprot.2013.143

Reddy, P., Jacquier, A. C., Abovich, N., Petersen, G., & Rosbash', M. (1986). The period clock Locus of D. melanogaster codes for a proteoglycan. *Cell*, *46*, 53–61.

Richardson, J. R., Quan, Y., Sherer, T. B., Greenamyre, J. T., & Miller, G. W. (2005). Paraquat neurotoxicity is distinct from that of MPTP and rotenone. *Toxicological Sciences*, *88*(1), 193–201. https://doi.org/10.1093/toxsci/kfi304

Rihn, B. H., Bottin, M. C., Coulais, C., Rouget, R., Monhoven, N., Baranowski, W., Edorh, A., & Keith, G. (2000). Genotoxicity of 3-methylcholanthrene in liver of transgenic Big Blue® mice. *Environmental and Molecular Mutagenesis*, *36*(4), 266–273. https://doi.org/10.1002/1098-2280(2000)36:4<266::AID-EM2>3.0.CO;2-H

Ringel, R., Sologub, M., Morozov, Y. I., Litonin, D., Cramer, P., & Temiakov, D. (2011). Structure of human mitochondrial RNA polymerase. *Nature*, *478*(7368), 269–273. https://doi.org/10.1038/nature10435

Rolfe, D. F. S., & Brown, G. C. (1997). Cellular Energy Utilization and Molecular Origin of Standard Metabolic Rate in Mammals. *Physiological Reviews*, *77*(3), 731–758.

Rostovtseva, T., & Colombini, M. (1996). ATP Flux Is Controlled by a Voltage-gated Channel from the Mitochondrial Outer Membrane*. *The Journal of Biological Chemistry*, *271*(45), 28006–28008. http://www-jbc.stanford.edu/jbc/

Sancak, Y., Markhard, A. L., Kitami, T., Kovács-Bogdán, E., Kamer, K. J., Udeshi, N. D., Carr, S. A., Chaudhuri, D., Clapham, D. E., Li, A. A., Calvo, S. E., Goldberger, O., & Mootha, V. K. (2013). EMRE is an essential component of the mitochondrial calcium uniporter complex. *Science*, *342*(6164), 1379–1382. https://doi.org/10.1126/science.1242993

Savouret, J.-F., Antenos, M., Quesne, M., Xu, J., Milgrom, E., & Casper, R. F. (2001). 7-Ketocholesterol Is an Endogenous Modulator for the Arylhydrocarbon Receptor. *Journal of Biological Chemistry*, *276*(5), 3054–3059. https://doi.org/10.1074/jbc.M005988200

Scheller, K., Sekeris, C. E., Krohne Georg, Hock, R., Hansen, I. A., & Scheer, U. (2000). Localization of glucocorticoid hormone receptors in mitochondria o f human cells Glucocorticoid receptor-mitochondria-immunolocalization-green fluorescent protein-HeLa cells-Hep-2 cells. *European Journal of Cell Biology*, *9*(7). http://www.urbanfischer.de/journals/ejcb

Schmidt, J. V, HUEI-TING Sutt, G., Reddy, J. K., CELESTE SIMONt, M., & Bradfield, C. A. (1996). Characterization of a murine Ahr null allele: Involvement of the Ah receptor in hepatic growth and development (dioxin/2,3,7,8-tetrachlorodibenzo-p-dioxin/gene targeting/liver) (Vol. 93). https://www.pnas.org

Schoemaker, H., Bliss, M., & Yamamura, H. I. (1981). Specific high-affinity saturable binding of [3H]Ro5-4864 to benzodiazepine binding sites in the rat cerebral cortex. *European Journal of Pharmacology*, *71*, 173.

Schreij, A. M., Chaineau, M., Ruan, W., Lin, S., Barker, P. A., Fon, E. A., & McPherson, P. S. (2015). LRRK 2 localizes to endosomes and interacts with clathrin-light chains to limit Rac1 activation. *EMBO Reports*, *16*(1), 79–86. https://doi.org/10.15252/embr.201438714

Seok, S. H., Ma, Z. X., Feltenberger, J. B., Chen, H., Chen, H., Scarlett, C., Lin, Z., Satyshur, K. A., Cortopassi, M., Jefcoate, C. R., Ge, Y., Tang, W., Bradfield, C. A., & Xing, Y. (2018). Trace derivatives of kynurenine potently activate the aryl hydrocarbon receptor (AHR). *Journal of Biological Chemistry*, *293*(6), 1994–2005. https://doi.org/10.1074/jbc.RA117.000631

Sharma, M. R., Koc, E. C., Datta, P. P., Booth, T. M., Spremulli, L. L., & Agrawal, R. K. (2003). Structure of the Mammalian Mitochondrial Ribosome Reveals an Expanded Functional Role for Its Component Proteins. *Cell*, *115*, 97–108. www.cell.com/cgi/content/

Shen, R.-S., Abell, C. W., Gessner, W., & Brossi, A. (1985). Serotonergic conversion of MPTP and dopaminergic accumulation of MPP+. *FEBS*, *189*(2), 225–230.

Shimizu, S., Narita, M., & Tsujimoto, Y. (1999). Bcl-2 family proteins regulate the release of apoptogenic cytochrome c by the mitochondrial channel VDAC. *Nature*, *399*, 483–487.

Shrestha, S., Parks, C. G., Umbach, D. M., Richards-Barber, M., Hofmann, J. N., Chen, H., Blair, A., Beane Freeman, L. E., & Sandler, D. P. (2020). Pesticide use and incident Parkinson's disease in a cohort of farmers and their spouses. *Environmental Research*, *191*. https://doi.org/10.1016/j.envres.2020.110186

Sinal, C. J., & Bend, J. R. (1997). Aryl Hydrocarbon Receptor-Dependent Induction of Cyp1a1 by Bilirubin in Mouse Hepatoma Hepa 1c1c7 Cells. *Molecular Pharmacology*, *52*, 590–599.

Singer, T. P., & Kearney, E. B. (1954). Solubilization, assay, and purification of succinic dehydrogenase. *Biochimica et Biophysica Acta*, *15*, 151–153.

Sjostrand, F. (1953). Electron microscopy of mitochondria and cytoplasmic double membranes. *Nature*, *171*(4340), 30–31.

Steger, M., Tonelli, F., Ito, G., Davies, P., Trost, M., Vetter, M., Wachter, S., Lorentzen, E., Duddy, G., Wilson, S., Baptista, M. A. S., Fiske, B. K., Fell, M. J., Morrow, J. A., Reith, A. D., Alessi, D. R., & Mann, M. (2016). Phosphoproteomics reveals that Parkinson's disease kinase LRRK2 regulates a subset of Rab GTPases. *ELife*, *5*(JANUARY2016). https://doi.org/10.7554/eLife.12813.001

Sutter, T. R., Tang, Y. M., Hayes, C. L., Wo, Y. Y. P., Jabs, E. W., Li, X., Yin, H., Cody, C. W., & Greenlee, W. F. (1994). Complete cDNA sequence of a human dioxin-inducible mRNA identifies a new gene subfamily of cytochrome P450 that maps to chromosome 2. *Journal of Biological Chemistry*, *269*(18), 13092–13099. https://doi.org/10.1016/s0021-9258(17)36803-5

Szabadkai, G., Bianchi, K., Várnai, P., De Stefani, D., Wieckowski, M. R., Cavagna, D., Nagy, A. I., Balla, T., & Rizzuto, R. (2006). Chaperone-mediated coupling of endoplasmic reticulum and mitochondrial Ca2+ channels. *Journal of Cell Biology*, *175*(6), 901–911. https://doi.org/10.1083/jcb.200608073

Taketani, S., Kohno, H., Furukawa, T., & Tokunaga, R. (1995). Involvement of peripheral-type benzodiazepine receptors in the intracellular transport of heme and porphyrins1. *J. Biochem*, *117*, 875–880.

Tanguay, R. L., Abnet, C. C., Heideman, W., & Peterson, R. E. (1999). Cloning and characterization of the zebrafish (Danio rerio) aryl hydrocarbon receptor 1. *Biochimica et Biophysica Acta*, *1444*, 35–48. http://kiwi.bcm.edu:8088/

Tani, M., Kamata, Y., Deushi, M., Osaka, M., & Yoshida, M. (2018). 7-Ketocholesterol enhances leukocyte adhesion to endothelial cells via p38MAPK pathway. *PLoS ONE*, *13*(7). https://doi.org/10.1371/journal.pone.0200499

Tanos, R., Patel, R. D., Murray, I. A., Smith, P. B., Patterson, A. D., & Perdew, G. H. (2012). Aryl hydrocarbon receptor regulates the cholesterol biosynthetic pathway in a dioxin response element-independent manner. *Hepatology*, *55*(6), 1994–2004. https://doi.org/10.1002/hep.25571

Tappenden, D. M., Lynn, S. G., Crawford, R. B., Lee, K. A., Vengellur, A., Kaminski, N. E., Thomas, R. S., & LaPres, J. J. (2011). The aryl hydrocarbon receptor interacts with ATP5α1, a subunit of the ATP synthase complex, and modulates mitochondrial function. *Toxicology and Applied Pharmacology*, *254*(3), 299–310. https://doi.org/10.1016/j.taap.2011.05.004

Taylor, B. L., & Zhulin, I. B. (1999). PAS Domains: Internal Sensors of Oxygen, Redox Potential, and Light. *Microbiology and Molecular Biology Reviews*, *63*(2), 479–506. www.llu.edu/medicine/micro/PAS.

Tian, Y., Lv, J., Su, Z., Wu, T., Li, X., Hu, X., Zhang, J., Wu, L., & Key, B. (2021). LRRK2 plays essential roles in maintaining lung homeostasis and preventing the development of pulmonary fibrosis. *Proceedings of the National Academy of Sciences*, *118*. https://doi.org/10.1073/pnas.2106685118/-/DCSupplemental

Titcomb, T. J., & Tanumihardjo, S. A. (2019). Global Concerns with B Vitamin Statuses: Biofortification, Fortification, Hidden Hunger, Interactions, and Toxicity. *Comprehensive Reviews in Food Science and Food Safety*, *18*(6), 1968–1984. https://doi.org/10.1111/1541-4337.12491

Toyofuku, T., Okamoto, Y., Ishikawa, T., Sasawatari, S., & Kumanogoh, A. (2020). LRRK 2 regulates endoplasmic reticulum–mitochondrial tethering through the PERK -mediated ubiquitination pathway . *The EMBO Journal*, *39*(2). https://doi.org/10.15252/embj.2018100875

Tu, L. N., Morohaku, K., Manna, P. R., Pelton, S. H., Butler, W. R., Stocco, D. M., & Selvaraj, V. (2014). Peripheral benzodiazepine receptor/translocator protein global knock-out mice are viable with no effects on steroid hormone biosynthesis. *Journal of Biological Chemistry*, *289*(40), 27444–27454. https://doi.org/10.1074/jbc.M114.578286

Uemura, H., Arisawa, K., Hiyoshi, M., Kitayama, A., Takami, H., Sewachika, F., Dakeshita, S., Nii, K., Satoh, H., Sumiyoshi, Y., Morinaga, K., Kodama, K., Suzuki, T. I., Nagai, M., & Suzuki, T. (2009). Prevalence of metabolic syndrome associated with body burden levels of dioxin and related compounds among Japan's general population. *Environmental Health Perspectives*, *117*(4), 568–573. https://doi.org/10.1289/ehp.0800012

Van Itallie, C. M. (1992). Dexamethasone Treatment Increases Mitochondrial RNA Synthesis in a Rat Hepatoma Cell Line*. *Endocrinology*, *130*(2), 567–576. https://academic.oup.com/endo/article/130/2/567/2535765

Vaziri, C., & Faller, D. V. (1997). A Benzo[a]pyrene-induced Cell Cycle Checkpoint Resulting in p53-independent G 1 Arrest in 3T3 Fibroblasts*. *The Journal of Biological Chemistry*, *272*(5), 2762–2769. http://www-jbc.stanford.edu/jbc/

Verma, A., Ebanks, K., Fok, C. Y., Lewis, P. A., Bettencourt, C., & Bandopadhyay, R. (2021). In silico comparative analysis of LRRK2 interactomes from brain, kidney and lung. *Brain Research*, *1765*. https://doi.org/10.1016/j.brainres.2021.147503

Verma, A., Nye, J. S., & Snyder, S. H. (1987). Porphyrins are endogenous ligands for the mitochondrial (peripheral-type) benzodiazepine receptor (diazepam/metailoporphyrins/hemin/harderian gland). *Proceedings of the National Academy of Sciences USA*, *84*, 2256–2260.

Wang, H., Sun, X., Lin, M. S., Ferrario, C. M., Van Remmen, H., & Groban, L. (2018). G protein-coupled estrogen receptor (GPER) deficiency induces cardiac remodeling through oxidative stress. *Translational Research*, *199*, 39–51. https://doi.org/10.1016/j.trsl.2018.04.005

Warner, M., Mocarelli, P., Brambilla, P., Wesselink, A., Patterson, D. G., Turner, W. E., & Eskenazi, B. (2014). Serum TCDD and TEQ concentrations among Seveso women, 20 years afte. The explosion. *Journal of Exposure Science and Environmental Epidemiology*, *24*(6), 588–594. https://doi.org/10.1038/jes.2013.70

Warner, M., Mocarelli, P., Brambilla, P., Wesselink, A., Samuels, S., Signorini, S., & Eskenazi, B. (2013). Diabetes, metabolic syndrome, and obesity in relation to serum dioxin concentrations: The Seveso Women's Health Study. *Environmental Health Perspectives*, *121*(8), 906–911. https://doi.org/10.1289/ehp.1206113

Weed, D. L. (2021). Does paraquat cause Parkinson's disease? A review of reviews. *NeuroToxicology*, *86*, 180–184. https://doi.org/10.1016/j.neuro.2021.08.006

West, A. B., Moore, D. J., Biskup, S., Bugayenko, A., Smith, W. W., Ross, C. A., Dawson, V. L., & Dawson, T. M. (2005). *Parkinson's disease-associated mutations in leucine-rich repeat kinase 2 augment kinase activity*. www.pnas.orgcgidoi10.1073pnas.0507360102

Wikenheiser, K. A., Vorbroker, D. K., Rice, W. R., Clark, J. C., Bachurski, C. J., Oiet, H. K., & Whitsett, J. A. (1993). Production of immortalized distal respiratory epithelial cell lines from surfactant protein C/simian virus 40 large tumor antigen transgenic mice. *Cell Biology*, *90*, 11029–11033. https://www.pnas.org

Willis, A. W., Roberts, E., Beck, J. C., Fiske, B., Ross, W., Savica, R., Van Den Eeden, S. K., Tanner, C. M., Marras, C., Alcalay, R., Schwarzschild, M., Racette, B., Chen, H., Church, T., Wilson, B., & Doria, J. M. (2022). Incidence of Parkinson disease in North America. *Npj Parkinson's Disease*, *8*(1). https://doi.org/10.1038/s41531-022-00410-y

Xia, D., Esser, L., Tang, W. K., Zhou, F., Zhou, Y., Yu, L., & Yu, C. A. (2013). Structural analysis of cytochrome bc1 complexes: Implications to the mechanism of function. In *Biochimica et Biophysica Acta - Bioenergetics* (Vol. 1827, Issues 11–12, pp. 1278–1294). https://doi.org/10.1016/j.bbabio.2012.11.008

Xiao, H. X., Song, B., Li, Q., Shao, Y. M., Zhang, Y. Bin, Chang, X. L., & Zhou, Z. J. (2022). Paraquat mediates BV-2 microglia activation by raising intracellular ROS and inhibiting Akt1 phosphorylation. *Toxicology Letters*, *355*, 116–126. https://doi.org/10.1016/j.toxlet.2021.11.017

Xing, W., Liu, J., Cheng, S., Vogel, P., Mohan, S., & Brommage, R. (2013). Targeted disruption of leucine-rich repeat kinase 1 but not leucine-rich repeat kinase 2 in mice causes severe osteopetrosis. *Journal of Bone and Mineral Research*, *28*(9), 1962–1974. https://doi.org/10.1002/jbmr.1935

Xu, L., Li, A. P., Kaminski, D. L., & Ruh, M. F. (2000). 2,3,7,8 Tetrachlorodibenzo-p-dioxin induction of cytochrome P4501A in cultured rat and human hepatocytes. *Chemico-Biological Interactions*, *124*, 173–189. www.elsevier.com/locate/chembiont

Yang, S.-H., Liu, R., Perez, E. J., Wen, Y., Stevens, S. M. †, Valencia, T., Brun-Zinkernagel, A.-M., Prokai, L., Will, Y., Dykens, J., Koulen, P., & Simpkins, J. W. (2004). Mitochondrial localization of estrogen receptor. *The Proceedings of the National Academy of Sciences*, *101*(12), 4130–4135. www.pnas.orgcgidoi10.1073pnas.0306948101

Yang, T. T., Hsu, C. T., & Kuo, Y. M. (2009). Cell-derived soluble oligomers of human amyloid-β peptides disturb cellular homeostasis and induce apoptosis in primary hippocampal neurons. *Journal of Neural Transmission*, *116*(12), 1561–1569. https://doi.org/10.1007/s00702-009-0311-0

Yeliseev, A. A., & Kaplan, S. (1995a). A sensory transducer homologous to the mammalian peripheral-type benzodiazepine receptor regulates photosynthetic membrane complex formation in Rhodobacter sphaeroides 2.4.1. *Journal of Biological Chemistry*, *270*(36), 21167–21175. https://doi.org/10.1074/jbc.270.36.21167

Yeliseev, A. A., & Kaplan, S. (1995b). A sensory transducer homologous to the mammalian peripheral-type benzodiazepine receptor regulates photosynthetic membrane complex formation in Rhodobacter sphaeroides 2.4.1. *Journal of Biological Chemistry*, *270*(36), 21167–21175. https://doi.org/10.1074/jbc.270.36.21167

Yoshikawa, S., Shinzawa-Itoh, K., & Tsukihara, T. (1998). Crystal Structure of Bovine Heart Cytochrome c Oxidase at 2.8 A Resolution. *Journal of Bioenergetics and Biomembranes*, *30*(1).

Yu, C.-A., & Yu, L. (1981). Ubiquinone-binding proteins. *Biochimica et Biophysica Acta*, *639*, 99–128.

Zaglia, T., Ceriotti, P., Campo, A., Borile, G., Armani, A., Carullo, P., Prando, V., Coppini, R., Vida, V., Stølen, T. O., Ulrik, W., Cerbai, E., Stellin, G., Faggian, G., De Stefani, D., Sandri, M., Rizzuto, R., Di Lisa, F., Pozzan, T., … Mongillo, M. (2017). Content of mitochondrial calcium uniporter (MCU) in cardiomyocytes is regulated by microRNA-1 in physiologic and pathologic hypertrophy. *Proceedings of the National Academy of Sciences of the United States of America*, *114*(43), E9006–E9015. https://doi.org/10.1073/pnas.1708772114

Zeno, S., Zaaroor, M., Leschiner, S., Veenman, L., & Gavish, M. (2009). CoCl2 induces apoptosis via the 18 kDa translocator protein in U118MG human glioblastoma cells. *Biochemistry*, *48*(21), 4652–4661. https://doi.org/10.1021/bi900064t

Zhang, W., Gao, J. H., Yan, Z. F., Huang, X. Y., Guo, P., Sun, L., Liu, Z., Hu, Y., Zuo, L. J., Yu, S. Y., Cao, C. J., Wang, X. M., & Hong, J. S. (2018). Minimally toxic dose of lipopolysaccharide and α-synuclein oligomer elicit synergistic dopaminergic neurodegeneration: Role and mechanism of microglial NOX2 activation. *Molecular Neurobiology*, *55*(1), 619–632. https://doi.org/10.1007/s12035-016-0308-2

Zhao, A. H., Tu, L. N., Mukai, C., Sirivelu, M. P., Pillai, V. V., Morohaku, K., Cohen, R., & Selvaraj, V. (2016). Mitochondrial translocator protein (TSPO) function is not essential for heme biosynthesis. *Journal of Biological Chemistry*, *291*(4), 1591–1603. https://doi.org/10.1074/jbc.M115.686360

Zimprich, A., Müller-Myhsok, B., Farrer, M., Leitner, P., Sharma, M., Hulihan, M., Lockhart, P., Strongosky, A., Kachergus, J., Calne, D. B., Stoessl, J., Uitti, R. J., Pfeiffer, R. F., Trenkwalder, C., Homann, N., Ott, E., Wenzel, K., Asmus, F., Hardy, J., … Gasser, T. (2004). The PARK8 Locus in Autosomal Dominant Parkinsonism: Confirmation of Linkage and Further Delineation of the Disease-Containing Interval. *American Journal of Human Genetics*, *74*, 11–19.

Zuo, J., Brewer, D. S., Arlt, V. M., Cooper, C. S., & Phillips, D. H. (2014). Benzo [a]pyrene-induced DNA adducts and gene expression profiles in target and non-target organs for carcinogenesis in mice. *BMC Genomics*, *15*(1). https://doi.org/10.1186/1471-2164-15-880